



PONTIFICIA UNIVERSIDAD CATÓLICA DE CHILE

Facultad de Ciencias Biológicas

Programa de Doctorado en Ciencias Biológicas

Mención Biología Celular y Molecular

ROLE OF GALECTIN-8 AND DYSFUNCTIONS BY AUTOANTIBODIES IN THE BRAIN

Tesis entregada a la Pontificia Universidad Católica de Chile en cumplimiento parcial de los requisitos para optar al grado de Doctor en Ciencias con mención en Biología Molecular y Celular.

Por: M. FRANCISCA BARAKE SABBAGH

Director de Tesis: Dr. Alfonso González de la Rosa

Co-Directora de Tesis: Dra. Betty Diamond

Enero 2021

This work is dedicated to my family and friends, specially to my father looking after me from the skies, my mother for her tremendous help and dedication in helping me with everything, my amazing brother for always been there, my children Trini and Jorge for putting my world upside down and to my partner in life Alex for always making me laugh.

ACKNOWLEDGMENTS

I would like to thank Dr. Alfonso Gonzalez for giving me the opportunity to work with him and encouraging my love for science. And to all the members and past members from his laboratory for their friendship and continuous help. Specially in this thesis to Claudio Retamal for the microscopy analysis, Adely de la Peña for preparing Gal-8, Claudia Oyanadel for preparing Gal-8 and purifying antibodies, Carmen Espinoza for teaching me many techniques used here and helping me with the behavior assays, Evelyn Pardo and Andrea Soza for establishing the bases of this thesis by performing the pull-down and Mass-Spec sequencing, to Laura Hernandez for letting me teach her and for the performance of experiments, to Beatriz Vasquez for cloning the Gal-8 N-CRD, to Loreto Massardo and Claudia Cárcamo for the sera collection, Javier Venegas for his invaluable technical help and to Irma Castillo for her great managing help. I am also thankful to Mariana Labarca, Lisette Sandoval, Ronan Shaughnessy, Claudia Metz, Patricia Gajardo, Marcela Bravo, Jonathan Barra, Milena Mimica and Catalina Grabowski for their friendship and tremendous support throughout these years.

I would also greatly thank Dr. Betty Diamond for accepting me in her laboratory permitting me to learn and grow there. I am especially thankful to Venkatesh Jeganathan for his invaluable help with the human and mouse monoclonal antibodies and his friendship, and Susan Malkiel for teaching me the flow cytometry technique. I am also thankful to Lior Brimberg, Simone Mader, Czeslawa Kowal amongst many others laboratory members for their help and companionship.

I would also like to thank from the Feinstein Institute to Bruce Volpe and Patricio Huerta and their laboratory members Roseann Berlin and Tomás Huerta respectively, for teaching me and their friendship.

To Dr. Alejandra Álvarez for giving me a place at her laboratory and to all of her laboratory members, specially Nancy Leal for preparing all the primary cultured neurons.

To Dr. Mathew Sharp laboratory specially to Susan Buhl for the helping with the mouse monoclonal fusion.

To Dr. Nibaldo Inestrosa and his laboratory, specially to Juan Francisco Codocedo and Carolina Oliva for the realization of the electrophysiology experiments.

To Dr. Waldo Cerpa and his laboratory for permitting the use of their behavioral suite and specially to Francisco Carvajal for performing electrophysiology experiments.

To the personnel at the Flow Cytometry Core Facility, Feinstein Institute for Medical Research for the performance of the flow cytometric analysis and assistance.

To the services provided by UC CINBIOT Animal Facility funded by PIA CONICYT ECM-07 Program for Associative Research, of the Chilean National Council for Science and Technology.

Finally, I would like to thank UNESCO and L'Oreal for their financing and the amazing opportunity to receive the prize in France together with training and permitting me meet amazing scientific women.

This thesis was financed by CONICYT National Doctoral studies fellowship Chile (21120650), CONICYT International fellowship Chile, VRI International Fellowship (PUC) Chile, For Women in Science International Fellowship UNESCO/L'Oreal France, Programa de Apoyo a Centros con Financiamiento Basal AFB170005 to the Center for Aging and Regeneration (CARE) and AFB170004 to Fundación Ciencia & Vida.

INDEX

ACKNOWLEDGMENTS	i
FIGURE INDEX	vii
TABLE INDEX	ix
ABBREVIATIONS	x
RESUMEN	xii
ABSTRACT	xv
1. INTRODUCTION	1
1.1. <i>Problem Statement</i>	<i>1</i>
1.2. <i>Literature review</i>	<i>5</i>
1.2.1. Galectins	<i>5</i>
1.2.1.1 Galectin-8 (Gal-8).....	<i>5</i>
1.2.1.2 Anti-Galectin-8 antibodies	<i>6</i>
1.2.2 Glutamatergic Synapse	<i>7</i>
1.2.2.1. AMPA receptors (AMPA).....	<i>7</i>
1.2.2.2. NMDA receptors (NMDAR).....	<i>8</i>
1.2.2.3. Synaptic plasticity.....	<i>9</i>
1.2.2.4. GABA receptors (GABAR)	<i>10</i>
1.3. <i>Hypothesis and Objectives</i>	<i>11</i>
1.3.1. Hypothesis: “Gal-8 modulates glutamatergic functions that can be interfered with anti-Gal-8 autoantibodies”.....	<i>11</i>
1.3.2. Objectives:	<i>11</i>
2. MATERIALS AND METHODS	12
2.1. <i>Materials</i>	<i>12</i>
2.1.1. Animals	<i>12</i>
2.1.2. Patients Samples	<i>12</i>
2.1.3. Antibodies	<i>12</i>
2.1.4. Reagents	<i>13</i>
2.1.5. Plasmid	<i>13</i>
2.2. <i>Methods</i>	<i>14</i>
2.2.1. Cellular biology techniques.....	<i>14</i>
2.2.1.1. Rat primary Neuronal Culture.	<i>14</i>

2.2.1.2. Cell Surface Biotinylation.	14
2.2.1.3. Neurons Live Immunofluorescence.....	15
2.2.1.4. Endocytosis assay.	15
2.2.1.5. Recycling assay.	16
2.2.1.6. HEK-293 transfection.	16
2.2.2. Biochemical techniques	17
2.2.2.1. Fusion protein-GST and recombinant protein production.	17
2.2.2.2. Pull-Down assay.	17
2.2.2.3. Co-Immunoprecipitation.	18
2.2.2.4. Antibody purification.....	18
2.2.2.5. Post synaptic Densities (PSD) preparation.	19
2.2.2.6. Gel electrophoresis and western blot.....	19
2.2.3. Animal procedures	20
2.2.3.1. Electrophysiology.....	20
2.2.3.2. Behavioral tests.....	22
2.2.4. Statistical Analysis	22
3. RESULTS	24
3.1. <i>Gal-8 binds AMPAR</i>	24
3.2. <i>Gal-8 increases AMPAR levels on the cell surface</i>	28
3.3. <i>Gal-8 increases recycling of AMPAR to the cell surface</i>	33
3.4. <i>PKA and FAK pathways are involved in Gal-8 effects on AMPAR levels at the neuronal surface</i>	35
3.5. <i>Gal-8 enhances or inhibits glutamatergic synaptic transmission depending on its concentration</i>	38
3.6. <i>Blocking endogenous Gal-8 with Gal-8 N-CRD inhibits synaptic transmission</i>	43
3.7. <i>Function-blocking anti-Gal-8 autoantibodies inhibit CA3-CA1 synaptic plasticity</i>	45
3.8. <i>Gal-8 KO mice have reduced postsynaptic density AMPAR levels, impaired plasticity and altered spatial memory</i>	47
4. DISCUSSION	52
4.1. <i>Gal-8 binds AMPAR</i>	53
4.2. <i>Gal-8 increases AMPAR surface levels by modulating its traffic</i>	54
4.3. <i>Gal-8 in synaptic transmission</i>	58
4.4. <i>Endogenous functions of Gal-8</i>	60
4.5. <i>Relevance</i>	62

4.5.1. Gal-8 expression levels in the brain.....	62
4.5.2. Other galectins involved in glutamatergic functions.....	63
4.5.3. Glycosylation patterns in the brain.....	63
4.5.4. Anti-Gal-8 autoantibodies inhibit Gal-8 function	66
5. CONCLUSIONS	69
<i>ADDENDUM: Generation of mice and human monoclonal antibodies against ribosomal P epitope and their effect on hippocampal glutamatergic transmission</i>	
A.1. INTRODUCTION.....	70
A.2. MATERIALS AND METHODS	73
<i>A.2.1. Materials.....</i>	<i>73</i>
A.2.1.1. Animals.....	73
A.2.1.2. Patients Samples	73
A.2.1.3. Antibodies.....	73
A.2.1.4. Reagents	74
A.2.1.5. Plasmids.....	75
<i>A.2.2 Methods.....</i>	<i>75</i>
A.2.2.1. Mouse Monoclonal	75
A.2.2.1.1. Mice immunization	75
A.2.2.1.2. Hybridomas.....	75
A.2.2.2. Human Monoclonal	76
A.2.2.2.1. Fluorescent P-Epitope preparation.	77
A.2.2.2.2. Sorting.	77
A.2.2.2.3. Complementary DNA (cDNA) Preparation.	77
A.2.2.2.4. Immunoglobulin variable region amplification.....	78
A.2.2.2.5. Cloning amplification round.	79
A.2.2.2.6. Cloning.....	79
A.2.2.2.7. Transformation.....	80
A.2.2.2.8. Miniprep.	80
A.2.2.2.9. HEK 293-T transfections for antibody production.	80
A.2.2.3. Cellular biology techniques	81
A.2.2.3.1. HEK-293 Immunofluorescence.....	81
A.2.2.4. Biochemical techniques.....	81
A.2.2.4.1. Fusion protein-GST and recombinant protein production.....	81
A.2.2.4.2. Gel electrophoresis and western blot.	82
A.2.2.4.3. Enzyme-linked immunosorbent (ELISA) assays.....	82
A.2.2.4.4. Antibody purification.	83
A.2.2.5. Animal procedures	84
A.2.2.5.1. Electrophysiology.....	84
A.3. RESULTS	87

<i>A.3.1 Murine monoclonal antibodies</i>	87
<i>A.3.2 Human monoclonal antibodies</i>	89
A.4. DISCUSSION	98
<i>A.4.1 Murine monoclonal anti-P antibodies</i>	98
<i>A.4.2 Human monoclonal anti-P antibodies</i>	99
<i>A.4.3. Conclusions</i>	99
BIBLIOGRAPHY	101

FIGURE INDEX

Figure 1: Gal-8 interacts through its sialic acid-binding (N-CRD) domain with AMPAR but not NMDAR subunits in the brain.	27
Figure 2: Gal-8 increases the levels of GluA1 at the neuronal surface.	30
Figure 3: Gal-8 increases the neuronal surface levels of GluA2 but not GluN2B.	31
Figure 4: Gal-8 increases the levels of GluA1 at dendrites.	32
Figure 5: Gal-8 enhances GluA1 endocytosis and recycling to the surface.	34
Figure 6: Gal-8 increases GluA1 levels at the cell surface involving FAK and PKA activity. .	37
Figure 7: Gal-8 increases spontaneous excitatory or inhibitory spikes at different concentrations.	40
Figure 8: Gal-8 enhances excitatory or inhibitory synaptic transmission.	41
Figure 9: Gal-8 has inhibitory influence upon glutamatergic transmission, enhances GABA _A R cell surface levels and binds GABA _A R.	42
Figure 10: Gal-8 N-CRD decreases synaptic transmission.	44
Figure 11: Function blocking anti-Gal-8 autoantibodies from patients with multiple sclerosis inhibit synaptic plasticity.	46
Figure 12: Endogenous Gal-8 contributes to AMPAR levels on the postsynaptic densities (PSD).	49
Figure 13: Endogenous Gal-8 contributes to synaptic plasticity.	50
Figure 14: Endogenous Gal-8 contributes to memory.	51
Figure 15. Model of Gal-8 glutamatergic functions	68
Figure A.1: Mouse monoclonal antibodies.	88
Figure A.2: C-terminal biotinylated P-Epitope as the best choice for detecting anti-P memory B cells.	91

Figure A.3: Cell sorter setup for the identification of memory B cells expressing cell surface anti-P-IgG.	93
Figure A.4: Human anti-P monoclonal antibody cDNAs cloned from single sorted memory B cells.....	96
Figure A.5: Properties of human monoclonal antibody C12 (hmabC12) that resemble anti-P antibodies.	97

TABLE INDEX

Table 1: Gal-8 interactors..... **26**

Table A.1: Primer sequences for amplification and cloning of the variable regions of heavy and light immunoglobins chains..... **86**

Table A.2: Summary of populations obtained when setting the cell sorting parameters. **94**

ABBREVIATIONS

α -(2,3)SL	α -(2,3)-Sialyllactose
α -(2,6)SL	α -(2,6)-Sialyllactose
AMPA	α -amino-3-hydroxy-5-methyl-4-isoxazolepropionic acid receptors
ANOVA	Analysis of variance
anti-dsDNA	anti-double stranded DNA
anti-P	anti-ribosomal P protein antibodies
APV	D-2-amino-5-phosphonovalerate
BBB	Blood brain barrier
BSA	Bovine serum albumine
CamKII	Calmodulin-dependent protein kinase II
CD	Cognitive dysfunction
cDNA	complementary DNA
CRD	Carbohydrate recognition domain
CSF	Cerebrospinal fluid
DMEM	Dulbecco's Modified Eagle Medium
DMSO	Dimethyl sulfoxide
DNRab	anti-dsDNA antibodies that cross-react with NMDAR
DIV	Days in vitro
ELISA	Enzyme-linked immunosorbent assay
FACS	Fluorescence-activated cell sorting
FAK	Focal adhesion Kinase
FAKi	Focal adhesion kinase inhibitor
FBS	Fetal bovine serum
fEPSP	Field excitatory postsynaptic potentials
GABA _A R	Gamma-aminobutyric acid type A receptors
Gal-8	Galectin-8
GS	Glutathion Sepharose
HBSS	Hanks' Balanced Salt Solution
HFS	High frequency stimulation
hmabC12	Human monoclonal antibody clone 12
HRP	Horseradish peroxidase
IgG	Inmmunoglobulin G
IgM	Inmmunoglobulin M
IPTG	Isopropyl β - d-1-thiogalactopyranoside
KO	Knockout
LB	Luria Broth

LTD	Long-term depression
LTP	Long-term potentiation
MAP	Multiantigenic peptide
MS	Multiple Sclerosis
MUA	Multiunit activity
NBQX	2,3-dioxo-6-nitro-7-sulfamoyl-benzo[f]quinoxaline
NEEA	Non-essential aminoacids
NMDARs	N-methyl-D-aspartate receptors Non-significant
NSPA	Neuronal surface P antigen
ON	Over night
P/S	Penicilin/Streptamicin
PBMC	Peripheral blood mononuclear cells
PBS	Phosphate buffered saline
PCR	Polimerase chain reaction
PFA	Paraformaldehyde
PKA	Protein Kinase A
PPF	Pair pulse facilitation
PSD	Postsynaptic densities
PSD-95	Postsynaptic density-95
PTX	Picrotoxin
RT	Room temperature
RT-PCR	Reverse transcriptase PCR
SEM	Standard error of the mean
SLE	Systemic Lupus Erythematosus
TARP	Transmembrane AMPAR regulatory protein
TBS	Tetha burst stimulation
TDG	Thiodigalactoside
WT	Wild type

RESUMEN

Galectina-8 pertenece a una familia de proteínas que regulan una variedad de procesos celulares al interactuar con residuos β -galactósidos presentes en las glicoproteínas. Galectina-8 tiene dos dominios de reconocimiento de carbohidratos unidos por una cadena peptídica y es única entre otras galectinas por su alta preferencia por los ácidos siálicos en α -2,3 por su dominio de reconocimiento de carbohidratos N-terminal (N-CRD). En el cerebro, trabajos previos en nuestro laboratorio han demostrado que Galectina-8 tiene funciones inmunosupresoras y neuroprotectoras. Galectina-8 se encuentra en el líquido cefalorraquídeo de los seres humanos y una de sus principales regiones de expresión en el cerebro es el plexo coroideo, la estructura responsable de la generación de líquido cefalorraquídeo. Por tanto, se espera que esta proteína bañe la mayoría de las regiones del cerebro y, en principio, puede contribuir a generar un entorno neuroprotector y quizás modular la función neuronal. Nuestro laboratorio describió autoanticuerpos contra Galectina-8 en varias afecciones inflamatorias, incluyendo pacientes con enfermedades autoinmunes, como el lupus eritematoso sistémico y esclerosis múltiple. Curiosamente, un análisis proteómico de sinaptosomas sugiere que Galectina-8 podría interactuar con los receptores de ácido α -amino-3-hidroxi-5-metil-4-isoxazolpropiónico (AMPA). Este receptor es un receptor glutamatérgico ionotrópico que junto con los receptores de N-metil-D-aspartato (NMDAR) representan los principales receptores ionotrópicos excitatorios en el cerebro. En el hipocampo, AMPAR y NMDAR son abundantes y subyacen la plasticidad sináptica involucrada en la memoria, las emociones y otros procesos cognitivos. Por tanto, proponemos la **hipótesis** de que *“Galectina-8 modula funciones glutamatérgicas que pueden ser interferidas con anticuerpos anti-Galectina-8”*.

Nuestros resultados primero corroboran mediante ensayos de *pull-down* que Galectina-8 se une a AMPAR y esta interacción involucra ácidos siálicos α -2,3 y el N-CRD de Galectina-8. Los ensayos de biotilación e inmunofluorescencia de la superficie celular en cultivo primario neuronal revelan que Galectina-8 aumenta los niveles de AMPAR en la superficie celular en tan solo 1 hora de tratamiento. El mecanismo implica un mayor reciclaje a la superficie celular sin afectar la endocitosis, como lo muestran las imágenes de células vivas de neuronas transfectadas con GluA1 etiquetado con pH-fluorina sensible al pH (GluA1-SEP) y mediante ensayos de biotina reducible, respectivamente. Este efecto requiere la actividad de la proteína quinasa A (PKA), que se sabe que aumenta el reciclaje de AMPAR a la superficie celular, así como la quinasa de adhesión focal (FAK), un efector río abajo de las integrinas. Ni los inhibidores de AMPAR ni de NMDAR afectan el aumento de los niveles de superficie celular de AMPAR mediado por Galectina-8, descartando así un papel de la actividad de estos receptores. Los ensayos de electrofisiología en el circuito hipocampal CA3-CA1 en cortes de cerebro *ex vivo* revelan que Galectina-8 tiene efectos potenciadores o inhibidores sobre la transmisión glutamatergica de AMPAR, a concentraciones bajas o altas, respectivamente. Las concentraciones elevadas de Galectina-8 estimulan la transmisión inhibitoria de los receptores de ácido gamma-aminobutírico tipo A (GABA_AR). Los experimentos en neuronas primarias muestran que Galectina-8 también aumenta los GABA_AR de la superficie celular implicando interacciones mediadas por ácido siálico con glicanos de superficie. El mecanismo sigue siendo desconocido. A continuación, probamos el efecto de el dominio N-CRD de Galectina-8 y los autoanticuerpos anti-Galectina-8 como herramientas para inhibir las funciones de Galectina-8. Curiosamente, el N-CRD de Galectina-8 redujo fuertemente la transmisión sináptica glutamatergica y con los anticuerpos anti-Galectina-8 de pacientes con esclerosis múltiple encontramos una reducción de la potenciación a largo plazo. Estos resultados indican un papel estimulante de la Galectina-8 endógena sobre la transmisión glutamatergica y sugieren que los anticuerpos anti-Galectina-8 podrían desempeñar funciones patogénicas inhibiendo los procesos cognitivos

dependientes de Galectina-8. Apoyando estas posibilidades, encontramos que los ratones carentes de Galectina-8 tienen niveles más bajos de AMPAR en el postsináptico, plasticidad sináptica reducida y memoria espacial deteriorada en comparación con los ratones silvestres.

Además, en esta tesis se incluyen estudios sobre autoanticuerpos contra las proteínas P ribosomales (anti-P) de pacientes con Lupus Eritematoso Sistémico, que se asocian con psicosis y disfunción cognitiva en esta enfermedad autoinmune. Nuestro laboratorio describió que los anticuerpos anti-P reaccionan de forma cruzada con una proteína de función desconocida que expone un epítipo-P en la superficie de la célula neuronal y de alguna manera se requiere en la transmisión glutamatérgica. Como herramienta para estudiar los mecanismos patogénicos de estos anticuerpos, generamos anticuerpos monoclonales de ratones y humanos contra el epítipo-P conocido conformado por una secuencia de 11 residuos (SDEDMGFGLFD) en un esfuerzo de colaboración con la Dra. Betty Diamond (Instituto Feinstein de Investigación Médica, Nueva York, EE. UU.). Los anticuerpos anti-P se obtuvieron de hibridomas murinos y de ADNc clonado individualmente de células B de memoria de un paciente con lupus eritematoso sistémico. Demostramos que estos anticuerpos monoclonales se unen al epítipo-P en ensayos ELISA y perturban la transmisión sináptica, lo que promueve a una mayor caracterización.

En resumen, los principales estudios de esta tesis revelaron que Galectina-8 es un nuevo regulador sináptico de la transmisión glutamatérgica, que puede verse potencialmente interferido por anticuerpos anti-Galectina-8 contribuyendo a disfunciones cognitivas.

ABSTRACT

Galectin-8 belongs to a family of proteins that regulate a variety of cellular processes by interacting with beta-galactoside moieties present in glycoproteins. Galectin-8 has two carbohydrate recognition domains linked by a peptide chain and is unique among other galectins in the high preference for α -2,3 sialic acids of its N-terminal carbohydrate recognition domain (N-CRD). In the brain, previous work in our laboratory has shown that Galectin-8 has immunosuppressor and neuroprotective functions. Galectin-8 is found in the cerebrospinal fluid in humans and one of the major regions of expression in the brain is the choroid plexus, the structure responsible for the generation of cerebrospinal fluid. Thus, this protein is expected to bathe most brain regions and may in principle contribute to generate a neuroprotective environment and perhaps modulate neuronal function. Our laboratory described autoantibodies against Galectin-8 in several inflammatory conditions, including patients with the autoimmune diseases Systemic Lupus Erythematosus and Multiple Sclerosis. Interestingly, a proteomic analysis of synaptosomes suggests that Galectin-8 might interact with α -amino-3-hydroxy-5-methyl-4-isoxazolepropionic acid receptors (AMPA). This receptor is an ionotropic glutamatergic receptor that together with N-methyl-D-aspartate receptors (NMDAR) account for the principal excitatory ionotropic receptors in the brain. In the hippocampus, AMPAR and NMDAR are abundant and underlie synaptic plasticity involved in memory, emotions and other cognitive processes. Therefore, we propose **the hypothesis** that *“Galectin-8 modulates glutamatergic functions that can be interfered with anti-Gal-8 antibodies”*.

Our results first corroborate by pull-down assays that Galectin-8 binds AMPAR and this interaction involves α -2,3 sialic acids and the Galectin-8 N-CRD. Cell surface biotinylation

and immunofluorescence assays in neuronal primary culture reveal that Galectin-8 increases the cell surface levels of AMPAR in just 1 hour treatment. The mechanism involves an enhanced recycling to the cell surface without affecting endocytosis, as shown by live-cell imaging of neurons transfected with pH-sensitive pHluorin-tagged GluA1 (GluA1-SEP) and by reducible biotin assays, respectively. This effect requires the activity of protein kinase A (PKA), known to increase AMPAR recycling to the cell surface, as well as focal adhesion kinase (FAK), a downstream effector of integrins. Neither AMPAR nor NMDAR inhibitors affect the Galectin-8-mediated increase of AMPAR cell surface levels, thus discarding a role of the activity of these receptors. Electrophysiology assays in the CA3-CA1 hippocampal circuit in *ex vivo* brain slices reveal that Galectin-8 has enhancing or inhibitory effects upon AMPAR glutamatergic transmission, at low or high concentrations, respectively. High Galectin-8 concentrations stimulate the inhibitory gamma-aminobutyric acid type A receptors (GABA_AR) transmission. Experiments in primary neurons show that Galectin-8 also augments cell surface GABA_AR involving sialic acid mediated interactions with surface glycans. The mechanism remains unknown. Next we tested the effect of Galectin-8 N-CRD and anti-Galectin-8 autoantibodies as tools to inhibit Galectin-8 functions. Interestingly, Galectin-8 N-CRD strongly reduced glutamatergic synaptic transmission and with anti-Galectin-8 antibodies from Multiple Sclerosis patients we find reduction of long-term potentiation. These results indicate a stimulating role of endogenous Galectin-8 upon glutamatergic transmission and suggest that anti-Galectin-8 antibodies might play pathogenic roles inhibiting Galectin-8-dependent cognitive processes. Supporting these possibilities, we find that Galectin-8 knockout mice have lower AMPAR levels in the postsynaptic, reduced synaptic plasticity and impaired spatial memory compared to wild type mice.

In addition, this thesis includes studies dealing with autoantibodies against ribosomal P proteins (anti-P) from Systemic Lupus Erythematosus patients, which associate with

psychosis and cognitive dysfunction in this autoimmune disease. Our laboratory described that anti-P antibodies cross-react with a protein of unknown function that exposes a P-Epitope at the neuronal cell surface and is somehow required in glutamatergic transmission. As a tool to study the pathogenic mechanisms of these antibodies we generated murine and human monoclonal antibodies against the known P-epitope conformed by a sequence of 11 residues (SDEDMGFGLFD) in a collaborative effort with Dr. Betty Diamond (Feinstein Institute for Medical Research, NY., USA). Anti-P antibodies were obtained from murine hybridomas and from cloned cDNA from single cell memory B cells from a Systemic Lupus Erythematosus patient. We show that these monoclonal antibodies bind to the P-Epitope on ELISA assays and perturb synaptic transmission, thus prompting further characterization.

In summary, the main studies in this thesis revealed Galectin-8 as a new synaptic regulator of glutamatergic transmission, which can be potentially interfered by anti-Galectin-8 antibodies and contribute to cognitive dysfunctions.

1. INTRODUCTION

1.1. Problem Statement

Galectins are a family of proteins that bind carbohydrates (lectins) of glycoproteins and glycolipids and have been involved in a variety of cellular processes and pathogenic conditions (Barake et al., 2020; Johannes et al., 2018). The 15 members of this family of lectins share affinity for β -galactosides through a homologous carbohydrate recognition domain (CRD). In the brain, different galectins have been found to play roles in neuroinflammation (Barake et al., 2020; Siew & Chern, 2018), axon growth, myelination and re-myelination, neurogenesis, neuroprotection and memory (Barake et al., 2020; Chen et al., 2017; de Jong et al., 2019; Imaizumi et al., 2011; Lekishvili et al., 2006; Sakaguchi et al., 2011; Sakaguchi et al., 2007; Sakaguchi et al., 2010). This makes them particularly interesting to study as therapeutic targets in neurologic diseases.

Galectins have redundant complementary or antagonistic functions provided by their distinct preferences for glycan arrangements (Barake et al., 2020; de Jong et al., 2019) and are considered to decode a vast array of glycan structures called the “sugar code” or “glycome”, which varies under physiological and pathogenic conditions (Kaltner et al., 2019). Galectins are synthesized in the cytosol where they establish protein-protein interactions with functions in the cytoplasm and nucleus (Barake et al., 2020). Remarkably, Galectin-3 (Gal-3), Gal-8 and Gal-9 constitute a protection surveillance system that detect damaged endo-lysosomes and mediate their autophagic removal, repair and replacement (Barake et al., 2020). They can also be secreted by unconventional mechanisms and can play complementary or completely different roles (Barake et al., 2020). In the extracellular space,

galectins bind glycans from membrane proteins, extracellular matrix and glycolipids, thus mediating cell signaling, cell adhesion and cell-cell interactions (Barake et al., 2020). Galectins also modulate intracellular trafficking of cell surface proteins (Johannes et al., 2018). In contrast to the classic concept of one ligand one receptor, galectins interact with many glycoproteins at the same time and therefore exert a more global cell regulation (Barake et al., 2020).

Galectins are classified by the number of CRD they possess having the prototypic type one CRD (Gal-1, Gal-2, Gal-5, Gal-7, Gal-10, Gal-11, Gal-13, Gal-14, and Gal-15), the tandem repeat type two, which are linked by a single polypeptide chain of variable length (Gal-4, Gal-6, Gal-8, Gal-9 and Gal-12), and the chimera type, where Gal-3 is the only known member, has one CRD with a collagen-like N-terminal region (Barake et al., 2020). Only Gal-1, Gal-3, Gal-4, Gal-8 and Gal-9 have been found expressed in the brain (Barake et al., 2020). We are interested in the tandem repeat Gal-8, which is unique among other galectins because its N-terminal CRD (N-CRD) has high affinity for terminal α -(2,3)-sialic acid (Cagnoni et al., 2020; Ideo et al., 2011) and our laboratory has described as immunosuppressor and neuroprotective factor that presumably counteracts several damaging agents in the brain (Pardo et al., 2019; Pardo et al., 2017). Analysis in mice have shown that Gal-8 is expressed in different zones of the brain, including the hippocampus, and is particularly expressed at high levels in the choroid plexus, very likely accounting for its presence in the human cerebrospinal fluid (CSF) (Pardo et al., 2019; Pardo et al., 2017). The presence in the choroid plexus and CSF suggests that Gal-8 may be reaching the whole brain. Therefore, it is important to assess whether it has additional roles upon neuronal function.

Interestingly, preliminary proteomic study in our laboratory showed that Gal-8 binds the excitatory glutamatergic α -amino-3-hydroxy-5-methyl-4-isoxazolepropionic acid receptors

AMPA (Table 1). Glutamatergic receptors are main effectors of brain neuronal excitatory synaptic transmission, underlying cognitive processes, including memory, as well as behavior and emotional functions (Citri & Malenka, 2008; Nicoll, 2017; Volk et al., 2015). This system is composed mostly by two postsynaptic ionotropic receptors, namely, the N-methyl-D-aspartate receptors (NMDAR) and the AMPAR (Kessels & Malinow, 2009). The inhibitory counterpart of these excitatory glutamatergic receptors, though not located in the same synapse, are gamma-aminobutyric acid receptors (GABA_AR) (B. Luscher et al., 2011).

Our laboratory has also described function-blocking autoantibodies that neutralize the effects of Gal-8 in several cellular processes (Carcamo et al., 2006; Norambuena et al., 2009; Pardo et al., 2019; Pardo et al., 2017; Vicuña et al., 2013). These antibodies can be found in patients with Systemic Lupus Erythematosus (SLE), Multiple Sclerosis (MS), rheumatoid arthritis and sepsis (Massardo et al., 2009; Pardo et al., 2006; Pardo et al., 2017). We presented evidence that anti-Gal-8 antibodies can be biomarkers of worse prognosis in MS patients, very likely blocking an immunosuppressive function of Gal-8 in the brain (Pardo et al., 2017). Also, the neuroprotective function of Gal-8 is blocked by anti-Gal-8 autoantibodies reducing hippocampal neuron viability in primary culture (Pardo et al., 2019). Autoantibodies have been increasingly recognized as a cause of brain disorders acting as inflammatory agents or directly affecting cellular function by binding cell surface targets (Brimberg et al., 2015; Kello et al., 2019; Zong et al., 2017). The excitatory glutamatergic system has been the most studied target of autoantibodies in diseases such as autoimmune encephalitis, psychosis, epilepsy and SLE (Gardoni et al., 2021; Gibson et al., 2020, Kello, 2019 #4483). In particular, cognitive dysfunction (CD) is relatively common in SLE and MS (Kello et al., 2019; Sumowski et al., 2018) and might be driven by neuropathogenic autoantibodies that affect glutamatergic receptors (Kello et al., 2019). It is possible that Gal-8 could have glutamatergic functions eventually blocked by anti-Gal-8 antibodies, contributing

to CD frequently found in MS and SLE patients. All this adds to the relevance of defining the range of functions that Gal-8 might play in the brain. In this thesis we ask whether Gal-8 has glutamatergic functions that might be blocked by anti-Gal-8 antibodies from autoimmune diseases.

An additional aspect studied in this thesis deals with an autoantibody against ribosomal P proteins (anti-P) originally described to associate with psychosis in SLE patients (Bonfa et al., 1987). These antibodies recognize the P-epitope defined by 11 terminal amino acids (SDEDMGFGLFD) shared by the ribosomal phosphoproteins P0, P1 and P2 (Elkon et al., 1985; Mahler et al., 2003). Our laboratory described that these anti-P antibodies cross-react with a cell surface membrane protein that exposes a P-Epitope to the neuronal cell surface, thus named neuronal surface protein P antigen (NSPA) (Matus et al., 2007). Through NSPA, the anti-P antibodies can induce calcium influx or increase AMPAR and NMDAR currents, with a consequent perturbation of synaptic transmission leading to memory impairment (Bravo-Zehnder et al., 2014; Matus et al., 2007; Segovia-Miranda et al., 2015). Our laboratory has also described that these anti-P antibodies associate with CD in SLE (Massardo et al., 2015). Advances in understanding the neuropathogenic mechanism of anti-P antibodies are usually difficult due to the need of screening large number of SLE patients. We originally proposed to study these mechanisms generating mouse monoclonal antibodies and recombinant human monoclonal antibodies. However, due to technical problems we decided to change the main theme of the thesis to the role of Gal-8 exposed above. The achievements regarding the generation of monoclonal anti-P antibodies as a tool to be used in the future will be presented in the addendum section.

1.2. Literature review

1.2.1. Galectins

Galectins are carbohydrate binding proteins that recognize β -galactosides (N-acetyl-lactosamine (LacNAc), a disaccharide of galactose and N-acetyl-glucosamine (GlcNAc), (Gal β 1-4GlcNAc) (Barake et al., 2020). The 15 members of this protein family have in common the presence of one or two carbohydrate recognition domains (CRD) (Barake et al., 2020). CRDs have variations conferring distinct affinities for different β -galactoside arrangements (density, repeats and branching) or terminal modifications, such as sialic acid and sulfate groups, providing the different galectins with redundant, complementary or antagonistic functions (Barake et al., 2020; de Jong et al., 2019).

1.2.1.1 Galectin-8 (Gal-8)

Gal-8 belongs to the tandem repeat galectins that have an N-terminal and C-terminal CRD linked by a peptide region (Barake et al., 2020; Cagnoni et al., 2020). The N-CRD of Gal-8 has high affinity for sulfated oligosaccharides and sialic acid in α -2,3 configuration, while its C-CRD preferentially binds non-sialylated oligosaccharides (Cagnoni et al., 2020; Ideo et al., 2011), presumably underlying different functions (Cagnoni et al., 2020). In humans, there are three isoforms of Gal-8 protein that vary on their linker length, referred as Gal-8S(small), Gal-8M(medium) and Gal-8L(long). Gal-8M is the most frequent isoform (Cagnoni et al., 2020; Troncoso et al., 2014) thus it is the one we will use here with a linker of 32 amino acids and a molecular weight of 34 kDa (Bidon et al., 2001). Of note, Gal-8L holds a site that can be proteolyzed with thrombin (Nishi et al., 2006). Gal-8 also has protein-protein interactions with the nuclear domain 10 protein 52 (NDP52), actin and K-Ras4B (Cagnoni et al., 2020; Meinohl et al., 2020).

Gal-8 most studied roles are related to cancer (Cagnoni et al., 2020; Troncoso et al., 2014) and the immune system (Tribulatti et al., 2020). In the brain, Gal-8 has an immunomodulatory role ameliorating autoimmune encephalomyelitis by modulating the balance of helper T cell polarization and T regulatory cells (Pardo et al., 2017). Also, Gal-8 is neuroprotective against several damaging agents *in vitro* and *in vivo*, acting through β 1 integrins (Pardo et al., 2019). Gal-8 is expressed in several brain regions including the hippocampus, with the highest levels in the choroid plexus, and accordingly has been detected in CSF (Pardo et al., 2019; Pardo et al., 2017). The presence in the choroid plexus suggests it is secreted to the CSF and bathes the whole brain (Pardo et al., 2017).

1.2.1.2 Anti-Galectin-8 antibodies

Anti-Galectin-8 (anti-Gal-8) antibodies have been described in SLE, MS, rheumatoid arthritis and sepsis (Massardo et al., 2009; Pardo et al., 2006; Pardo et al., 2017). Anti-Gal-8 antibodies from MS and SLE are function-blocking antibodies, as demonstrated by the inhibition of Gal-8 functions in the immune system and as neuroprotector in primary cultured neurons (Carcamo et al., 2006; Norambuena et al., 2009; Pardo et al., 2019; Pardo et al., 2017; Vicuña et al., 2013). So far, the only pathogenic associations found for anti-Gal-8 have been lymphopenia in SLE (Massardo et al., 2009) and worse prognostic in patients with the relapsing-remitting form of MS (Pardo et al., 2017). Assays in murine experimental autoimmune encephalomyelitis (EAE), the preferred model of MS, suggest that Gal-8 has an immunosuppressive role in the brain that might be blocked by autoantibodies (Pardo et al., 2017). Given the variety of functions that Gal-8 might exert interacting with different cell surface glycoproteins, it is very likely that anti-Gal-8 antibodies have other pathogenic roles too. Because SLE and MS patients frequently present cognitive dysfunctions (Filippi et al., 2018; González & Massardo, 2018; Kello et al., 2019; Sumowski et al., 2018), we found it

attractive to explore the role of Gal-8 in the glutamatergic system and a related neuropathogenic role of anti-Gal-8 antibodies.

Our finding of anti-Gal-8 autoantibodies with prognostic potential in MS contribute to evidence for a pathogenic role of autoantibodies in this autoimmune disease, an issue largely debated (Filippi et al., 2018). Although the CSF of MS patients have several autoantibodies, including targets such as myelin and other antigens found in oligodendrocytes, astrocytes and immune cells (Fraussen et al., 2014), a convincing pathologic mechanism is still lacking. Therapies that deplete B cells, antibody producers, do not change their levels in spite of clinical improvement (Filippi et al., 2018; Fraussen et al., 2014). In particular, whether antibodies play roles in the cognitive dysfunction of patients remains unknown, precluding the design of targeted therapies (Sumowski et al., 2018).

1.2.2 Glutamatergic Synapse

Ionotropic AMPAR and NMDAR in the postsynaptic region conform the main excitatory system in the brain, (Nicoll, 2017) and mediate multiple cognitive functions including memory (Volk et al., 2015). Their major neurotransmitter agonist is glutamate, though NMDAR need a co-agonist like glycine or D-serine (Armada-Moreira et al., 2020).

1.2.2.1. AMPA receptors (AMPA)

Structurally, AMPAR are heterotetramers of homologous GluA1, GluA2, GluA3 and GluA4 subunits (Henley & Wilkinson, 2016). GluA4 is almost exclusively present during development, while the majority of adult hippocampal AMPAR are composed by GluA1/GluA2 (80%) and GluA2/GluA3 (20%) (Buonarati et al., 2019; Henley & Wilkinson, 2016). AMPAR mostly conduct Na^{2+} (Purkey & Dell'Acqua, 2020) while the infrequent GluA1 homotetramers are also calcium permeable (Purkey & Dell'Acqua, 2020). GluA subunits have 4 domains exposing the N-terminal domain and the ligand-binding domain to the extracellular media. The transmembrane domain contains the pore and towards the cytosol lies the C-terminal

domain where many posttranslational regulatory modifications occur (Herguedas et al., 2019; Purkey & Dell'Acqua, 2020). Their affinity for glutamate is low and therefore their activation requires close location to the glutamate releasing sites from the presynaptic neuron (Choquet & Hosy, 2020). However, a characteristic of AMPAR is their constant moving into and out the synapses involving lateral diffusion and endocytic trafficking as highly regulated processes (Collingridge et al., 2004; M. Park, 2018). Auxiliary proteins regulate their traffic and function. For instance, the transmembrane AMPAR regulatory protein $\gamma 8$ (TARP $\gamma 8$) anchor them to the scaffold protein postsynaptic density-95 (PSD-95) (Buonarati et al., 2019). Recent studies also involve the N-terminal domain in this entrapment (Díaz-Alonso et al., 2017; Watson et al., 2017).

1.2.2.2. NMDA receptors (NMDAR)

Structurally, NMDAR are heterotetramers of 2 GluN1 mandatory subunits assembled together with 2 GluN2 (A-D) or 2 GluN3 (Paoletti et al., 2013) subunits. Subunits GluN2A and GluN2B predominate at the hippocampus. They are distinctly distributed in the neuron. Although still debated, there is synaptic predominance of GluN2B during development and GluN2A in adulthood (Paoletti et al., 2013). NMDAR are mainly calcium channels that have an extracellular N-terminal and an extensive intracellular C-terminal, which binds many signaling and scaffolding proteins, principally PSD-95, and also undergoes posttranslational modifications that control the receptor activity and trafficking (Paoletti et al., 2013). These receptors have been implicated in survival and apoptotic signaling by calcium excitotoxicity (Armada-Moreira et al., 2020), presumably involving the extrasynaptic GluN2B subunits (Armada-Moreira et al., 2020). In the steady state, fast excitatory synaptic transmission is provided mostly by AMPAR that deliver Na^{2+} into the neuron, while NMDAR have Mg^{2+} blocking their pore (Nicoll, 2017). Under increased activity AMPAR currents depolarize the cell membrane releasing the Mg^{2+} of NMDAR and permitting Ca^{2+} entrance. Therefore,

NMDAR require both glutamate and membrane depolarization from AMPAR to be activated (Nicoll, 2017).

1.2.2.3. Synaptic plasticity

Synaptic plasticity is the process in which synaptic strength is modified principally by changes in the levels of AMPAR at the synapsis (Moretto & Passafaro, 2018; Nicoll, 2017). Under conditions of sustained AMPAR activation, the calcium permeated through NMDAR activates a series of signaling events that can increase or decrease the levels of AMPAR at the cell surface, eliciting the phenomena of long-term potentiation (LTP) or long-term depression (LTD), respectively, also known as Hebbian synaptic plasticity (Buonarati et al., 2019; Moretto & Passafaro, 2018; Nicoll, 2017). Hippocampal LTP and LTD are considered the biologic correlates of learning and memory (Moretto & Passafaro, 2018). There are different forms of LTP and LTD, but the classic one includes differential calcium signaling from NMDAR activation (Moretto & Passafaro, 2018). AMPAR are also involved in another kind of synaptic plasticity called homeostatic plasticity, in response to chronic non-physiologic processes that attempts to restore signaling (Moretto & Passafaro, 2018). For instance, chronic reduced activation increases AMPAR while chronic excessive activation reduces it (Moretto & Passafaro, 2018). Thus, changes in the amount of synaptic AMPAR determine synaptic strength during Hebbian and homeostatic synaptic plasticity (Moretto & Passafaro, 2018).

AMPAR are endocytosed and recycled back to the synaptic membrane by a series of signaling events during LTP induction (Ehlers, 2000). The most studied is calmodulin-dependent protein kinase II (CamKII) activation, which phosphorylates TARP subunits leading to an increased binding to PSD-95 and thus accumulating AMPAR in the synapse (Buonarati et al., 2019; Opazo et al., 2010). Also, protein kinase A (PKA) phosphorylation of GluA1 in Ser845 enhances cell surface delivery of AMPAR from recycling endosomes and

reduces their endocytosis (Buonarati et al., 2019; Diering & Huganir, 2018; Ehlers, 2000). In contrast, during LTD AMPAR are rapidly endocytosed and re-routed to lysosomes for degradation (Diering & Huganir, 2018; Ehlers, 2000; Moretto & Passafaro, 2018).

1.2.2.4. GABA receptors (GABAR)

The principal inhibitory counterpart of glutamatergic receptors are GABA type A receptors (B. Luscher et al., 2011). They are heteropentamers composed of α 1-6, β 1-3, γ 1-3, δ , ϵ , θ , π and ρ 1-3 subunits (B. Luscher et al., 2011). Most frequently, they are found as combinations of 2 α and 2 β with a single γ 2 or δ subunits (B. Luscher et al., 2011). GABA_AR are Cl⁻ channels that upon activation hyperpolarize the neuron through enhanced Cl⁻ entrance, thus inhibiting transmission (Jacob et al., 2008). GABA_AR are responsible for fast GABA actions (Jacob et al., 2008; B. Luscher et al., 2011). The γ 2 subunit is the most common subunit found in synapses and is essential for postsynaptic clustering of GABA_AR (Jacob et al., 2008; B. Luscher et al., 2011). The functional strength of inhibitory synapses is proportional to synaptic GABA_AR levels that are also highly regulated by endocytic trafficking and lateral entrapment, mainly through the intracellular scaffold protein gephyrin (B. Luscher et al., 2011).

1.3. Hypothesis and Objectives

1.3.1. Hypothesis: *“Gal-8 modulates glutamatergic functions that can be interfered with anti-Gal-8 autoantibodies”*

1.3.2. Objectives:

1. To evaluate Gal-8 interaction with glutamatergic receptors of the excitatory system (AMPA and NMDAR).
 - 1.1. To evaluate Gal-8 interaction with AMPAR and NMDAR.
 - 1.2. To evaluate carbohydrate dependency.
 - 1.3. To evaluate involvement of the unique Gal-8 N-CRD.
2. To assess the effect of Gal-8 on the surface levels of these receptors.
 - 2.1. To evaluate if Gal-8 can either increase or decrease neuronal surface levels of these receptors.
 - 2.2. To define potential mechanisms involved.
3. To define functional effects of Gal-8 in glutamatergic functions in the brain.
 - 3.1. To define the effects of Gal-8 on synaptic transmission.
 - 3.2. To evaluate the effects of the N-terminal domain of Gal-8 and anti-Gal-8 autoantibodies isolated from MS patients.
 - 3.3. To assess the consequence of lacking Gal-8 expression on postsynaptic levels of glutamatergic receptors, synaptic plasticity and spatial memory.

ADDENDUM: As the original proposal of this thesis focused on the pathogenic role of autoantibodies directed against ribosomal P proteins (anti-P) that cross-react with NSPA, we include at the end of the present objectives the generation of mice and human anti-P monoclonal antibodies and their effects in glutamatergic transmission, as the work done during an internship abroad of 1.5 years in Dr. Betty Diamond’s laboratory.

2. MATERIALS AND METHODS

2.1. Materials

2.1.1. Animals

Sprague-Dawley rats and mice were housed at the Faculty of Biological Sciences of Pontificia Universidad Católica de Chile. All protocols were approved by the Institutional Animal Care and Use Committee of this facility. All animals were maintained under conditions of strict confinement, which included automatic control of temperature (21°C) and photoperiod (12 h light / 12 h dark) and received water and food *ad libitum*. Lgals8/Lac-Z knock-in (here called Gal-8 KO) mice were generated from C57BL/6NTac mice engineered in Regeneron Pharmaceuticals Inc., New York, using Velocigene technology for replacing the entire coding region of the mouse Lgals8 gene (18,427 bp) with LacZ lox-Ub1-EM7-Neo-lox Cassette containing the LacZ gene that encodes β -galactosidase (Pardo et al., 2019; Pardo et al., 2017). Details of the Lgals8 KO mice and PCR genotyping assay, including the predicted PCR products and the primers, are available at the Velocigene website (www.velocigene.com/komp/detail/14305).

2.1.2. Patients Samples

Blood samples were collected from MS patients and healthy controls according to protocols approved the Faculty of Medicine, Pontificia Universidad Católica de Chile ethics committee with written informed consent from all participants.

2.1.3. Antibodies

Mouse anti-GluN1 (75-272) (1:1,000 dilution), mouse anti-GluN2A (75-288) (1:500 dilution), mouse anti-GluN2B (75-101) (1:1,000 dilution), mouse anti-GluA1 (75-327) (1:1,000 dilution), mouse anti-GluA2 (75-002) (1:1,000 dilution) and mouse anti-PSD95 (75-028)

(1:10,000 dilution) from UC Davis/NIH/NeuroMab Facility (UCLA, Davis, CA, USA). Mouse anti- β -actin (ab6276) (1:10,000 dilution) from Abcam. Rabbit Anti-GABA_AR γ 2 (G0545) (1:500 dilution) from Sigma.

Primary antibodies were recognized with horseradish peroxidase (HRP) conjugated antibodies (Rockland) for western blots (1:5,000 dilution) or with Alexa conjugated antibodies (Molecular Probes) for immunofluorescence (1:500 dilution).

2.1.4. Reagents

Lipofectamine 2000, Opti-MEM medium, Neurobasal medium, penicillin/streptomycin (P/S), B27 supplement, glutamine, Dulbecco's Modified Eagle Medium (DMEM), Isopropyl-1-thio-h-d- galactopyranoside (IPTG) (15529-010), nitrocellulose membrane (88018), fetal bovine serum (FBS) from Invitrogen. Bradford reagent and Affi-10 resin from Bio-Rad. Dimethyl sulfoxide (DMSO) from MERK. Focal Adhesion Kinase inhibitor (FAK inhibitor-14), ampicillin, MESNA (M1511), Iodoacetamide, Thrombin from human plasma (T1063), AP solution in tablets, Poly-L-lysine hydrobromide (P2636) and D -2-Amino-5-phosphonovaleric acid (APV) from Sigma. Protein-G-Sepharose (200209) from GenScript. EZ-Link sulfo NHS-Biotin (21217), EZ-Link Sulfo-NHS-SS-Biotin (cleavable biotin) (21331), Neutravidin-agarose (29201), BCA assay from Thermo. Amicon Ultra 0.5 ml 30,000 Da and Immobilon Forte Western HRP substrate (WBLUF0500) from Millipore. Picrotoxin (PTX) (1128) and 2,3-Dioxo-6-nitro-1,2,3,4-tetrahydrobenzo[f]quinoxaline-7-sulfonamide disodium salt (NBQX) (0373) from Tocris. Thiodigalactoside (TDG), α -2,3-sialyllactose (α -2,3-SL) and α -2,6-sialyllactose (α -2,3-SL) from Carbosynth. Glutathione Sepharose 4 Fast Flow Media from GE.

2.1.5. Plasmid

pCI-SEP-GluR1 was a gift from R. Malinow (Addgene plasmid # 24000; <http://n2t.net/addgene:24000>; RRID: Addgene_24000) and described in (Kopec, 2006).

2.2. Methods

2.2.1. Cellular biology techniques

2.2.1.1. Rat primary Neuronal Culture. Cortex or hippocampus neuronal rat cultures were prepared as previously described (Vargas et al., 2014). E18 pups' cortexes or hippocampi were dissected in ice cold Hanks' Balanced Salt Solution with 5.56 mM glucose, pH 7.4 (HBSS-Glu). The tissue was then incubated with 0.25% trypsin for 15 min in HBSS-Glu at 37°C, afterwards, drops of serum were added and then the tissue was triturated with Pasteur pipettes. Disaggregated cells were pelleted at 1,000 rpm for 1 min and then resuspended in DMEM 10% horse serum 1% P/S and plated in pre-treated plates with 0.1% poly-L-Lysine in 0.1 M borate buffer pH 8.4 and afterwards washed with water. Next day medium was changed to Neurobasal media supplemented with 2 mM glutamine, P/S, B27 supplement and 2 μ M 1- β -D cytosine Arabinoside. Neurons were grown at 37°C in 5% CO₂. Fresh medium was added every 3 days.

2.2.1.2. Cell Surface Biotinylation. 9-11 days in vitro (DIV) cortical neurons plated at 1.5 mill in 6-well plates were treated as indicated in their complete media using 2 wells per condition. When indicated α -2,3-SL or vehicle was preincubated with Gal-8 for 30 min at 37°C before adding to each well. Inhibitors (NBQX, APV, FAKi and H89) or the corresponding vehicle, were added to each well 30 min before Gal-8 treatments. After the indicated treatments, cells were washed once with 1 ml ice cold PBS with 0.1 mM CaCl₂ and 1 mM MgCl₂ (PBS-CM) and incubated with biotin at 0.5 mg/ml in PBS-CM for 40 min at 4°C. Then, cells were washed twice with 100 mM Glycine in PBS-CM and then incubated with the same 2 times for 10 min. Finally, cells were washed once with PBS-CM and frozen at -80°C until processing. Neurons were lysed in lysis buffer with protease inhibitors and spun at 14,000 rpm for 1 minute. Lysates were added to 35 μ l of Neutravidin-agarose previously washed with lysis buffer at 900 g and then incubated for 2 h at 4°C. 5% of the lysate was used for input.

Neutravidin complexes were washed three times with lysis buffer for 5 min and then eluted in sample buffer for western blotting.

2.2.1.3. Neurons Live Immunofluorescence. 16 DIV hippocampal neurons cultured in 12 mm coverslips were treated as indicated, then washed twice with ice cold PBS-CM and incubated at 4°C with anti-GluA1 at 1:30 dilution in PBS-CM for 30 min at 4°C then gently washed and fixed at room temperature (RT) with 4% PFA 4% Sucrose in PBS for 10 min. Cells were permeabilized with 0.2% Triton X-100 in PBS for 10 min then blocked for 30 min in 0.2% blocking buffer then incubated with Phalloidin-488 (1:20) in blocking buffer overnight (ON) at 4°C. Coverslips were washed and incubated with anti-mouse-555 for 30 min at 37°C. Coverslips were washed and mounted in Fluoromont. Images were acquired in a Leica tcs SP8 spectral confocal microscopy (×63 oil immersion objective, 1.4 N.A.) running the LASX Leica software. Area of GluA1 puncta from neurite 50 µm segments were analyzed and quantified with particle analyzer plug-in from Fiji software (Schindelin et al., 2012).

2.2.1.4. Endocytosis assay. 9-11 DIV cortical neurons were plated at 1.5 mill in 6 well plates. 3 wells were used per condition. Cells were washed twice with PBS-CM, saving the media, and then incubated with cleavable biotin (Sulfo-NHS-SS-Biotin) at 0.4 mg/ml for 30 min at 4°C. Cells were washed with 100 mM Glycine in PBS-CM twice then incubated twice for 5 min and then washed 3 times with PBS-CM. 2 conditions were incubated at 4°C, one for total biotinylated and one for total reduced. The rest were incubated at 37°C for 30 min in the saved media with the indicated treatment. Then, cells were washed twice with PBS-CM and incubated, except for total biotinylated, with freshly prepared 22 mM MESNA in reducing buffer for 45 min at 4°C (50 mM Tris-HCl, 100 mM NaCl, pH 8.6). Cells were washed and then alkylated with freshly prepared 20 mM iodoacetamide in PBS-CM for 10 min at 4°C. Finally, cells were washed twice with PBS-CM and frozen at -80°C until neutravidin precipitation and western blotting.

2.2.1.5. Recycling assay. 675,000 hippocampal neurons were plated in 35 mm live cell imaging plates in Neurobasal supplemented with P/S, glutamine and B27. Media was changed the next day and fresh media was added every 3 days. Cells were transfected at 4-5 DIV. Before transfection neuronal media was saved at 37°C and fresh media was added. Two solutions were prepared in 75 µl of Optimem. One had 0.5 µl of Lipofectamine 2000 and the other 0.25 µg of GluA1-SEP plasmid. After 5 min at RT both solutions were mixed, and after 10 min the mix was placed in drops on top of the cells. After 1 h, the media with Lipofectamine/DNA was eliminated, and the saved media was re-added to the cells. At 21 DIV cells were placed in a temperature-controlled recording chamber in 37°C warm recording solution (137 mM NaCl, 5 mM KCl, 2 mM CaCl₂, 1 mM MgCl₂, 20 mM Glucose, 10 mM HEPES, pH 7.4). Transfected neurons were visualized in a Leica tcs SP8 spectral confocal microscopy (×63 oil immersion objective, 1.4 N.A.) running the LASX Leica software. Dendrites were photobleached for 3 x 5 pulses at 100% laser power using the frap booster configuration and then recorded every 5 s. Finally, few drops of HCl were added to the media which corroborated GluA1-SEP surface location by fluorescence quenching. Videos were analyzed offline in the LASX Leica software measuring fluorescence recovery after photobleaching.

2.2.1.6. HEK-293 transfection. 1.9 million cells were plated the day before in 60mm plates in 5% FBS 1% P/S DMEM. For transfection, two solutions were prepared in 190 µl of Opti-MEM. One had 9.5 µl of Lipofectamine 2000 and the other 3.7 µg of GluA1-SEP plasmid. After 5 min at RT both solutions were mixed, and after 10 min both were placed in drops on top of the cells. After 48 h of transfection cells were lysed in lysis buffer (50 mM HEPES pH 7.4, 150 mM NaCl, 1 mM EGTA, 2 mM MgCl₂, 10% Glycerol, 1% Triton X-100), supplemented with protease inhibitors (4 µg/ml leupeptin, 4 mM PMSF, 4 µg/ml pepstatin) centrifuged for 15 min at 12,000 g and the supernatant was used for pull-down experiments.

2.2.2. Biochemical techniques

2.2.2.1. Fusion protein-GST and recombinant protein production. Recombinant proteins and fusion proteins were obtained following previously described procedures (Carcamo et al., 2006). Transformed Bacteria with pGEX-4T-3 (Pharmacia Biotech) plasmid with the desired protein were grown ON in LB supplemented with ampicillin (50-100 µg/ml) (LB-amp) at 37°C in agitation. Then a 1:100 dilution was made also in LB-amp and grown 3-4 h for Gal-8-GST, Gal-8 N-CRD and GST. IPTG was added at 0.1 mM final concentration for 4 h at 37°C. Medium was centrifuged in 250 ml aliquots at 5000 rpm for 10 min, the supernatants were discarded, and the bacterial pellets were frozen at -80°C until further use. Pellets were resuspended in 1 ml of PBS with bacterial antiproteases cocktail concentration at 1 x per 100 ml of initial culture. Lysozyme was added for 30 min at 100 µg/ml on ice. Then, Triton 100x was added at final 1% concentration. The resuspension was sonicated and then incubated for 30 min at 4°C in agitation. Lysates were centrifuged at 12,000 g for 10 min and the supernatants were collected and then incubated with 125 µl Glutation-Sepharose per 250 ml of initial culture previously washed once with water and twice with PBS, for 2 h at 4°C in rotation. Afterwards, the beads were washed at least 5 times with PBS and centrifuged at 500 g. If elution was needed, 1 U of Thrombin was used per 50 µl of beads for 4 h. The beads were centrifuged at 500 g for 5 min and the protein in the eluant was measured with Bradford.

2.2.2.2. Pull-Down assay. Total membrane fractions (P2) of hippocampus and cortex were prepared by homogenizing in ice-cold sucrose buffer containing 0.32 M sucrose, 10 mM Hepes, 3 mM EGTA and protease inhibitors as previously described in (Espinoza et al., 2020). Homogenates were spun twice at 1,000 g for 10 min. The supernatant was collected and spun at 12,000 g for 20 min. The pellet was resuspended in lysis buffer with protease inhibitors. Protein extracts were incubated with GST-Glutation Sepharose column,

for 1 h at 4°C. The beads were centrifuged and then the supernatant was incubated for 2 h at 4°C with Gal-8-GST-Glutation-Sepharose previously incubated for 1 h with the indicated inhibitor or vehicle as described in (Pardo et al., 2019). Beads were then washed 3 times with lysis buffer at 4°C then 3 times at RT for 5 min and eluted with loading buffer for western blot.

2.2.2.3. Co-Immunoprecipitation. 5 µg of anti-GluA1 was incubated ON with 25 µl of Protein G and washed 3 times with lysis buffer. 500 µg of WT or KO hippocampus and cortex P2 extracts, with or without 50 µg of recombinant human Gal-8, were incubated for 2 h at 4°C then washed 6 times with lysis buffer at 4°C. Proteins were eluted in sample buffer and blotted against anti-hGal-8 isolated from MS patients.

2.2.2.4. Antibody purification. The resin for affinity purification was prepared as follows. 1 ml of Affi-10 was washed with 15 ml of distilled water then PBS with centrifugations at 1,000 rpm for 5 min. Then, the resin was incubated with 1 mg of Gal-8 in PBS for 3 h at 4°C then centrifuged and washed with PBS. 1 ml of PBS and 200 µL of ethanolamine/1 M HCl (freshly prepared with 61 µl ethanolamine and 939 µl HCl 1 N) was added for 1 h at 4°C then extensively washed with PBS and stored in 0.05% sodium azide PBS until further use. Before use, the resin was washed extensively with PBS and then, patient serum was incubated at 4°C ON. The resin and sera were centrifuged at 1,000 rpm, serum was recuperated, and the resin was washed extensively with PBS. 10 ml of 0.1-0.2 M Glycine HCl pH 2.5-3 was added and eluates were collected in 400 µL fractions neutralized with 125 µL of 1M K₂HPO₄. The fractions were vortexed and rapidly put on ice. To determine the fractions to be concentrated, 5 µl of each elusion was sampled on a dot blot. Fractions were spun on Amicon Ultra 0.5 ml 30,000 Da at 14,000 g for 5 min. After concentrating the fractions of interest, the buffer was exchanged for PBS 3 times. Concentration was measured with Bradford.

2.2.2.5. Post synaptic Densities (PSD) preparation. Cortex of WT or Gal-8 KO mice were dissected on ice and homogenized in homogenization buffer (0.32 M sucrose, 0.5 mM EGTA, 5 mM Hepes, pH 7.4) supplemented with protease inhibitors using 5 ml of buffer per 1 gr of tissue with a Potter homogenizer as previously described in (Wyneken et al., 2001). Cell debris and nuclei were discarded by centrifuging twice at 1,000 g for 10 min at 4°C recuperating the Homogenate (H) in the supernatant. H was centrifugated at 12,000 g for 20 min at 4°C, the pellet was resuspended in gradient buffer (0.32 M Sucrose, 0.5 mM EGTA, 5 mM Tris, 1 mM DTT, pH 8.1) obtaining the crude membrane fraction (P2). P2 fraction was loaded on top of a first sucrose gradient at 1/1.2 M (1 M Sucrose, 5 mM Tris/1.2 M Sucrose, 5 mM Tris) and centrifuged at 200,000 g for 60 min. All ultracentrifugations were done in an Hitachi Himac CP80WX centrifuge. The synaptosome fraction was collected from the interphase and lysed in lysis buffer (5 mM Tris, 0.5 mM EGTA) for 30 min at 4°C in agitation. The lysate was centrifuged at 33,000 g for 30 min. The pellet was resuspended in gradient buffer obtaining the P2B fraction which was then loaded on a second sucrose gradient at 1/1.2 M and centrifuged 200,000 g for 60 min. Synaptic membranes (P2B2) were collected from the 1/1.2 M interphase and suspended in 0.32 M sucrose, 5 mM Tris and delipidated in equal volume of delipidating buffer (0.32 M sucrose, 0.025 mM CaCl₂, 1% Triton X-100, 2 mM DTT, 10 mM Tris) homogenizing manually. Delipidated synaptic membranes were centrifuged at 33,000 g for 30 min. The pellet was resuspended in 50 mM HepesNa tampon pH 7.4 and centrifuged at 70,000 g for 10 min. The pellet was resuspended in 50 mM HepesNa, 0.15 % SDS, pH 7.4 freshly prepared, yielding the postsynaptic density (PSD) fraction. Protein concentration was determined using the BCA assay. Samples were denatured with loading buffer for western blot.

2.2.2.6. Gel electrophoresis and western blot. Protein samples were resolved in sodium dodecyl sulfate polyacrylamide gel electrophoresis (SDS-PAGE) at different

percentages depending on the protein of interest. Loading buffer contained 100 mM DTT as a reducing agent. After electrophoresis, samples were transferred into a nitrocellulose membrane in 25 mM Tris-HCl, Glycine 192 mM and 20% methanol at 450 mA for 1-2 h depending on the analyzed protein. After transferring, membranes were blocked with PBS-5% skim milk for 1 h at RT. Primary antibodies were incubated ON at 4°C in blocking buffer and then washed five times for 10 min with PBS 0.5% Tween 20. Secondary antibodies conjugated with horseradish peroxidase (HRP) were incubated 1 h in blocking buffer then washed. HRP conjugated antibodies were developed with chemiluminescent HRP substrate following manufacturer's instructions. Chemiluminescent images were acquired in G:Box gene tools detection system (Syngene) with the corresponding filter. Densitometric band analysis was performed with FIJI software (Schindelin et al., 2012).

2.2.3. Animal procedures

2.2.3.1. Electrophysiology. Acute coronal slices from adult wild type male and female mice were prepared and recorded as described in (Oliva & Inestrosa, 2015). Immediately after removal, the brains were placed in ice cold cutting solution (85 mM NaCl, 75 mM Sucrose, 3 mM KCl, 1.25 mM NaH₂PO₄, 25 mM NaHCO₃, 10 mM Glucose, 3.5 mM MgSO₄, 0.5 mM CaCl₂, 3 mM Na-Pyruvate, 0.5 mM Na-Ascorbate, 305 mOsm, pH 7.4) thoroughly oxygenated with 95% O₂/5% CO₂. 350 µm brain slices were obtained and left at 36°C for 30 min for recovery then placed in oxygenated recording solution (126 mM NaCl, 3.5 mM KCl, 1.25 mM NaH₂PO₄, 25 mM NaHCO₃, 10 mM Glucose, 2 mM MgSO₄, 2 mM CaCl₂, 3 mM Na-Pyruvate, 0.5 mM Na-Ascorbate, 305 mOsm, pH 7.4) at RT. For recording, slices were placed in a submerged-style chamber in recording solution at 30-32°C. Schaffer collaterals between CA3 and CA1 were stimulated with a bipolar concentric electrode (World Precision Instruments, Sarasota, FL, United States) connected to an ISO-Flex stimulus generator (A.M.P.I., Jerusalem, Israel). Evoked field excitatory postsynaptic potentials

(fEPSPs) were recorded in the stratum radiatum of CA1, using a borosilicate glass electrode (World Precision Instruments, United States) of 0.5-1 M Ω pulled on a P-97 Flaming/Brown Micropipette Puller (Sutter Instruments, United States) filled with the recording solution. The signals were recorded using a MultiClamp 700B amplifier (Axon CNS, Molecular Devices LLC, United States), and digitally sampled at 30 kHz using a Digidata-1440A interface (Axon CNS, Molecular Devices). Two pulses (R1 and R2) separated 50 ms each, were applied with the stimulus generator every 60 s. The fEPSP slope of the first pulse (R1) was averaged during 15 to 20 min and once a stable basal signal was obtained, the corresponding treatments were added. To evaluate synaptic plasticity in these slices, long-term potentiation (LTP) experiments were performed with a theta burst stimulation (TBS), consistent of 5 bursts at 100 Hz every 20 s. The analyses were done offline using pClamp 10.3 (Molecular Devices LLC, United States). Spontaneous activity in the form of multiunit activity (MUA, spikes) was also recorded. To do that, the signal was band-pass filtered between 2 kHz-300 Hz, digitally sampled at 30 kHz, and analyzed using Spike2 (Cambridge Electronics Design Limited). Spikes were selected using the Wave Mark tool and the templates for detection of different spikes. All the spikes spontaneously generated were counted along the experiments and selected in 7 different classifications by their shape and amplitude. For WT and Gal-8 KO mice the recordings were done as above with the following modifications as described in (Carvajal et al., 2018), briefly, coronal slices were of 400 μ m and after cutting they were recuperated in recording solution at RT for 1 hour. Recordings were done adding picrotoxin (PTX; 50 μ M) to suppress inhibitory GABAR transmission. One pulse (R1) was applied every 15 s and sampled at 4.0 kHz using an A/D converter (National Instrument, Austin, TX, USA), and stored with the WinLTP program. To generate LTP, a high-frequency stimulation (HFS) was used, which consisted of 3 or 4 trains of 100 pulses at 100 Hz of stimuli with an inter-train interval of 20 s.

2.2.3.2. Behavioral tests. 2 to 4-month-old male WT and Gal-8 KO mice were moved from the animal facility to a behavioral suite. Mice were extensively handled in at least 8 sessions (1 or 2 per day) of 5 min each. The open field test was carried out in a 47 x 47 cm arena in a 10 min session per mouse. After at least one day of resting, mice were tested in the Water Maze as in (Vingtdoux et al., 2016; Vorhees & Williams, 2006) but with modifications. In the first phase, mice were launched into a pool of 1 m diameter filled with water around 22°C with a platform of 10 cm diameter above water level with a flag. Each mouse was launched in turns facing the wall of the pool until they found the platform or after they completed 60 s. If they could not find the platform, they were gently directed to it. The mice were left on the platform for 15 s and then dried and returned to their respective cages. The procedure was repeated 4 times per mouse in one day changing the platform quadrant and launching site with no giving sequence. Next day, the flag was removed, and the platform was hidden 1-1.5 cm below surface level. The water was clouded with non-toxic white paint. Signs were placed around the pool and the platform was located in the same position for the next 4 days. Each mouse was launched in turns, in 4 trials per day varying the launching position. The time to reach the platform (latency) was measured. On the fifth day, the probe test was performed. The platform was removed, and the mice were launched once for 30 s. The time they spend on each quadrant was measured off-line. On the reversal phase the platform was located on the opposite quadrant from the previous phase. Each mouse was launched in turns in 4 trials per day for 4 days. On day 5 the probe test was repeated. Data were collected using a video tracking system coupled to Honestech TVR 2.5 program and analyzed off-line in ANY-MAZE software (Stoelting Co, Wood Dale, IL, USA).

2.2.4. Statistical Analysis

Student's t test was used for two-group comparison, and one- or two-way analysis of variance (ANOVA) was used for comparisons of more than two groups with Bonferroni's post-

hoc test, $p < 0.05$ was considered statistically significant higher p values were considered non-significant (ns). All analysis was performed using PRISM software. Data points and error bars in the figures represent mean and standard error of the mean (SEM).

3. RESULTS

3.1. Gal-8 binds AMPAR

To detect possible interactors of Gal-8 in the brain we performed mass spectrometry analysis on Gal-8-GST pulled down proteins from whole brain synaptosomes and identified GluA1, GluA2, GluA3 and GluA4 subunits of the AMPA receptor (Table 1). Therefore, we performed pull-down assays to confirm such interactions. Immunoblots of Gal-8-GST pulled down proteins revealed AMPAR subunits GluA1 and GluA2 but not NMDA receptor subunits GluN1, GluN2A and GluN2B (Fig. 1A). Displacement with Thiodigalactoside (TDG) demonstrated carbohydrate dependent interactions (Fig. 1A). Also, α -(2,3)-Sialyllactose (α -(2,3)SL) inhibited the binding compared to α -(2,6)SL, implying N-terminal Gal-8 carbohydrate specific interaction (Fig. 1B). To test the role of N-terminal domain in the interaction with GluA1 we performed pull-down experiments using recombinant Gal-8 N-Terminal CRD (Gal-8 N-CRD) and analyzed the presence of GluA1. Effectively, we found GluA1 in the pulled down proteins except when α -(2,3)SL was added for displacement (Fig. 1C). These data demonstrate that the N-terminal of Gal-8 binds AMPAR through sialic acid.

The reverse experiments of immunoprecipitating GluA1 showed evidence of an interaction with endogenous Gal-8. The anti-Gal-8 immunoblots showed a band at 34 kDa corresponding to the electrophoretic mobility of Gal-8 in cortex samples from WT but not Gal-8 KO mice (Fig. 1D). We further confirmed the specificity of the Gal-8 detected in the immunoblot by adding recombinant Gal-8 to the anti-GluA1 immunoprecipitation assay, which showed the expected increased band in the immunoblot (Fig. 1D). These results indicate that just a proportion of AMPAR interacts with endogenous Gal-8, as suggested by the increased

amount of Gal-8 that co-immunoprecipitated with GluA1 when we added an excess recombinant Gal-8.

All these results indicate that Gal-8 interacts with AMPAR and whether this interaction has a functional meaning is studied below.

Table 1: Gal-8 interactors. Identification of proteins from a pull-down assay with Gal-8-GST by Mass Spec analysis. Possible interactors were analyzed from 4 bands of the indicated molecular weight which are listed by accession number. In blue AMPA receptor subunits.

Band of 17 kDa		Band of 26 kDa		Band of 31 kDa		Band of 95-100 kDa	
GSTM1_RAT	K1C19_RAT	VDAC1_RAT	TBB5_RAT	ADT1_RAT	TPM3_RAT	AT1A3_RAT	LEG8_RAT
SNP25_RAT	K2C7_RAT	BDH_RAT	LRP2_RAT	ADT2_RAT	ACTC_RAT	AT1A1_RAT	SORT_RAT
GSTM4_RAT	TRY1_RAT	ATPG_RAT	CH076_RAT	PHB_RAT	SYPH_RAT	AT1A2_RAT	K2C1B_RAT
GSTM5_RAT	K1C17_RAT	VDAC2_RAT	OSBL1_RAT	1433Z_RAT	RTN3_RAT	SV2A_RAT	KCNA4_RAT
RAB3C_RAT	DYHC_RAT	MPCP_RAT	K2C4_RAT	MOG_RAT	K1C14_RAT	DLG4_RAT	BSN_RAT
RAB3A_RAT	K1C42_RAT	C1QBP_RAT	PDS5B_RAT	K1C10_RAT	NPTXR_RAT	CD166_RAT	GRIA4_RAT
MOG_RAT	LIN7B_RAT	K1C10_RAT	ACON_RAT	GSTA3_RAT	DHSB_RAT	SV2B_RAT	KCNA6_RAT
RAB3D_RAT	RAB21_RAT	K2C1_RAT	CC130_RAT	K2C1_RAT	DDR1_RAT	AT1A4_RAT	DLG2_RAT
GSTM2_RAT	K1C14_RAT	NB5R1_RAT	CCD80_RAT	VAPA_RAT	LPHN3_RAT	MAG_RAT	S4A4_RAT
K1C10_RAT	CPT1B_RAT	GHC2_RAT	RBM43_RAT	SNG1_RAT	FTHFD_RAT	DPP10_RAT	CALX_RAT
GSTA3_RAT	NPTXR_RAT	K2C6A_RAT	GFAP_RAT	LEG8_RAT	GPSN2_RAT	ATP4A_RAT	DYHC_RAT
RALA_RAT	ITPR2_RAT	PRIO_RAT	MBP_RAT	K2C6A_RAT	PRIO_RAT	AP2A2_RAT	ITPR3_RAT
RAB3B_RAT	APOB_RAT	K2C5_RAT	LTBP2_RAT	RAB12_RAT	MYO5A_RAT	NLGN2_RAT	PDE2A_RAT
NDUV2_RAT	UN13B_RAT	ACTG_RAT	UGDH_RAT	K2C5_RAT	TRY1_RAT	LRC8A_RAT	S6A11_RAT
RAB14_RAT	RTN3_RAT	LEG8_RAT	KPRP_RAT	GSTA5_RAT	ERC2_RAT	AT12A_RAT	DBC1_RAT
RAB8A_RAT	SMBT1_RAT	AT1A3_RAT	CENG1_RAT	1433G_RAT	APBA3_RAT	4F2_RAT	KCNC2_RAT
CB047_RAT	HXK1_RAT	CLUS_RAT	CAPZB_RAT	1433F_RAT	K2C7_RAT	S6A17_RAT	MELT_RAT
TPIS_RAT	PLEC1_RAT	EAA1_RAT	AT1B1_RAT	AT1A3_RAT	DYHC_RAT	CTNB1_RAT	KCNA3_RAT
K2C6A_RAT	CAC1H_RAT	VDAC3_RAT	SMBT1_RAT	DNJC5_RAT	ZFR_RAT	SHPS1_RAT	AT2A1_RAT
K2C5_RAT	SNG1_RAT	STX1A_RAT	KIF1B_RAT	M2OM_RAT	SNIP_RAT	NLGN3_RAT	CAC1H_RAT
GSTA6_RAT	DDR1_RAT	DYHC_RAT	K22E_RAT	RAB3D_RAT	DNJB6_RAT	K1C10_RAT	AT1B1_RAT
K2C1_RAT	CSPG4_RAT	MAP1B_RAT	MYST3_RAT	RAB35_RAT	ITSN1_RAT	EAA1_RAT	SPEG_RAT
VDAC1_RAT	CA142_RAT	TRY1_RAT	CE037_RAT	LIN7C_RAT	CAD23_RAT	GRIA2_RAT	UBIQ_RAT
HCD2_RAT	K22E_RAT	ETBR2_RAT	SURF1_RAT	RAB14_RAT	ABCA2_RAT	NLGN1_RAT	TRY1_RAT
AT1A3_RAT	SPTA2_RAT	DHB12_RAT	UD2A1_RAT	1433T_RAT	TSKS_RAT	K2C6A_RAT	ACTN4_RAT
CSK2B_RAT	MYH9_RAT	TBA1A_RAT	WDR7_RAT	1433B_RAT	CENPT_RAT	PLEC1_RAT	LRC8E_RAT
K2C1B_RAT	GFAP_RAT	AT1A1_RAT	FBX6_RAT	RAB15_RAT	PCSK5_RAT	K2C1_RAT	PDZD2_RAT
LEG8_RAT	ITPR3_RAT	K2C8_RAT	ABCC8_RAT	PLEC1_RAT	MYOG_RAT	NCAM1_RAT	GUC2E_RAT
RAB1B_RAT	TAOK2_RAT	PGAM5_RAT	SPTN2_RAT	MPCP_RAT	SMBT1_RAT	K2C5_RAT	CAC1B_RAT
RAB4A_RAT	RB6I2_RAT	PLEC1_RAT	ESR2_RAT	GSTA4_RAT	DNSL1_RAT	KCNA2_RAT	CAC1A_RAT
K2C8_RAT	MPCP_RAT	TBA1C_RAT	ITPR3_RAT	COQ5_RAT	SPEG_RAT	GRIA1_RAT	FAS_RAT
RAB4B_RAT	ROCK2_RAT	NB5R3_RAT	TBA8_RAT	SYT1_RAT	WNK4_RAT	AP2B1_RAT	AT2B1_RAT
RAB15_RAT	PLCB3_RAT	DDR1_RAT	CSPG2_RAT	AT1B1_RAT	DHX30_RAT	ACTN1_RAT	DISC1_RAT
K2C4_RAT	CHIN_RAT	CAD23_RAT	UN13B_RAT	K2C4_RAT	GPR37_RAT	DLG1_RAT	DDX4_RAT
K1C15_RAT	ADCK3_RAT	K2C7_RAT	FACD2_RAT	K2C8_RAT	K1C17_RAT	GRIA3_RAT	IGS10_RAT
K1C13_RAT	PPM1H_RAT	DUOX2_RAT	RGS9_RAT	APOD_RAT	NMD3A_RAT	A4_RAT	KCNA5_RAT
ADT1_RAT	MYH11_RAT	CO4_RAT	CELR3_RAT	VAPB_RAT	PCDH3_RAT	SL9A1_RAT	DPP6_RAT
EAA1_RAT	ADT2_RAT	VATE1_RAT	SYT2_RAT	ITPR3_RAT	LKAP_RAT	SCAM5_RAT	DCMC_RAT
LIN7A_RAT	CD166_RAT	ITPR2_RAT	ZFR_RAT	AT1A1_RAT	TBA1B_RAT	LRC8C_RAT	KCNH2_RAT
LIN7C_RAT	AT1B1_RAT	ACSL1_RAT	ADT1_RAT	K1C42_RAT	TTLL1_RAT	GSTM5_RAT	AT2B4_RAT

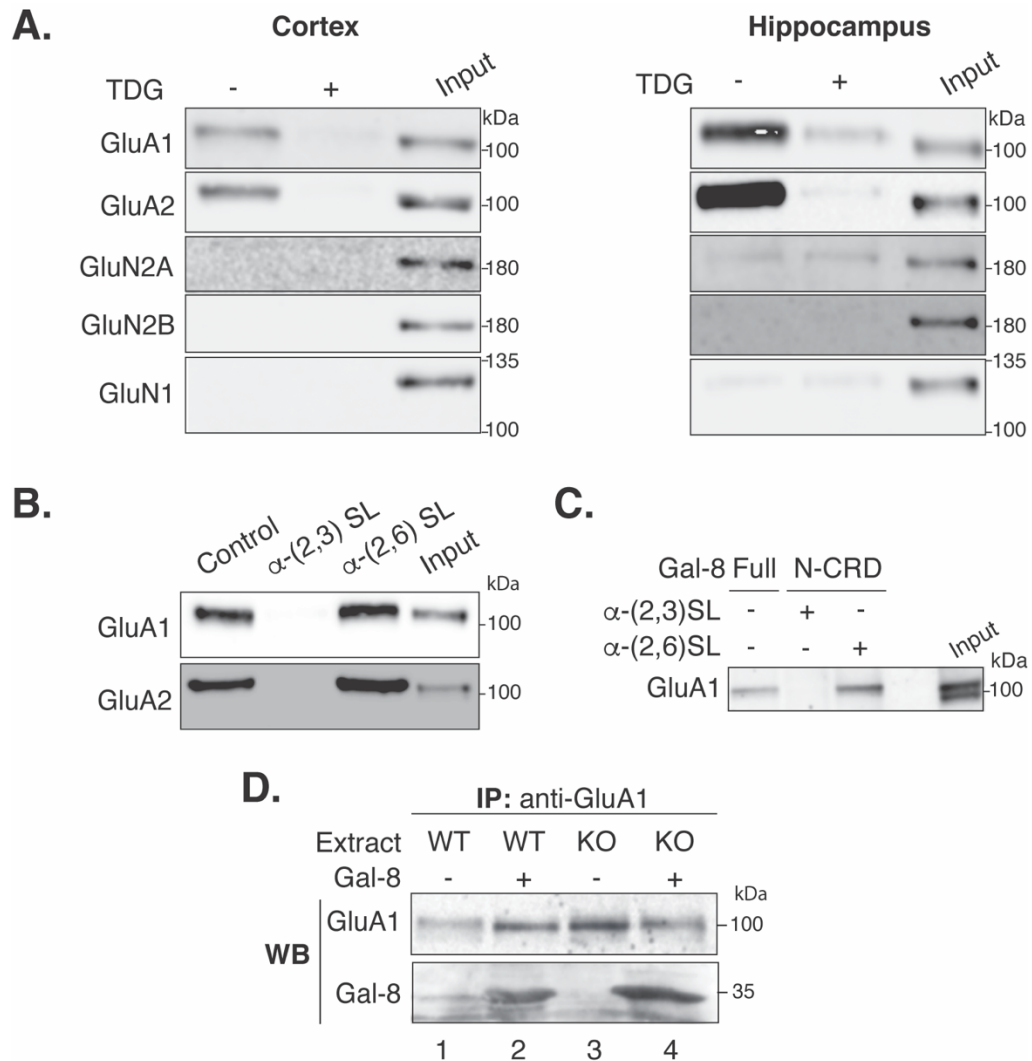


Figure 1: Gal-8 interacts through its sialic acid-binding (N-CRD) domain with AMPAR but not NMDAR subunits in the brain. **A.** Gal-8 interaction with AMPAR. Immunoblot of proteins pulled down by Gal-8-GST-GS from mouse cortex and hippocampus show interaction with AMPAR through β -galactosides, confirmed by TDG inhibition (20 mM) (n=3 for Cortex and n=4 for Hippocampus). **B.** Interaction of Gal-8 with GluA1 and GluA2 involves α -(2,3)-sialic acid. GluA1 and GluA2 pulled down by Gal-8-GST-GS is completely displaced by α -(2,3)-Sialyllactose (α -(2,3)SL; 10 mM) but not α -(2,6)SL (10 mM) (n=3). **C.** Gal-8 N-CRD binds AMPAR in an α -(2,3)-sialic acid-dependent manner. N-CRD-GST-GS pulled down GluA1 and this was displaced by α -(2,3)SL (10 mM) (n=2). **D.** Endogenous brain Gal-8 interacts with AMPAR. Anti-GluA1 antibodies co-immunoprecipitated Gal-8, as shown by the 34 kDa band in the immunoblot from WT (lane 1) but not Gal-8 KO mice (lane 3), as well as in the positive control of recombinant Gal-8 (50 μ g/ml) added to WT (lane 2) and KO (lane 4) extracts (n=1).

3.2. Gal-8 increases AMPAR levels on the cell surface

The function of AMPAR crucially depends on its neuronal surface levels, which in turn relays on strict control of their trafficking along endocytic and recycling routes (Collingridge et al., 2004; M. Park, 2018). Endocytic and exocytic trafficking of certain glycoproteins can be sensitive to interactions with galectins, impacting upon their cell surface levels (Johannes et al., 2018). An initial approach to examine whether Gal-8 interaction with AMPAR has functional consequences, was to analyze the levels of these glycoproteins at the surface of neurons in primary culture. A well-established cell surface biotinylation assay (Arancibia-Cárcamo et al., 2006) showed that Gal-8 (50 $\mu\text{g/ml}$) treatment for 4 hours increased the levels of GluA1 at the cell surface (Fig. 2A). As expected for an effect that depends on Gal-8 binding to terminal sialic acid, α -(2,3)SL abrogated this Gal-8-induced appearance of AMPAR at the cell surface (Fig. 2A), similar to the displacement observed in pull-down assays. We next analyzed the time at which this effect can be detected. Within 60 min of Gal-8 treatment we could observe the increased levels of GluA1 at the cell surface without changes in AMPAR total levels (Fig. 2B). Then we tested if lower concentrations could increase surface levels of AMPAR. No significant effects occurred within 1 h for Gal-8 treatments between 0.05 to 10 $\mu\text{g/ml}$ concentrations (Fig. 2C)

Likewise, the cell surface levels of GluA2 subunit of AMPAR also increased within an hour of Gal-8 treatment (Fig. 3A), whereas Gal-8 did not induce neuronal surface increments of GluN2B levels (Fig. 3B). To approach the effect of Gal-8 using a complementary technique we took advantage of an available antibody that recognizes an extracellular epitope in GluA1 and performed live cell immunofluorescence analysis. Gal-8 treatment for just 1 h increased the neuronal surface fluorescent pattern reflecting on GluA1 higher size of puncta in dendrites, which imply possible functional consequences on synaptic transmission (Fig. 4). These

results suggest that Gal-8 somehow selectively increases the presence of AMPAR at the neuronal cell surface.

Overall, these results indicate that Gal-8 interacts with AMPAR through the N-CRD and increases its cell surface presence.

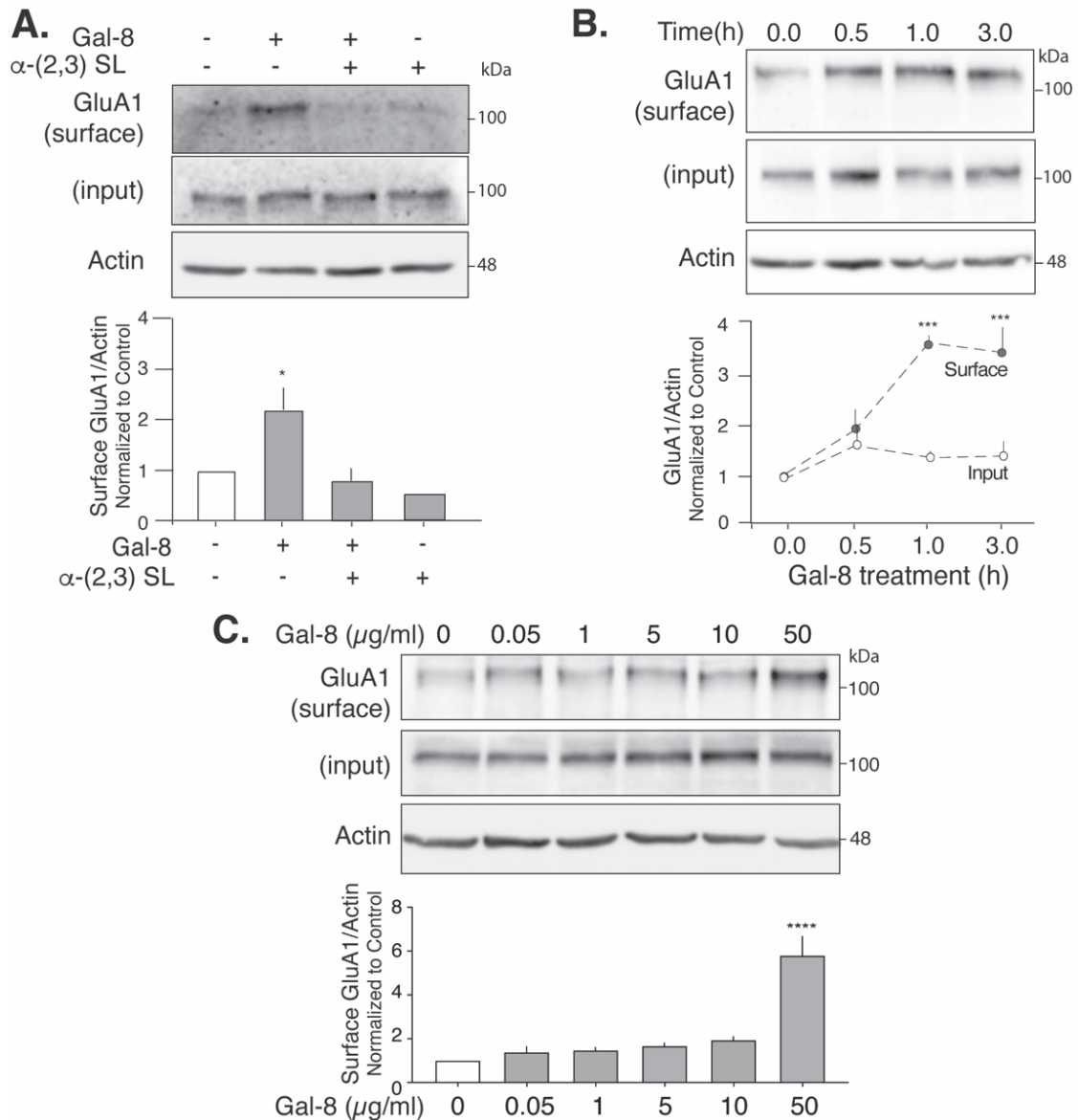


Figure 2: Gal-8 increases the levels of GluA1 at the neuronal surface. Cell surface biotinylation assays in primary neuronal rat cultured cells **A**. Gal-8 increases AMPAR depending on sialic acid. Neurons treated for 4 hours with Gal-8 (50 μ g/ml) show higher levels of AMPAR at the cell surface except when neurons are co-incubated with α -(2,3)-SL (10 mM). (n=3; Graph shows mean and SEM of densitometric band analysis of Surface GluA1/Actin normalized to control; ANOVA $p^* < 0.05$). **B**. Temporal analysis. Cell surface GluA1 levels increases reach a plateau after 1 h treatment with Gal-8. Input GluA1 levels remained unchanged (n=3; Graph shows mean and SEM of densitometric band analysis of Surface or Input GluA1/Actin normalized to control; ANOVA $p^{***} < 0.001$). **C**. Concentration analysis. Lower concentrations of Gal-8 (0.05-10 μ g/ml) for 1 h did not increase GluA1 at the cell surface (n=4; Surface GluA1/Actin normalized to control; ANOVA $p^{****} < 0.0001$).

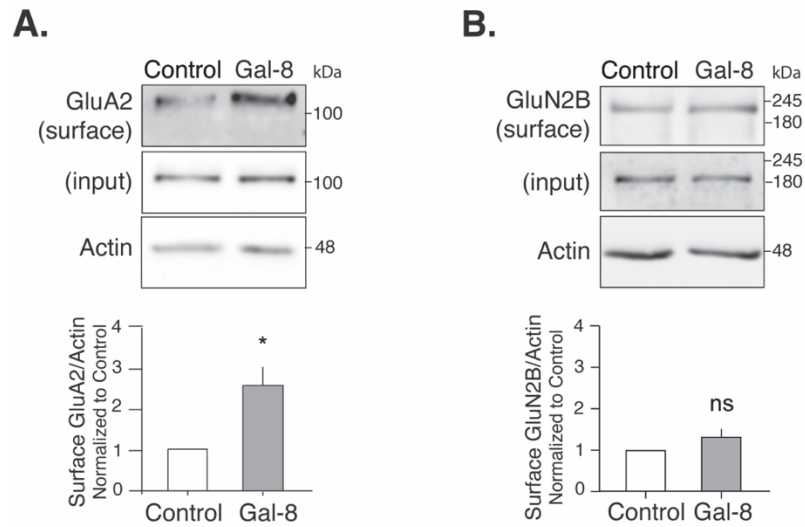


Figure 3: Gal-8 increases the neuronal surface levels of GluA2 but not GluN2B. Surface biotinylation analysis of GluA2 and GluN2B levels after 1 h treatment with Gal-8 (50 $\mu\text{g/ml}$) in primary neuronal rat culture. Gal-8 increases GluA2 subunit at the cell surface (n=3; Graph shows mean and SEM of densitometric band analysis of Surface GluA2/Actin normalized to control; t-test $p^* < 0.05$) (**A**). NMDAR GluN2B subunit levels are not affected by Gal-8 treatment (n=3; Graph shows mean and SEM of densitometric band analysis of Surface GluN2B/Actin normalized to control; t-test) (**B**).

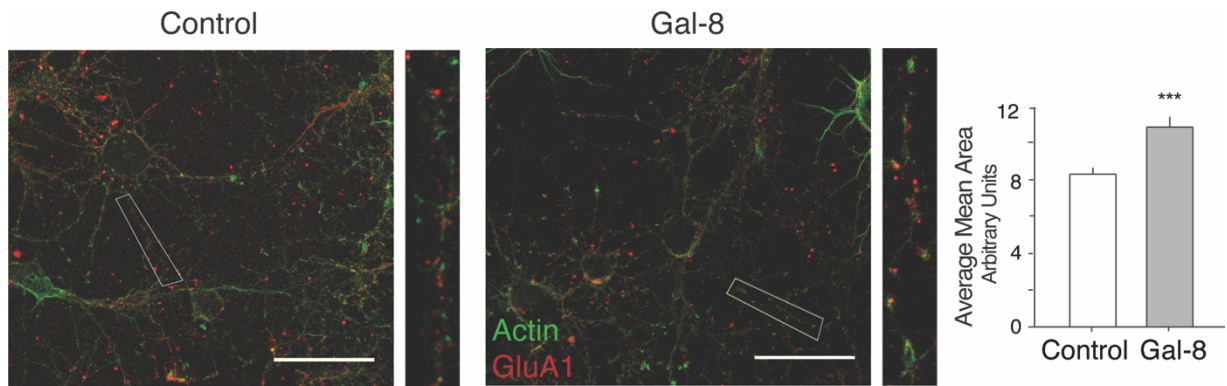


Figure 4: Gal-8 increases the levels of GluA1 at dendrites. GluA1 levels in live neurons. Hippocampal cultured neurons treated with Gal-8 (50 $\mu\text{g}/\text{ml}$) for 1 hour were incubated with anti-GluA1 at 4°C and then were fixed, permeabilized and analyzed by immunofluorescence. Inset exemplifies an analyzed area. Graph shows increased area of GluA1 puncta in dendrites of Gal-8 treated cells. Scale bar and ROI: 50 μm . (n=3; Graph shows mean and SEM of GluA1 puncta area; t-test $p^{***}<0.001$).

3.3. Gal-8 increases recycling of AMPAR to the cell surface

We focused the next experiments on the mechanism by which Gal-8 increases AMPAR levels. We first studied potential effects upon protein trafficking, which has been described for other galectins (Johannes et al., 2018). AMPAR is constantly endocytosed and recycled to the cell surface (Moretto & Passafaro, 2018). Thus, in principle, Gal-8 might increase AMPAR levels at the cell surface by inhibiting endocytosis or enhancing their recycling to the cell surface. To assess endocytosis, we used the widely described assay of labeling surface proteins with cleavable biotin reagent (Sulfo-NHS-SS-Biotin), which once internalized becomes resistant to a non-cell permeable reducing agent (Arancibia-Cárcamo et al., 2006). Unexpectedly, this approach revealed that Gal-8 increases endocytosed AMPAR (Fig. 5A). Therefore, Gal-8 is very likely promoting AMPAR endocytosis and recycling from internal compartments resulting in a positive balance towards a higher AMPAR residence at the cell surface. To approach this possibility, we used pH-sensitive pHluorin-tagged GluA1 (GluA1-SEP) that emits fluorescence at the surface and not in acidic endosomal compartments (Kopec, 2006), allowing the elimination of fluorescent emission from the cell surface by selective photobleaching. Afterwards, reappearance of fluorescence signal reflects exocytosis of internal GluA1-SEP or lateral diffusion (Hildick et al., 2012; Petrini et al., 2009; Roth et al., 2017). We first confirmed that Gal-8 binds this recombinant receptor, as shown by pull-down assays in GluA1-SEP transfected HEK-293 cells (Fig. 5B). Interestingly, under Gal-8 treatment, photobleached neuronal dendrites showed not only faster fluorescence recovery compared with control and Gal-8 co-incubated with α -(2,3)SL (Fig. 5C), but also an oscillatory fluorescence pattern at later times (Fig. 5C). This oscillating behavior is difficult to explain but the faster recovery very likely indicates faster recycling from endocytic compartments.

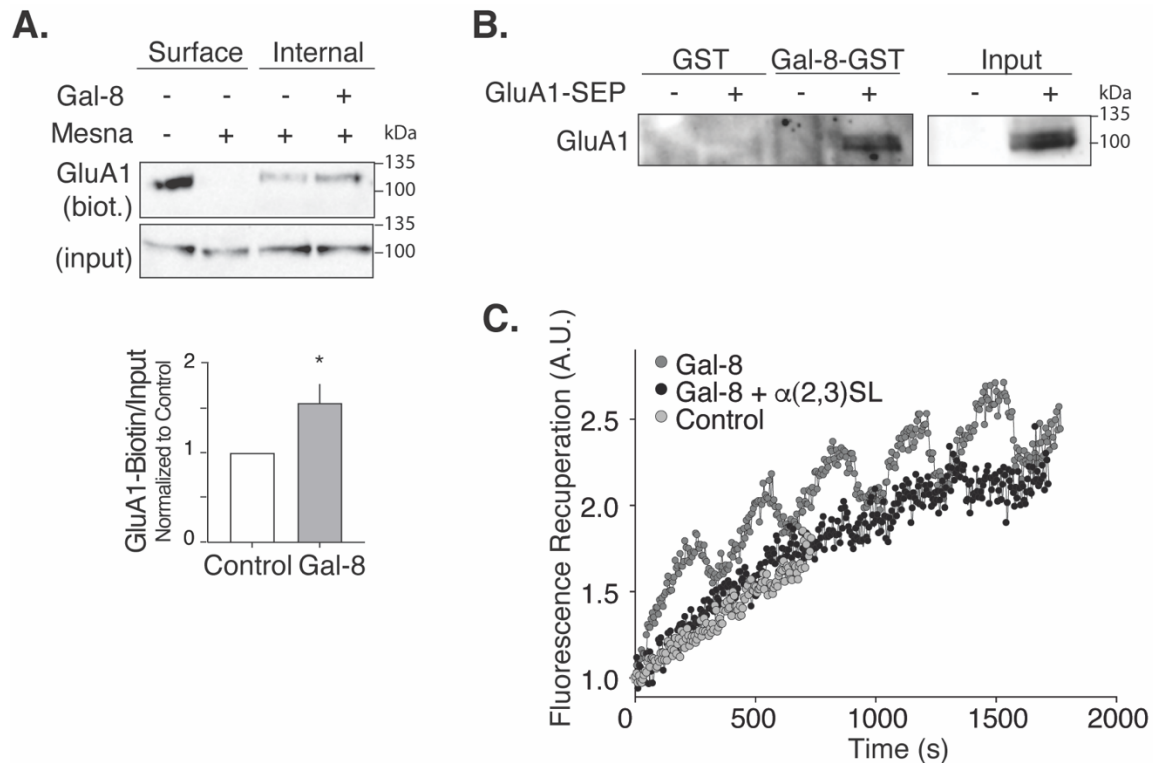


Figure 5: Gal-8 enhances GluA1 endocytosis and recycling to the surface. A. Gal-8 increases GluA1 endocytosis. Neurons were cell surface biotinylated with the reducible reagent sulfo-NSH-SS-biotin at 4°C and then incubated for 30 min at 37°C in the absence or presence of Gal-8 (50 µg/ml). Biotinylated GluA1 (GluA1-Biotin) remaining after cell surface reduction with Mesna reflects internalized protein. Graph shows an increased internalization of GluA1 after Gal-8 treatment (n=4; Graph shows mean and SEM of densitometric band analysis of GluA1-Biotin/Input normalized to control; t-test $p^* < 0.05$). **B.** Gal-8 binds recombinant pH-sensitive pHluorin-tagged GluA1 receptor (GluA1-SEP). Lysates of HEK-293 cells transfected or not with GluA1-SEP were incubated with either GST-GS or Gal-8-GST. Gal-8-GST pulled down GluA1-SEP (n=3). **C.** Gal-8 increases GluA1 recycling to the cell surface. Cultured hippocampal neurons were transfected with GluA1-SEP that emits fluorescence only at the neuronal surface. Fluorescence recuperation after photobleaching, which reflects exocytosis of GluA1-SEP from internal compartments, was faster under Gal-8 (50 µg/ml) treatment and then dropped and recovered cyclically every 300 s. Co-incubation with α -(2,3)SL (10 mM) abrogated this Gal-8 effect (n=2; Graph shows mean and SEM of fluorescence recuperation normalized to fluorescence after photobleaching 2 neurons for each condition of representative experiment).

3.4. PKA and FAK pathways are involved in Gal-8 effects on AMPAR levels at the neuronal surface

The most known mechanism leading to an increase of AMPAR at the cell surface underlying long-term potentiation, involves NMDAR activity that triggers signaling pathways towards vesicular trafficking (Nicoll, 2017). NMDAR become activated when the activity of AMPAR is enough to depolarize the membrane, causing the release of a magnesium plug in the interior of the NMDAR ionic channel. Therefore, membrane depolarization and glutamate stimulation acting together leads to NMDAR activation (Nicoll, 2017). To test whether Gal-8 activates this mechanism we used AMPAR and NMDAR inhibitors, 2,3-dioxo-6-nitro-7-sulfamoyl-benzo[f]quinoxaline (NBQX) (Fig. 6A) and D-2-amino-5-phosphonovalerate (APV) (Fig. 6B) respectively, and found that none of these inhibitors affected the Gal-8-induced AMPAR increase at the cell surface (Fig. 6A and 6B). Therefore, Gal-8 is triggering another mechanism independent of AMPAR and NMDAR activation.

AMPAR recycling from endosomal compartments to the cell surface during LTP is controlled by several signaling pathways, including PKA activity downstream of NMDAR (Ehlers, 2000; Esteban et al., 2003). Interestingly, even when inhibition of NMDAR had no effect, the inhibition of PKA with H89 abrogated the increment of AMPAR induced by Gal-8 (Fig. 6C). It is possible that Gal-8 is somehow increasing the PKA activity involved in AMPAR recycling.

On the other hand, considering our previous findings of Gal-8 interaction with $\beta 1$ integrins in several cellular systems (Carcamo et al., 2006; Hadari et al., 2000; Oyanadel et al., 2018) including neurons (Pardo et al., 2019), we analyzed the role of FAK as an integrin downstream element, which we have shown to become activated by Gal-8 (Levy et al., 2001; Oyanadel et al., 2018; Smith et al., 2020; Zamorano et al., 2019). Unexpectedly, FAK inhibition with FAKi also annulled the Gal-8 induced AMPAR cell surface increment (Fig. 6C).

All these results indicate that Gal-8 induces AMPAR appearance at the cell surface promoting its recycling from internal compartments involving PKA and FAK dependent pathways.

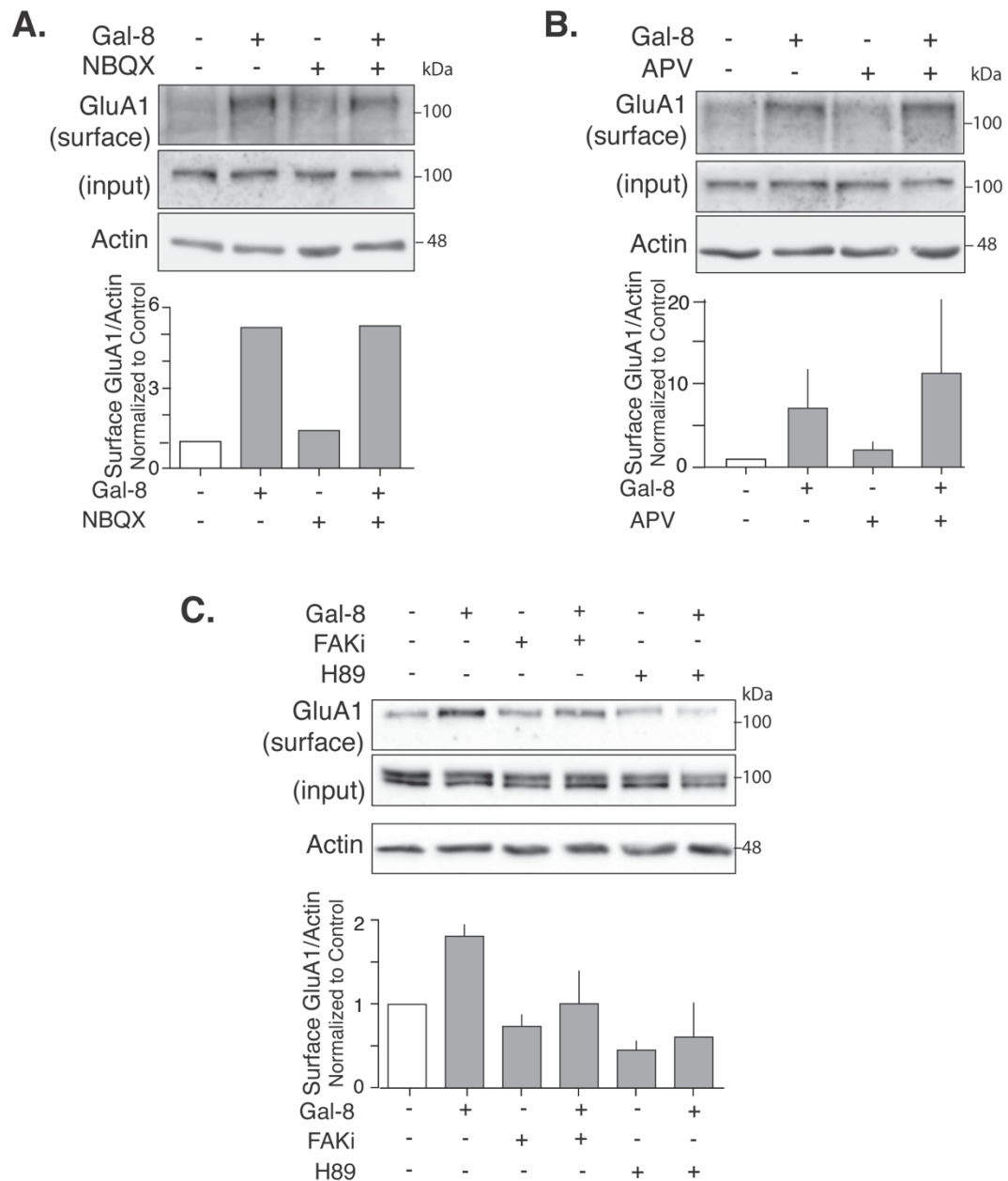


Figure 6: Gal-8 increases GluA1 levels at the cell surface involving FAK and PKA activity. Surface biotinylation followed by immunoblot of cultured rat neuronal cells show the levels of GluA1 after Gal-8 (50 μ g/ml) treatment in different conditions. **A** and **B**. GluA1 cell surface levels increase after 1 h Gal-8 treatment are not affected by AMPAR inhibition with NBQX (10 μ M) (n=1) (**A**) or NMDAR inhibition with APV (50 μ M) (n=2) (**B**) (Graph shows mean and SEM of densitometric band analysis of Surface GluA1/Actin normalized to control). **C**. Inhibitors of Focal Adhesion Kinase (FAKi; 5 μ M) and PKA (H89; 20 μ M) abrogate the cell surface increase of GluA1 induced by 1h Gal-8 treatment (n=2; Graph shows mean and SEM of densitometric band analysis of Surface GluA1/Actin normalized to control).

3.5. Gal-8 enhances or inhibits glutamatergic synaptic transmission depending on its concentration

Our previous experiments suggested that Gal-8 might play a role in glutamatergic transmission through the excitatory AMPAR. Therefore, we performed electrophysiological experiments adding exogenous Gal-8 in *ex vivo* brain slices. We first analyzed multiunit activity (MUA) recordings (i.e. extracellular spikes) in hippocampal slices and found that Gal-8 at 0.1 $\mu\text{g/ml}$ concentration augments mostly spontaneous excitatory action potentials (Fig. 7). Unexpectedly, at higher concentrations of 1-10 $\mu\text{g/ml}$, Gal-8 first interchanged excitatory for inhibitory transmission (Fig. 7). Next, we analyzed field excitatory post-synaptic potentials (fEPSP) in the CA3-CA1 circuit under different Gal-8 concentrations. Also, at low Gal-8 (0.1 $\mu\text{g/ml}$) concentrations, transmission was increased, and it decreased at higher (1 or 10 $\mu\text{g/ml}$) (Fig. 8). To evaluate whether this effect involved a presynaptic component we assessed the dynamics of pair pulse facilitation (PPF) by plotting the ratio of the second (R2) versus the first (R1) fEPSP slopes. The invariable paired pulse ratio (R2/R1 ratio) indicated that this effect did not involve a presynaptic contribution (Fig. 8). Overall, these results indicate that Gal-8 can increase or decrease synaptic transmission depending on its concentration.

The inhibitory effect of high concentrations of Gal-8 upon synaptic transmission might be due to reduction of excitatory transmission or to a superposed inhibitory GABA_AR activity. To test these possibilities, we blocked GABA_AR activity with Picrotoxin (PTX) and found a recovered synaptic transmission at 10 $\mu\text{g/ml}$ Gal-8 concentration, which increased even higher than the response elicited by 0.1 $\mu\text{g/ml}$ (Fig. 9A). We also added the AMPAR inhibitor NBQX that completely inhibited synaptic transmission confirming transmission through AMPAR (Fig. 9A). These results indicate that high concentrations of Gal-8 increase GABA_AR activity and shield the concomitant increase in AMPAR activity.

We then assessed cell surface levels of GABA_AR γ 2 subunit, that correspond to the subunit present primarily at synaptic locations (B. Luscher et al., 2011). Primary cultured neurons treated with Gal-8 (50 μ g/ml) for 1 h showed increased cell surface GABA_AR γ 2 subunit levels (Fig. 9B). Similar to AMPAR, pull-down assays showed that Gal-8-GST, and specifically Gal-8 N-CRD-GST, interacts with GABA_AR γ 2 subunit (Fig. 9C). Displacement with α -(2,3)SL but not α -(2,6)SL indicates that such interaction depends on the binding of N-terminal Gal-8 domain to sialic acids (Fig. 9C). All these results indicate that Gal-8 interacts with both AMPAR and GABAR and increases their cell surface presence. This implicates Gal-8 in opposed functions upon glutamatergic transmission at different concentrations.

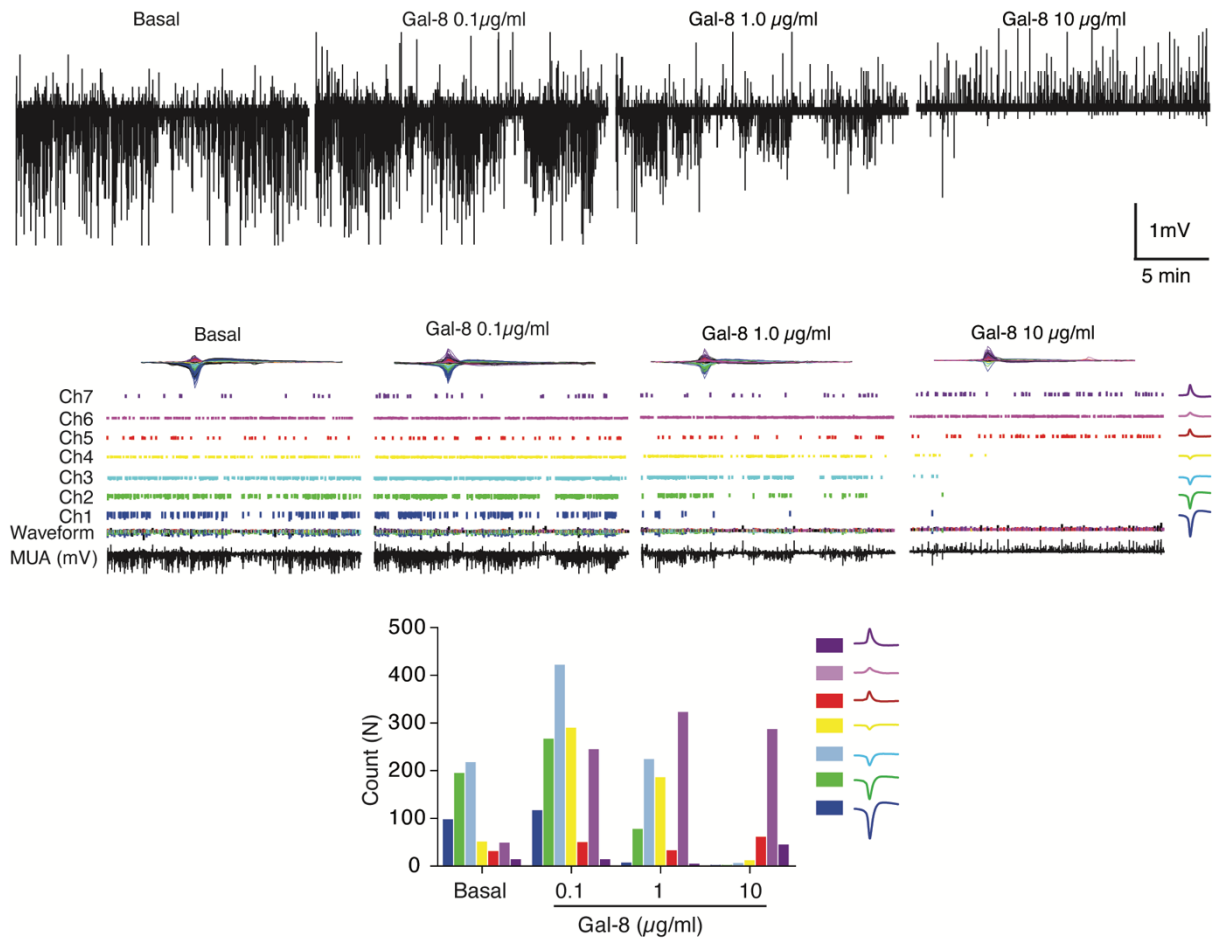


Figure 7: Gal-8 increases spontaneous excitatory or inhibitory spikes at different concentrations. Spontaneous Multiunit Activity (MUA) in CA1 hippocampus. Gal-8 enhances excitatory or inhibitory spikes at low (0.1 $\mu\text{g/ml}$) or high (10 $\mu\text{g/ml}$) concentrations, respectively. Excitatory and inhibitory spikes with different waveforms are overdrawn on the recording (Waveform) and placed in separate channels (Ch1-7). For convention, a spike wave with negative or positive deflection corresponds to an excitatory neuron or inhibitory neuron, respectively. Identified waveforms are depicted on the right with a particular color. The contribution of each spike is summarized in the graph.

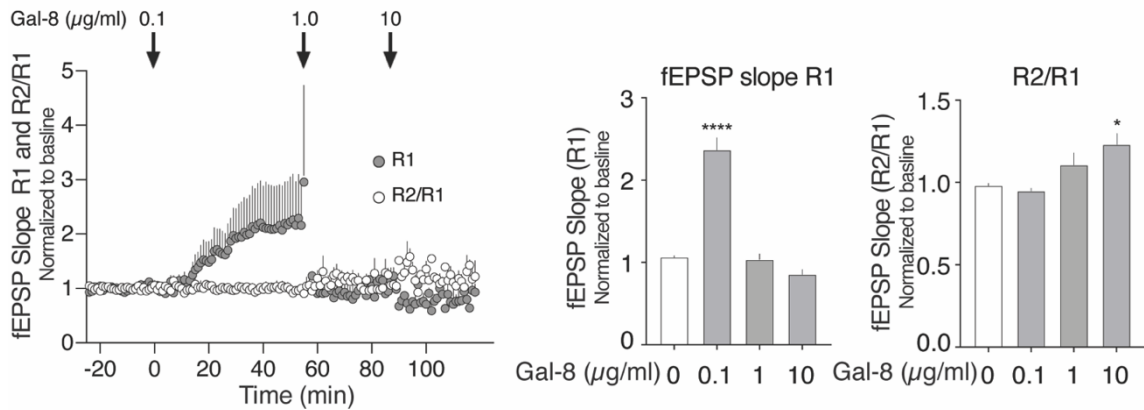


Figure 8: Gal-8 enhances excitatory or inhibitory synaptic transmission. Recordings of hippocampal CA3-CA1 field excitatory postsynaptic potentials (fEPSPs). Gal-8 increases or decreases evoked synaptic transmission at low or high Gal-8 concentrations respectively. Presynaptic involvement is discarded, as shown by unaltered facilitation index (R2/R1) of paired pulsed test at low concentrations and even increased R2/R1 at the highest Gal-8 concentration indicating a compensatory presynaptic (n=2; Point graph shows mean and SEM of Slope R1 and Slope R2/R1 normalized to basal transmission (left graph); Bar graph represents the mean and SEM of the last 5 minutes of recording for each indicated condition of R1 (middle graph) and R2/R1 (right graph); ANOVA $p^* < 0.05$ and $****p < 0.0001$).

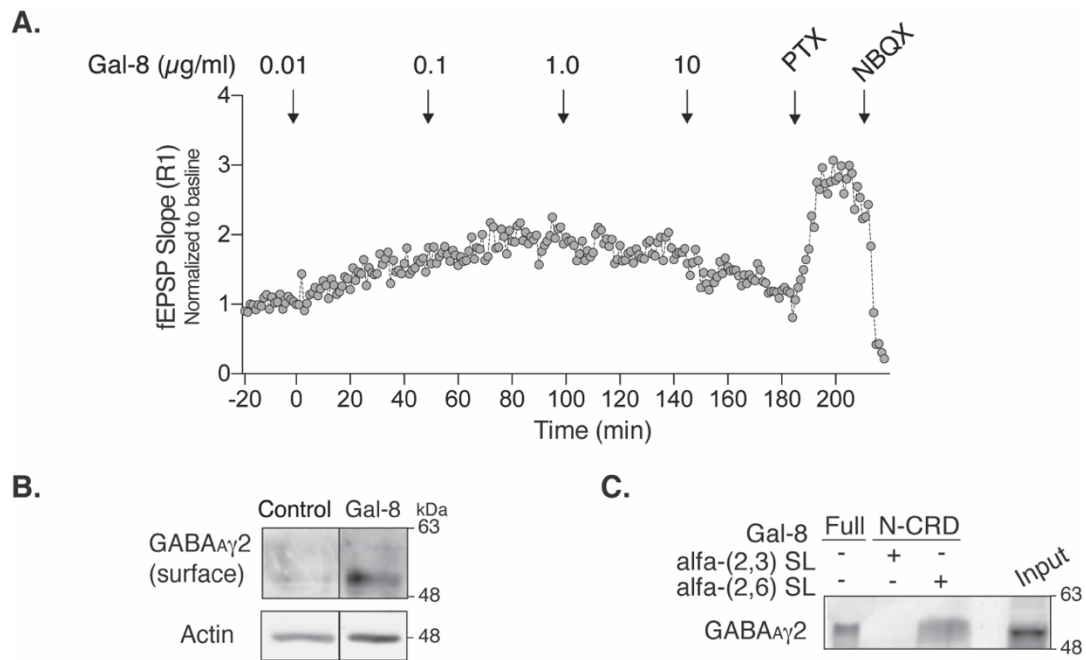


Figure 9: Gal-8 has inhibitory influence upon glutamatergic transmission, enhances GABA_AR cell surface levels and binds GABA_AR. **A.** GABA_AR is involved in Gal-8 inhibition at high doses. PTX (50 µM) abrogates the decrease in CA3-CA1 fEPSPs induced by high dose (10 µg/ml) of Gal-8 while AMPAR inhibition with NBQX (10 µM) completely blocks synaptic transmission (n=1; Graph shows mean and SEM of slope R1 normalized to basal transmission). **B.** Gal-8 increases GABA_AR at the cell surface, as revealed by biotinylation assay of treated neurons with Gal-8 (50 µg/ml) for 1 h (n=1) **C.** GABA_AR interaction with Gal-8 and its N-CRD. Immunoblots reveal GABA_ARγ2 in the pull-down of Gal-8-GST and N-CRD-GST from cortex, which is displaced by α-(2,3)SL but not α-(2,6)SL (n=1).

3.6. Blocking endogenous Gal-8 with Gal-8 N-CRD inhibits synaptic transmission

Because we found that recombinant Gal-8 N-CRD also binds to AMPAR (see Fig. 1C), we tested its effects on basal synaptic transmission. Interestingly, Gal-8 N-CRD caused sustained reduction of synaptic transmission which was not reversed by the GABA_AR inhibitor PTX and therefore did not involve a GABA_AR contribution (Fig. 10). This inhibitory effect upon fEPSP was due to a postsynaptic action as shown by the increased PPF ratio (Fig. 10). Gal-8 N-CRD very likely competes with endogenous Gal-8, negating its contribution to AMPAR mediated synaptic transmission.

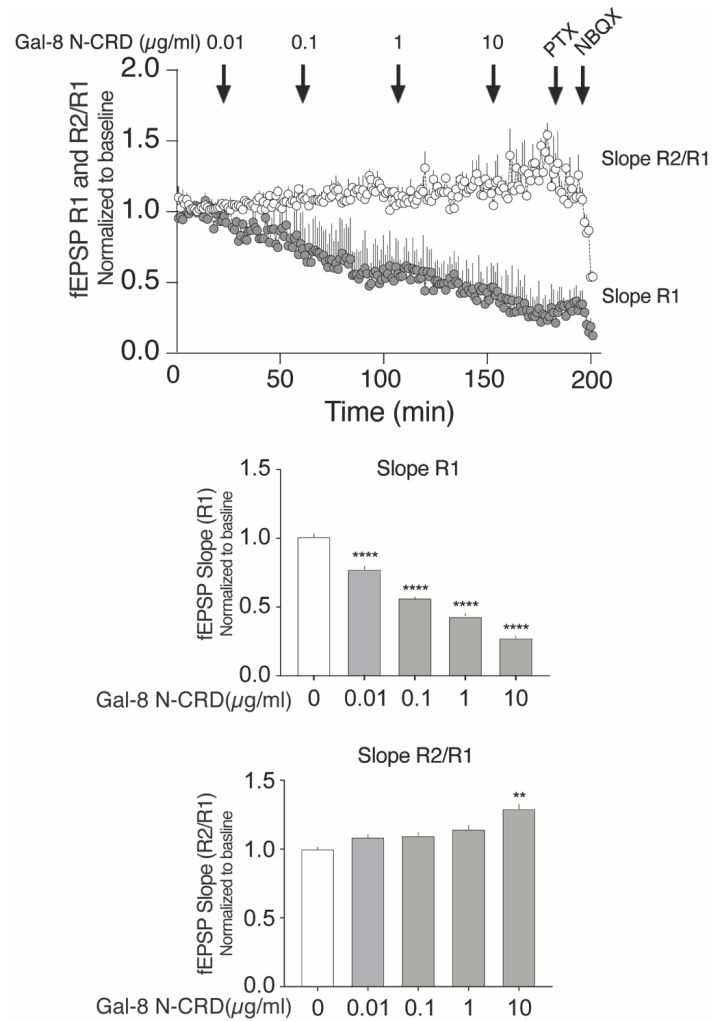


Figure 10: Gal-8 N-CRD decreases synaptic transmission. Brain slices incubated with increasing concentrations of Gal-8 N-CRD as indicated, show progressive decrease of fEPSP at the hippocampal CA3-CA1 circuit. Facilitation index (R2/R1) of paired pulsed test increases under Gal-8 N-CRD indicating a compensatory presynaptic enhancement (n=2; Point graph shows mean and SEM of Slope R1 and Slope R2/Slope R1 normalized to basal transmission (top graph); Bar graph represents the mean and SEM of the last 5 minutes of recording of each indicated condition of R1 (middle graph) and R2/R1 (bottom graph); ANOVA **p<0.01 and ****p<0.0001).

3.7. Function-blocking anti-Gal-8 autoantibodies inhibit CA3-CA1 synaptic plasticity

To further assess whether endogenous Gal-8 influences glutamatergic synaptic transmission as suggested by the previous experiments with Gal-8 N-CRD, we used function-blocking antibodies. Our laboratory has described that patients with SLE (Massardo et al., 2009; Pardo et al., 2006) and MS (Pardo et al., 2017), two diseases where cognitive dysfunction is frequently observed (Kello et al., 2019; Sumowski et al., 2018), generate autoantibodies that block Gal-8 interactions with glycoproteins and consequently block known Gal-8 functions (Carcamo et al., 2006; Norambuena et al., 2009; Vicuña et al., 2013). Furthermore, these anti-Gal-8 autoantibodies can be found in the CSF of patients with MS (Pardo et al., 2017). We affinity purified anti-Gal-8 antibodies from the serum of patients with MS and assessed their effects on synaptic transmission. Interestingly, these anti-Gal-8 antibodies slightly decreased basal synaptic transmission and inhibited LTP induction in WT brain slices (Fig. 11). These results further underscore a function of endogenous Gal-8 in synaptic transmission and plasticity. They also suggest that anti-Gal-8 autoantibodies from patients with autoimmune diseases such as SLE and MS have the potential to interfere with glutamatergic synaptic transmission and plasticity involved in memory processes, and eventually contribute to the cognitive dysfunction described in these diseases (Kello et al., 2019; Sumowski et al., 2018).

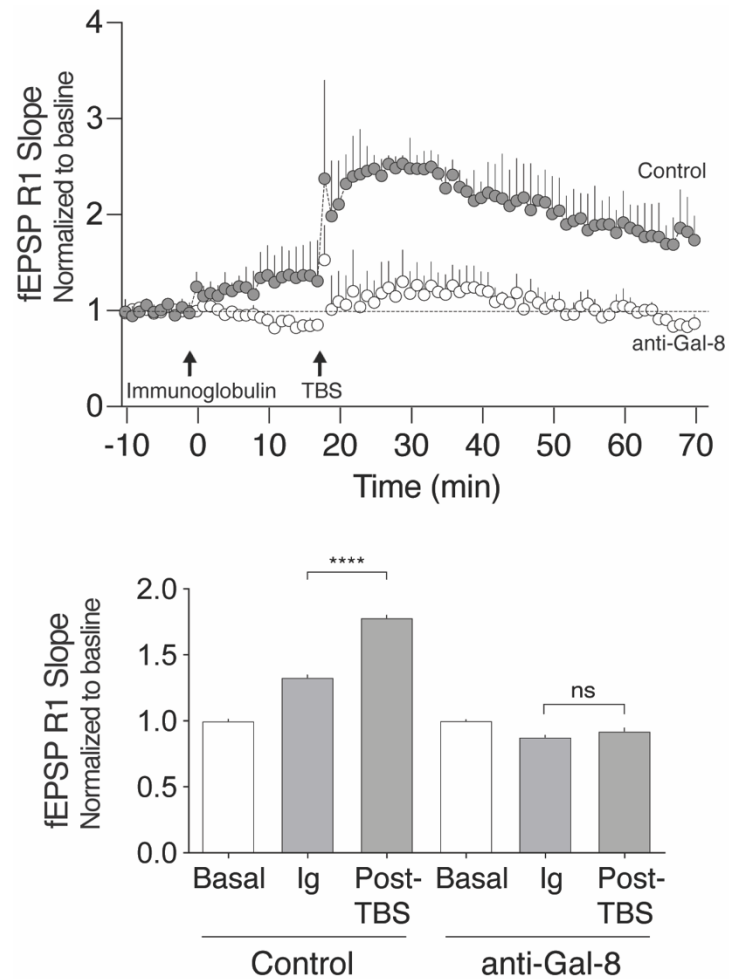


Figure 11: Function blocking anti-Gal-8 autoantibodies from patients with multiple sclerosis inhibit synaptic plasticity. fEPSP measurements in hippocampal CA3-CA1. Brain slices incubated with control immunoglobulin or anti-Gal-8 antibodies (0.25 $\mu\text{g}/\text{ml}$ affinity purified from serum of patients with MS. Anti-Gal-8 impairs LTP after induction with a theta burst stimulation (TBS) contrasting with control immunoglobulin ($n=3$; Point graph shows mean and SEM of slope R1 normalized to baseline; Bar graph represents mean and SEM of the last 5 minutes of recording for each condition (basal transmission before adding immunoglobulin; Ig before TBS and post TBS); ANOVA **** $p<0.0001$).

3.8. Gal-8 KO mice have reduced postsynaptic density AMPAR levels, impaired plasticity and altered spatial memory

Next, we used Gal-8 knockout mice (Gal-8 KO) to further evaluate a potential role of endogenous Gal-8 on glutamatergic synaptic function. We first prepared postsynaptic densities (PSD) from cortex and checked their purity analyzing pre- and postsynaptic markers (Fig. 12A). Strikingly, we found decreased levels of GluA1 and GluA2 AMPA receptor subunits in the PSDs of Gal-8 KO compared with WT mice (Fig. 12B). In contrast, we found increased levels of NMDA receptor subunit GluN2A in the PSDs of Gal-8 KO mice (Fig. 12B). These results suggest that endogenous Gal-8 contributes to determine the levels of glutamatergic receptors at the PSD.

The alterations in the levels of AMPAR and NMDAR at the PSD are expected to impact upon synaptic plasticity involved in memory processes. Therefore, we first analyzed LTP in the CA3-CA1 hippocampal circuit and then performed memory tests comparing Gal-8 KO and WT mice. We found impaired long-term potentiation LTP in the CA3-CA1 hippocampal circuit (Fig. 13). Then, we performed behavioral studies focused on spatial memory as an AMPAR-dependent process in the hippocampus (Kessels & Malinow, 2009). Firstly, we performed open field tests and found no significant differences between WT and Gal-8 KO mice, thus discarding anxiety behaviors (Carola et al., 2002) associated with the lack of Gal-8 expression (Fig. 14A). In water maze tests, starting with the visible platform paradigm, Gal-8 KO mice also behaved similarly to WT mice (Fig. 14B). However, the classic water maze paradigm that assesses spatial memory (Vorhees & Williams, 2006) revealed impaired performance by Gal-8 KO mice, as shown in the higher latencies displayed on day 2 and 4 (Fig. 14C) and by their reduced preference for the target quadrant in the probe test (Fig. 14C). Finally, we performed a reversal water maze to assess memory flexibility (Vorhees &

Williams, 2006). Gal-8 KO mice had higher overall latencies, but the probe test was not altered compared to WT mice (Fig. 14D).

All of these results reveal a role of Gal-8 on memory processes exerted upon the availability of AMPAR and NMDAR at the PSD that ensure appropriate synaptic plasticity.

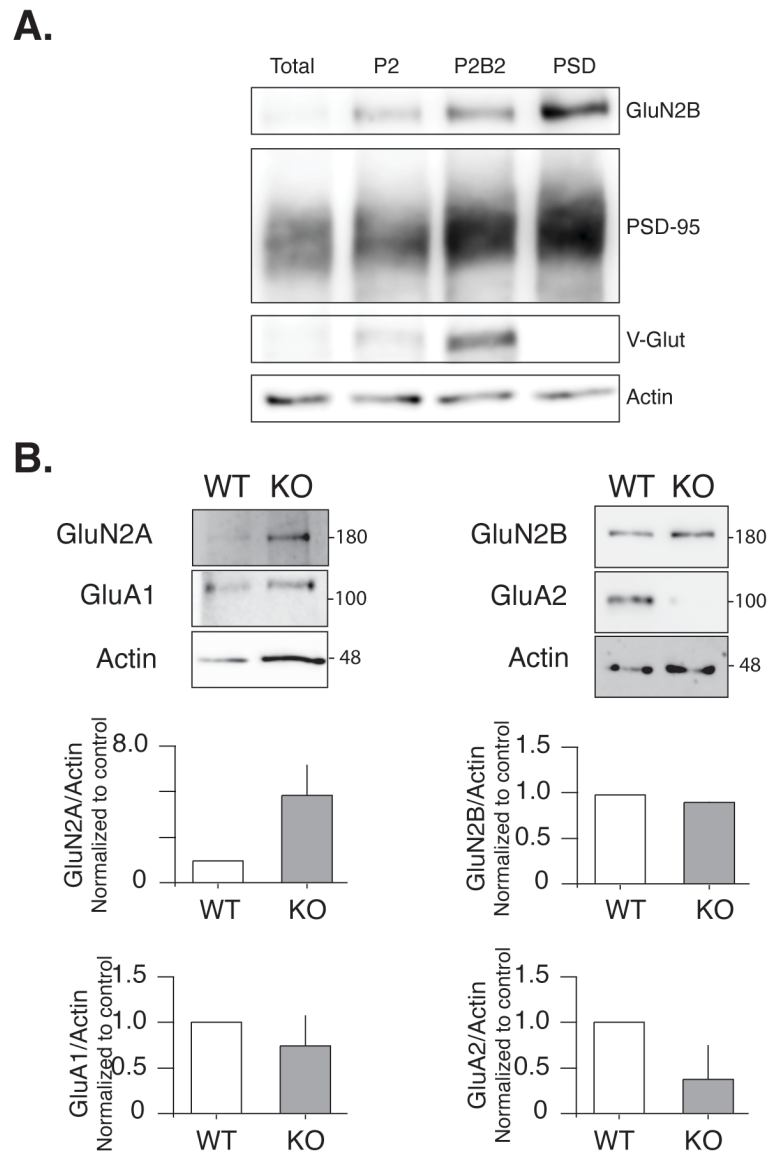


Figure 12: Endogenous Gal-8 contributes to AMPAR levels on the postsynaptic densities (PSD). **A.** Purity of postsynaptic densities (PSD) from mice cortex was proven using 10 μ g of each preparation of crude homogenates (H), crude membrane fraction (P2), synaptic membranes (P2B2) and postsynaptic densities (PSD) and immunoblotted against postsynaptic markers PSD-95 and GluN2B, presynaptic marker VGlut-1 and actin as loading control. **B.** PSD preparation from WT and Gal-8 KO mice. Cortex PSD from Gal-8 KO mice show decreased AMPAR subunits and elevated NMDAR subunits compared to WT mice (n=2; Graph shows mean and SEM of densitometric band analysis of indicated receptor/Actin normalized to control).

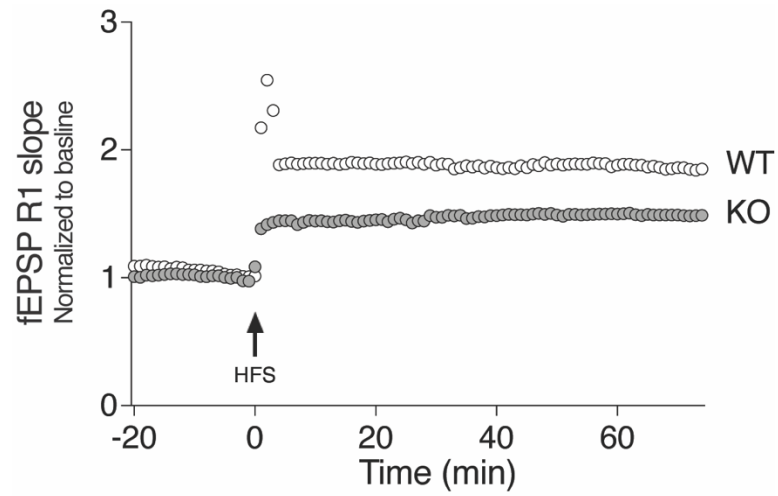


Figure 13: Endogenous Gal-8 contributes to synaptic plasticity. fEPSP measured in hippocampal CA3-CA1 of WT and Gal-8 KO mice. Gal-8 KO mice display decreased LTP in hippocampal CA3-CA1 after induction with a high frequency stimulation (HFS) as indicated (n=1 KO, n=1 WT; Graph shows mean and SEM of slope normalized to baseline).

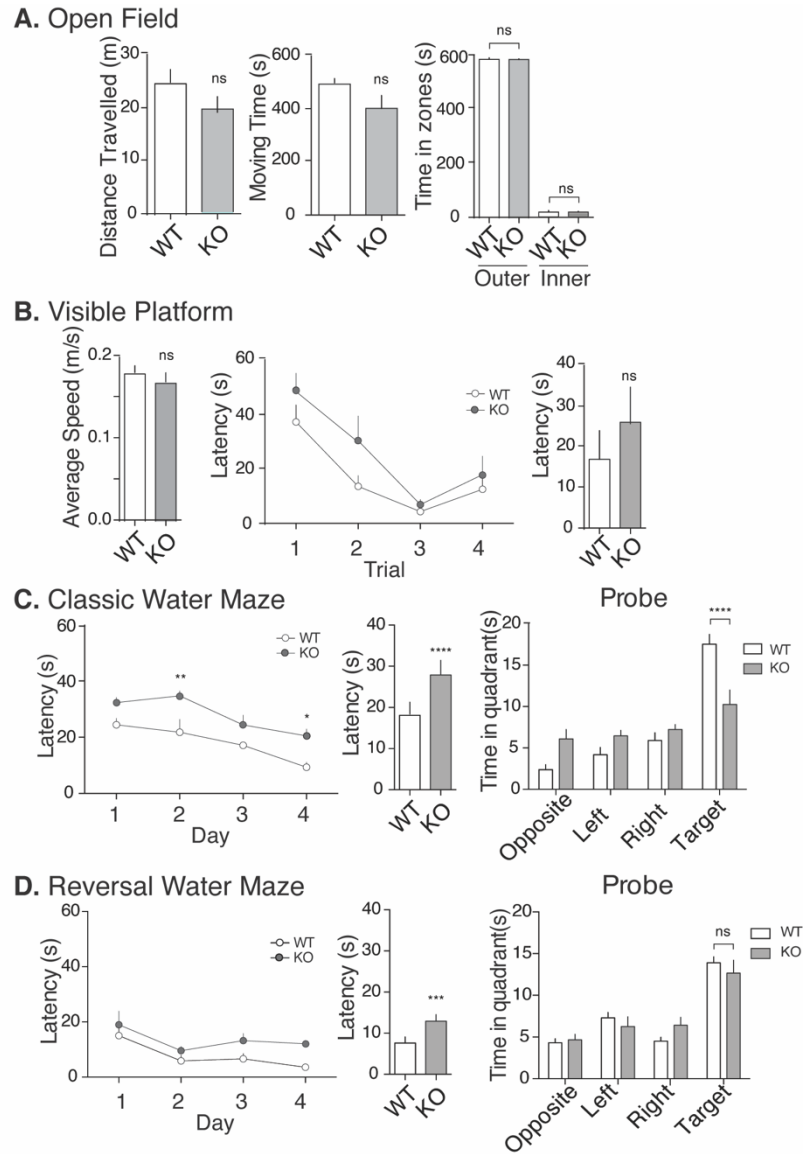


Figure 14: Endogenous Gal-8 contributes to memory. Behavioral tests comparing Gal-8 KO with WT mice. **A.** Open field show no differences (n=9 WT and KO; Graphs show mean and SEM of indicated parameters; t-test or ANOVA). **B.** Spatial cognition with a visible platform (4 trials in one day with a visible platform on a different location) also was similar in Gal-8 KO and WT mice (n=9 WT and KO; Graphs show mean and SEM of indicated parameters; t-test or ANOVA). **C.** Gal-8 KO mice show impaired spatial memory in Morris water maze test (4 trials a day for 4 days with a hidden platform in the same location; Probe test the platform is withdrawn) (n=9 WT, n=8 KO; Graphs show mean and SEM of indicated parameters; t-test and ANOVA; *p<0.05, **p<0.01, ****p<0.0001). **D.** Reversal water maze (Platform is located in the opposite quadrant respect the previous test; Probe test the platform is withdrawn) Gal-8 KO mice have overall slower performance but no differences in the probe test (n=9 WT, n=8 KO; Graphs show mean and SEM of indicated parameters; t-test and ANOVA; ***p<0.001).

4. DISCUSSION

We reveal an unexpected function of Gal-8 in memory that can be perturbed by function blocking anti-Gal-8 antibodies from MS patients but that are also present in SLE patients. Our results show that Gal-8 binds AMPAR and GABA_AR receptors and increases their cell surface levels in neurons. This involves Gal-8 N-CRD interactions with glycans that contain terminal sialic acid leading to an enhanced AMPAR endocytic recycling and PKA and FAK signaling pathways. The functional consequence is reflected in an enhancement or inhibition of glutamatergic synaptic transmission, depending on the concentration, and the requirement of Gal-8 in synaptic plasticity associated with memory. In addition, we find that anti-Gal-8 autoantibodies, previously described as function blocking antibodies from MS and SLE patients (Carcamo et al., 2006; Norambuena et al., 2009; Pardo et al., 2019; Pardo et al., 2017; Vicuña et al., 2013), block these Gal-8 functions in the brain and therefore might potentially contribute to the CD often found in these autoimmune diseases.

Galectins are proteins that interact with beta-galactosides of the carbohydrates exposed in glycoproteins and glycolipids on the cell surface and in damaged endolysosomes (Johannes et al., 2018). They modulate numerous cellular processes, including the trafficking of certain glycoproteins (Johannes et al., 2018). In the brain only Gal-1, Gal-3, Gal-4, Gal-8 and Gal-9 are expressed (Barake et al., 2020) and have been involved in microglia-mediated neuroinflammation, myelination and remyelination, adult neurogenesis, axonal growth, immunosurveillance and neuroprotection (Barake et al., 2020; Pardo et al., 2019; Sakaguchi & Okano, 2012; Siew & Chern, 2018; Velasco et al., 2013). Recently, we described that Gal-8 acts as an immunomodulator in autoimmune encephalitis (Pardo et al., 2017) and as neuroprotector against several pathogenic agents (Pardo et al., 2019). We also demonstrated

that Gal-8 is expressed in the hippocampus (Pardo et al., 2019), highly expressed in choroid plexus and is present in human CSF (Pardo et al., 2017). The presence of Gal-8 in the CSF suggests that Gal-8 has an anti-inflammatory and neuroprotective role in the immunosurveillance circuit of the brain, very likely bathing and penetrating the brain parenchyma (Brinker et al., 2014; Iliff et al., 2012; Pardo et al., 2019; Pardo et al., 2017; Simon & Iliff, 2016). Furthermore, anti-Gal-8 autoantibodies that have been described in SLE and MS (Massardo et al., 2009; Pardo et al., 2017) block its function and decrease neuronal survival (Carcamo et al., 2006; Norambuena et al., 2009; Pardo et al., 2019; Pardo et al., 2017) making them very likely neuropathogenic. Actually, detection of anti-Gal-8 at the moment of MS diagnosis predicts a worse prognosis within the first two years of disease evolution (Pardo et al., 2017).

4.1. Gal-8 binds AMPAR

To approach other possible functions of Gal-8 in the brain we first analyzed its protein interactome in rat brain synaptosomes. Among several interesting proteins, we chose AMPAR for further analysis considering its crucial function in synaptic plasticity and memory, and because its alterations lead to CD (Volk et al., 2015). CD is often found in patients with SLE or MS, where autoantibodies can play a pathogenic role (González & Massardo, 2018; Kello et al., 2019; Sumowski et al., 2018). As mentioned, we previously described function-blocking autoantibodies against Gal-8 both in SLE and MS patients (Massardo et al., 2009; Pardo et al., 2006; Pardo et al., 2017).

We corroborated that Gal-8 interacts with AMPAR subunits GluA1 and GluA2 from hippocampus and cortex where they have been described (Henley & Wilkinson, 2016). Even though GluA3 and GluA4 are also found in the proteomics analysis we did not assess their presence in Gal-8 pulled down proteins but they might be expected. We also pulled down AMPAR expressed in HEK-293 cells. However, we cannot discard that the interaction

between Gal-8 and AMPAR is indirect involving another glycoprotein. Immunoprecipitation experiments performed in brain extracts further indicate AMPAR interaction with Gal-8. Interestingly, NMDAR subunits are also highly glycosylated proteins (Everts et al., 1997), but nevertheless we did not detect them, neither in the proteomics nor in our pull-down experiments. This suggests that glycans in NMDAR subunits have configurations not recognized by Gal-8, a property common in the galectin family (Rabinovich & Croci, 2012). Highlighting this notion, we show that α -(2,3)-SL, but not α -(2,6)-SL, displaces AMPAR from the Gal-8 interaction. Indeed, the N-CRD of Gal-8, that is unique in the galectin family because of its high affinity for α -2-3-sialic acid, (Barake et al., 2020) also interacts with AMPAR in pull-down experiments.

4.2. Gal-8 increases AMPAR surface levels by modulating its traffic

To approach potential consequences of the interaction between Gal-8 and AMPAR we performed experiments in primary neurons and we found that Gal-8 increases the surface levels of GluA1 and GluA2 AMPAR subunits. This effect can be detected within 1 h treatment with Gal-8 without affecting GluN2B levels. Therefore, the Gal-8 effect is selective among these glutamatergic receptors.

Changes in the cell surface AMPAR levels within 1 h of Gal-8 treatment very likely reflect changes in the balance between endocytic uptake and recycling (M. Park, 2018). Galectins have been shown to inhibit or enhance endocytosis through different mechanisms (Johannes et al., 2018). For instance, Gal-3 through the formation of lattices can inhibit endocytosis or induce clathrin-independent endocytosis by interacting with endophilins and glycosphingolipids and clustering them in clathrin-independent carriers (CLICs), thus promoting the formation of tubular endocytic pits in a process termed glycolipid-lectin (GL-Lect) hypothesis (Johannes et al., 2018; Johannes et al., 2016; Lakshminarayan et al., 2014;

Lau et al., 2007; Straube et al., 2013). Gal-8 promotes endocytosis of different antigens and increases their degradation in antigen presenting cells (Prato et al., 2020), induces internalization of platelet coagulation factor V (Zappelli et al., 2012) and promotes endocytic pit formation through binding to endophilin-A3 producing the endocytosis of activated leukocyte cell adhesion molecule (ALCAM/CD166) (Renard et al., 2020). Here we use a cell surface reducible biotinylation assay and find higher levels of internalized AMPAR under Gal-8 treatment. Either Gal-8 increases the endocytic rate or deviates AMPAR from a degradation pathway. We did not find changes in the total levels of AMPAR and therefore a reduced degradation seems unlikely. Given the recent evidence that Gal-8 increases endocytosis in different cellular systems we think plausible that it is also increasing endocytosis of AMPAR. Interestingly, endocytosis of AMPAR can be clathrin independent and has been associated with endophilin (Chowdhury et al., 2006; Rial Verde et al., 2006; J. Zhang et al., 2017), which might eventually be promoted by Gal-8. In any case, a higher recycling would be necessary to explain the higher levels of these receptors at the cell surface.

After endocytosis, cargo is delivered to early endosomes and then either to lysosomal degradation routes or to recycling endosomes pathways back to the plasma membrane (Grant & Donaldson, 2009). The recycling route can be rapid from the early endosome or slower through the endocytic recycling compartment (Grant & Donaldson, 2009). AMPAR are constantly recycling in and out of the synapse and the plasma membrane even without activation using different endocytic routes and recycling routes depending on activity (Hanley, 2018; C. Luscher et al., 1999; Zheng et al., 2015). AMPARs in endosomes are indeed an important source for the synaptic increase of this receptor in LTP (Moretto & Passafaro, 2018; Z. Wang et al., 2008). We provide evidence of an increased recycling of AMPAR to the cell surface in the presence of Gal-8. In Gal-8 treated neurons, we observed higher fluorescence recuperation of transfected GluA1-SEP receptors after photobleaching,

reflecting an accelerated appearance of intracellular receptors at the cell surface and thus higher recycling. Then, an oscillatory behavior of the fluorescence suggests rapid disappearance and reappearance at the cell surface, suggesting that Gal-8 stimulates massive endocytosis and then recycling of AMPAR. After surface binding, Gal-8 can enter the cell into endosomes (Carlsson et al., 2007; Prato et al., 2020) and perhaps recycles together with AMPAR, intracellularly stimulating this pathway.

To approach possible mechanisms of AMPAR increases at the cell surface induced by Gal-8 we evaluated the role of NMDAR, and other signaling pathways. We found that blocking AMPAR and NMDAR did not interfere with Gal-8 effect.

The cytoplasmic tyrosine kinase FAK is particularly attractive. FAK associates with different receptors at the plasma membrane and recruits Src family kinases, especially fyn and src, involved in memory (Purcell & Carew, 2003; Sulzmaier et al., 2014). It has also scaffold functions (Kleinschmidt & Schlaepfer, 2017) and regulates endocytosis (Doherty et al., 2011; Kleinschmidt & Schlaepfer, 2017; Wu et al., 2005), including interactions with endophilin (Wu et al., 2005). FAK is enriched in the cortex and hippocampus and has been involved in several neuronal functions (Burgaya et al., 1995; Menegon et al., 1999; Srikanth et al., 2018; Stevens et al., 1996), including hippocampal synaptic plasticity and memory (Monje et al., 2012; Siciliano et al., 1996; Y. C. Yang et al., 2003). Gal-8 has been shown to activate FAK, associated with its role in cell migration and proliferation in different cell lines (Levy et al., 2001; Oyanadel et al., 2018), increased endothelial permeability (Zamorano et al., 2019) and fibronectin secretion in human gingival fibroblasts (Smith et al., 2020), most likely involving interactions with β 1-integrins (Carcamo et al., 2006; Diskin et al., 2009; Hadari et al., 2000; Nishi et al., 2003; Oyanadel et al., 2018; Pardo et al., 2019; Smith et al., 2020) that are the most important counterreceptors of FAK.

Our results show that FAK activity is required for Gal-8 induced increase of AMPAR at the cell surface. As AMPAR inhibitor NBQX does not abrogate Gal-8 function, it is unlikely AMPAR directly activates FAK. In neurons, FAK has been shown to be activated by NCAM (Beggs et al., 1997; R. Kleene et al., 2010; Kolkova et al., 2000; Niethammer et al., 2002), Trk receptors (Monje et al., 2012), EphB (Y. Shi et al., 2009) and integrins (Babayyan et al., 2012; Y. K. Park & Goda, 2016). Among all these proteins, only integrins have been reported to interact with Gal-8, although NCAM appeared in the proteomic analysis of Gal-8 interactors.

Integrins are heterodimers of α and β subunits acting as cell surface adhesion receptors and counter receptors of adjacent cells, connecting to the cytoskeleton and orchestrating signaling cascades (Y. K. Park & Goda, 2016). Integrins are one of the strongest activators of FAK (Kleinschmidt & Schlaepfer, 2017). Gal-8 binds several subunits including the $\beta 1$ subunit (Carcamo et al., 2006; Diskin et al., 2009; Hadari et al., 2000; Nishi et al., 2003; Oyanadel et al., 2018; Pardo et al., 2019; Smith et al., 2020) and has neuroprotective effects through $\beta 1$ integrins in neurons (Pardo et al., 2019). Integrins are highly expressed at synapses and contribute to synaptic transmission processes in memory and behavior (Lilja & Ivaska, 2018; Y. K. Park & Goda, 2016). GluA2 forms a complex with $\beta 3$ integrin and FAK that controls its abundance at the plasma membrane and homeostatic synaptic scaling (Cingolani & Goda, 2008; Cingolani et al., 2008; Pozo et al., 2012). FAK has been involved in the coordinated endocytosis and recycling of integrins (Ezratty et al., 2005; Kleinschmidt & Schlaepfer, 2017; Nader et al., 2016). Therefore, integrins are candidates to mediate the effects of Gal-8 on AMPAR cell surface levels.

Another pathway crucial in the regulation of AMPAR cell surface levels is PKA. PKA signaling has been involved in a variety of vesicular trafficking processes, including surface delivery from endosomal compartments, synaptic vesicles, exocrine and endocrine secretion (Seino & Shibasaki, 2005) and endocytosis and recycling of selective receptors, such as the

EGFR (Salazar & Gonzalez, 2002). Regarding GluA1 subunit, it is phosphorylated at Ser845 by PKA resulting in an increased recycling from the endosomes to the perisynaptic membrane (Buonarati et al., 2019; Diering & Huganir, 2018; Ehlers, 2000; Esteban et al., 2003). This PKA-mediated phosphorylation also prevents GluA1 endocytosis and sorting to lysosomes for degradation (Diering & Huganir, 2018; Ehlers, 2000; Purkey & Dell'Acqua, 2020). In neurons, PKA signaling is most frequently activated by cAMP produced after calcium signaling, but G-coupled receptors are also involved (Seino & Shibasaki, 2005). We show that PKA inhibition abrogates the Gal-8 induced AMPAR increase at the cell surface. The mechanism remains unknown. Gal-8 might increase PKA activation or promote its location close to AMPAR through scaffold proteins such as AKAP5 (AKAP79/150) (Buonarati et al., 2019; Purkey & Dell'Acqua, 2020; Tavalin et al., 2002; M. Zhang et al., 2013).

4.3. Gal-8 in synaptic transmission

To evaluate whether Gal-8 has a role in glutamatergic transmission we performed electrophysiological experiments in the hippocampus. We find that Gal-8 has postsynaptic effects and either increases or reduces excitatory synaptic transmission depending on its concentration. At relatively low concentrations of 0.01-0.1 $\mu\text{g/ml}$, Gal-8 increases glutamatergic transmission, while an inhibitory effect starts to be detected at 1 $\mu\text{g/ml}$ and reaches its maximum by 10 $\mu\text{g/ml}$. While the stimulatory effect can be related with our previous observation of an increased AMPAR recycling that elevates its cell surface levels, the inhibitory effect required further analysis. The addition of GABA_AR receptor inhibitor PTX abrogates the reduced transmission elicited by high Gal-8 concentration, thus involving a higher function of GABA_AR at these conditions.

Our demonstration of an interaction between Gal-8 and an AMPAR leading to an increasing cell surface level of these receptors, suggests a stimulating effect due stabilization and availability of these receptors at the synaptic cleft. AMPARs have low affinity for

glutamate and need to be located near glutamate release sites (Choquet & Hosy, 2020). Therefore, Gal-8 increase of AMPAR at the cells surface is not enough to account for the increased synaptic transmission, which reflects a higher level of functional AMPAR at the synaptic cleft. AMPARs reach this location through lateral diffusion after their exocytosis at perisynaptic regions (Choquet & Hosy, 2020; Penn et al., 2017). Both intracellular and extracellular proteins contribute to entrap AMPAR at postsynaptic densities (Choquet & Hosy, 2020; Sheng et al., 2018). TARPs anchor them intracellularly to the PSD-95 (Buonarati et al., 2019). Intracellular elements indeed might respond to the signaling pathways such as FAK and PKA triggered by Gal-8, which we previously involved in AMPAR recycling to the cell surface. In addition, the availability of more AMPAR at the cell surface by itself increases the probability of it to be included at the synaptic cleft. On the other hand, extracellularly, the amino terminal domain of AMPAR that is glycosylated has been shown to be important for synaptic localization and retention (Díaz-Alonso et al., 2017; Watson et al., 2017). Extracellular proteins such as, N-cadherin, LRRTM, SynCAM, neuroligins and neuroligins could also contribute to AMPAR nanoclustering (Choquet & Hosy, 2020; Keable et al., 2020). Interestingly, the interactome analysis in synaptosomes pulled down the three known neuroligins and therefore it would be important to corroborate their interaction with Gal-8. Galectins can certainly mediate clustering of glycoproteins and mediate interactions with the extracellular matrix (Johannes et al., 2018), which might eventually contribute to cluster AMPAR at the postsynaptic density.

The results involving GABA_AR in the inhibition of synaptic transmission under high Gal-8 concentrations prompted us to assess whether Gal-8 interacts with and modifies the cell surface levels of GABA_AR. Synaptic GABA_AR forms heteropentamers between two α , two β and one γ 2 subunits (B. Luscher et al., 2011). We used an antibody directed against the γ 2 subunit that is mostly present at the GABA_AR synapse (B. Luscher et al., 2011). Using a

similar approach as for AMPAR, our pull-down assays reveal an interaction between Gal-8 and GABA_AR, which similarly to the interaction with AMPAR, also involves Gal-8 N-CRD and sialic acid. Only α β subunits are known to be glycosylated in GABA_AR, at least in humans (Mueller et al., 2014). N-glycosylations in GABA_AR α subunits are important for assembly (Buller et al., 1994) and are directed towards the pore and those in β subunits are directed to the extracellular (Phulera et al., 2018). Therefore, in principle, only the N-glycans of β subunits would be accessible for galectin binding.

Biotinylation assays in primary neurons show that Gal-8 also increases GABA_AR at the cell surface. Similar to AMPAR, synaptic transmission of GABA_AR is regulated by their cell surface levels, which are in turn regulated by endocytosis, recycling and synaptic entrapment (B. Luscher et al., 2011; Petrini et al., 2004). Also similar to AMPAR, PKA phosphorylation of GABA_AR has been shown to reduce their endocytosis (B. Luscher et al., 2011), while neuroligins promote their synaptic location (B. Luscher et al., 2011). Further experiments are needed to assess the mechanisms of Gal-8 induced GABA_AR activity at the cell surface.

4.4. Endogenous functions of Gal-8

In all these findings we added exogenous Gal-8 at concentrations that are unknown to be physiological. Therefore, we decided to evaluate the function of endogenous Gal-8 through different complementary approaches, including an interference with the Gal-8 N-CRD and function-blocking autoantibodies against Gal-8, to then analyze Gal-8 KO mice. Our results in the electrophysiology setting show that Gal-8 N-CRD reduces synaptic transmission in a postsynaptic manner. This suggests a role of endogenous Gal-8 in CA3-CA1 hippocampal circuit favoring the excitatory synaptic transmission. This finding brings up the possibility of a regulatory mechanism that might operate under inflammatory conditions. In

humans, there is an isoform of Gal-8 with a longer linker between the CRD that bears a thrombin cleavage site (Nishi et al., 2006). This isoform is not as frequently produced as the non-cleavable isoform (Troncoso et al., 2014), but its cleavage with thrombin may be relevant in the case of stroke or trauma, were the blocking effect of Gal-8 N-CRD could be released. We also find that anti-Gal-8 antibodies purified from sera of MS patients slightly decrease synaptic transmission but completely abrogate synaptic plasticity. This observation reinforces the notion that endogenous Gal-8 promotes synaptic excitatory transmission and plasticity. These results also suggest that the pathogenicity of these antibodies may be extended to the CD of patients with MS or SLE. Furthermore, the low Gal-8 concentrations at which we observed an increased synaptic transmission seems to be more closely related with the physiologic function of Gal-8 in the brain.

We next used Gal-8 KO mice as a model for the lack of Gal-8 expression. Interestingly, Gal-8 KO mice have decreased AMPAR GluA1 and GluA2 in the postsynaptic densities. This suggests that endogenous Gal-8 regulates the levels of AMPAR at the synapse. Accordingly, the Gal-8 KO mice have reduced LTP in the CA3-CA1 hippocampal circuit. We also find an increment of some subunits of NMDAR receptors, suggesting a compensatory mechanism. These results led us to evaluate spatial memory functions were AMPAR participates in hippocampus (Kessels & Malinow, 2009). First, we discarded anxiety behaviors with the open field assay (Carola et al., 2002) and also discarded a great impairment showing no alterations in the visible platform (Vorhees & Williams, 2006). However, we find a defect in spatial memory reflected in impaired water maze assays (Vingtdeux et al., 2016; Vorhees & Williams, 2006). Although these results underscore a role of Gal-8 on hippocampal spatial memory, it is possible that Gal-8 is required for other AMPAR functions, such as emotions, addiction and autism (Kessels & Malinow, 2009).

We propose the following model: Gal-8 at the physiological intra-brain concentrations binds AMPAR and increases their endocytosis and recycling to the cell surface through PKA and β 1-integrin-mediated FAK activity. This leads to increased levels of AMPAR at the cell surface with consequential increase in the excitatory synaptic transmission, favoring plasticity and memory. Autoantibodies can inhibit this function. At higher Gal-8 concentrations, eventually achieved under pathogenic conditions, Gal-8 also binds GABA_AR, increases its surface levels and inhibitory transmission (Fig. 15).

4.5. Relevance

4.5.1. Gal-8 expression levels in the brain

Gal-8 in the brain is mainly expressed at the choroid plexus and its levels at the CSF seems to vary among different individuals (Pardo et al., 2017). This suggests that its expression levels might be under regulation by mechanisms still completely unknown. The extracellular availability of Gal-8 can be determinant for synaptic transmission and brain function especially since we found this dual function of increasing excitatory transmission and at higher concentrations increasing inhibitory transmission. The electrophysiologic experiments with Gal-8 N-CRD and anti-Gal-8 reveal that endogenous Gal-8 in the brain might be at an extracellular concentration favorable for excitatory transmission. The questions that remains is whether the high concentrations that lead to inhibition of this transmission can be achieved under certain conditions. Even though Gal-8 secretion occurs through unconventional mechanisms, Gal-8 is also found in the cytosol (Barake et al., 2020) and therefore pathogenic conditions, such as stroke, due to disrupted cells, could release enough intracellular Gal-8. Inflammatory conditions where its expression is upregulated (Tribulatti et al., 2020) might also increase its levels although this remains unexplored for the brain.

4.5.2. Other galectins involved in glutamatergic functions

Since galectins share common affinities to β -galactosides, but also distinct preferences, they are known to have complementary, redundant or antagonistic roles (Barake et al., 2020). Other galectins that have also been involved on memory and glutamatergic regulation are Gal-1 and Gal-3. Gal-1 can slow the desensitization of recombinant AMPAR and Kainate receptors (Copits et al., 2014). Gal-1 also participates in neurogenesis (Sakaguchi & Okano, 2012), that is involved in spatial memory (Anacker & Hen, 2017), increases of GluN1 subunit by unknown mechanisms and participates in hippocampus-dependent contextual and spatial learning (Lekishvili et al., 2006; Sakaguchi et al., 2011). Gal-3, negatively regulates synaptic plasticity, hippocampal memory processes of contextual fear conditioning and water maze paradigm (Chen et al., 2017) by binding α -3 integrin reducing FAK activation (Chen et al., 2017), in contrast with our results with Gal-8. Decreased sialylation can increase Gal-3 binding (Puigdellivol et al., 2020), and decrease the Gal-8 roles uncovered here. Therefore, it would be interesting to elucidate how Gal-1, Gal-3, Gal-8 or other galectins functionally intertwine.

4.5.3. Glycosylation patterns in the brain

Carbohydrates certainly possess different levels of regulation. Glycosylation patterns are flexible, non-template driven and are controlled by genetic variations of sugars transporters and glycosyltransferases, as well as by monosaccharide substrate availability and uptake (Mathew & Donaldson, 2019). Glycoproteins are principally glycosylated in asparagine (N-linked) or serine/threonine (O-linked) (Williams et al., 2020). In the endoplasmic reticulum N-glycosylation starts with en block transfer of a high mannose precursor (immature glycosylation) (Williams et al., 2020). Later, ER and Golgi enzymes reduce, or trim, mannoses and later other monosaccharides are added by glycosyltransferases giving way to hybrid and complex glycosylations (Williams et al., 2020).

O-glycosylations can be initiated in the ER or Golgi with a monosaccharide that is then extended. Glycolipids are also synthesized in the ER and Golgi (Williams et al., 2020). Proteoglycans that consist on a protein core with polysaccharide chains known as glycosaminoglycans (GAGs) are attached to asparagine, serine or threonine (Williams et al., 2020).

N-glycosylations, O-glycosylations, sialylation and polysialylation participate in several brain functions during development, regeneration and even memory (Ralf Kleene & Schachner, 2004; Reily et al., 2019; Taylor et al., 2014; B. Wang, 2009; Y. R. Yang et al., 2017). Therefore, galectin functions, including Gal-8 in memory, neuronal protection and immune modulation in the brain (Pardo et al., 2019; Pardo et al., 2017), might be finely tuned by changes in glycosylation patterns. The content of α -2,3-sialic acid that Gal-8 binds might change in the brain. Memory paradigms can change glycosylation patterns (Hidalgo et al., 2006) increasing the incorporation of sialic in the brain (B. Wang, 2009). In contrast, cell surface sialidase activity is increased and necessary after NMDAR independent LTP in mossy fiber-CA3 and in spatial memory and contextual fear conditioning (Minami et al., 2017; Minami et al., 2016). Glycosylation can be changed through diet and diseases. Sialic acid supplementation and breastfeeding increases the content of this sugar in the brain and can lead to faster learning in memory paradigms (Mudd et al., 2017; Oliveros et al., 2018; ten Bruggencate et al., 2014; B. Wang, 2009; B. Wang et al., 2003; B. Wang et al., 2007). Glucosamine feeding increases N-glycan branches increasing the substrate for galectin binding (Rahimian et al., 2019). Patients with Alzheimer's disease have different glycosylations than control subjects, with particular alterations in fucosylation and sialylation (Cho et al., 2019; Fang et al., 2020; Gaunitz et al., 2020; Regan et al., 2019). A β ₂₅₋₃₅ peptide induces neuroinflammation, reduction of α -2,3 and increase in α -2,6-sialic acid (Limon et al., 2011; Ramos-Martinez et al., 2018). During inflammation by lipopolysaccharide, Tau or

fibrillar A β , activated microglia secrete sialidase that desialylates glycans favoring Gal-3 binding (Allendorf, Franssen, et al., 2020; Allendorf, Puigdellivol, et al., 2020; Nomura et al., 2017) which would presumably inhibit Gal-8 binding as well. Glycosylation alterations are also described in schizophrenia particularly affecting AMPA, kainate and GABA receptors but not NMDAR (Mueller et al., 2014; J. Tucholski, Simmons, Pinner, Haroutunian, et al., 2013; J. Tucholski, Simmons, Pinner, McMillan, et al., 2013; Williams et al., 2020). Mutations in specific sialyltransferases in humans produce epilepsy, salt and pepper syndrome, intellectual disability, progressive motor neuropathy and cognitive dysfunction (Puigdellivol et al., 2020). Patients with mutations of ST3Gal3, the sialyltransferase that binds sialic acid to galactose in α -2,3, causes intellectual disability (Hu et al., 2011) or West syndrome, a syndrome that causes childhood epilepsy and intellectual disability (Edvardson et al., 2013). Null mice for ST3Gal3 have reduced terminal protein sialylation, myelination, motor alterations and altered passive avoidance behavior (Yoo et al., 2015). All of these particular changes in glycosylation and in particular of sialic acids can certainly increase or decrease Gal-8 function over AMPAR which is certainly interesting to study in the future.

Our findings may be expected in humans too because although different AMPAR subunits are differentially glycosylated as evaluated by lectin binding, they are highly conserved between different species comparing rat, tree shrew, macaque, and human frontal cortex tissue (Janusz Tucholski et al., 2014). AMPAR is known to have different glycoforms in the brain providing different substrates that could be favorable or unfavorable for Gal-8 binding (Bowen et al., 2017; Hanus et al., 2016; Hwang & Rhim, 2019; Kanno et al., 2010; Standley et al., 1998).

GABA_AR N-glycosylation is required for assembly, cell surface expression, channel gating properties and receptor function (Buller et al., 1994; Lo et al., 2010; Tanaka et al., 2008). Glycosylation alterations of GABA_AR have been found in schizophrenia (Mueller et al.,

2014) and specifically mutations in the β subunit are associated with childhood absence epilepsy and GABA_AR hyperglycosylation (Gurba et al., 2012; Tanaka et al., 2008). All of these glycosylation states could either increase or decrease Gal-8 binding to AMPAR or GABA_AR providing a vast amount of regulation that surely warrant future studies.

There are many diseases where AMPAR and GABA_AR surface regulation is found altered such as Alzheimer's disease, Fragile X, Rett syndrome, autism, epilepsy, anxiety disorders, mood disorders and schizophrenia (Lee et al., 2017; B. Luscher et al., 2011; Purkey & Dell'Acqua, 2020) making it particularly interesting to study if Gal-8 has a role in them.

4.5.4. Anti-Gal-8 autoantibodies inhibit Gal-8 function

Our group described that MS, SLE, rheumatoid arthritis and septic patients have autoantibodies that recognize Gal-8 (Massardo et al., 2009; Pardo et al., 2006; Pardo et al., 2017). Anti-Gal-1 and anti-Gal-3 antibodies have also been described in MS and SLE (de Jong et al., 2019; Lutomski et al., 1997; Nishihara et al., 2017; Z. R. Shi et al., 2015). In MS, anti-Gal-3 are associated with secondary progressive MS and they increase phospho-NF κ B and ICAM-1 in brain microvascular endothelial cells thus, they could contribute to BBB leakage (de Jong et al., 2019; Nishihara et al., 2017). In SLE, anti-Gal-8 antibodies are associated to lymphopenia (Massardo et al., 2009) and in MS they are an early prognostic marker for relapsing-remitting MS (Pardo et al., 2017). Furthermore, anti-Gal-8 autoantibodies from at least SLE and MS patients are function blocking impeding its interaction with cell surface glycoproteins (Carcamo et al., 2006; Norambuena et al., 2009; Pardo et al., 2019; Pardo et al., 2017; Vicuña et al., 2013). Our laboratory described that these anti-Gal-8 autoantibodies inhibit Gal-8 binding to β 1 and LFA1 (Vicuña et al., 2013), inhibit Jurkat cells and PBMCs adhesion (Carcamo et al., 2006; Pardo et al., 2017), protect from Gal-8 induced apoptosis in Jurkat cells (Norambuena et al., 2009) and activated Th17

cells (Pardo et al., 2017) and reduce hippocampal neuron viability in hippocampal primary culture (Pardo et al., 2019). Our results showing that these antibodies interfere with LTP suggest a new pathogenic role in cognitive functions that deserve further study in a clinical context. Autoantibodies in general could be present within brain parenchyma coming from the circulation under conditions that breach the blood brain barrier (Brimberg et al., 2015) or can be produced intrathecally in an autoimmune disease such as MS (Stock et al., 2017). Our group already described anti-Gal-8 antibodies in cerebrospinal fluid of MS patients (Pardo et al., 2017). The effects shown here on synaptic plasticity are novel and could be involved in CD in SLE and MS patients.

Other antibodies that affect AMPAR and GABA_AR function are described in limbic encephalitis (Gibson et al., 2020). Anti-AMPAR antibodies typically target GluA1 and GluA2 reducing their synaptic localization and inducing their degradation leading to altered synaptic plasticity and to compensatory increased excitability (Gibson et al., 2020; Gleichman et al., 2014; Hoftberger et al., 2015; Peng et al., 2015). They can produce loss of short term memory, confusion, psychiatric symptoms and seizures among other alterations (Gibson et al., 2020; Hoftberger et al., 2015). Indirectly affecting AMPAR, some patients have anti-LGI1 antibodies that reduce AMPAR clusters in the synapse (Gibson et al., 2020; Ohkawa et al., 2013) or anti-CASPR2 that may affect AMPAR trafficking or GABA_AR transmission (Gibson et al., 2020). Also, some patients present anti-GABA_AR antibodies that reduces its surface levels affecting inhibitory transmission which can produce seizures (Gibson et al., 2020). In SLE patients, anti-ribosomal P antibodies acting through NSPA can increase both AMPAR and NMDAR transmission affecting synaptic plasticity and memory (Bravo-Zehnder et al., 2014; Segovia-Miranda et al., 2015). Our results predict that anti-Gal-8 autoantibodies can mediate CD in SLE and MS, a possibility that remains to be studied in the future.

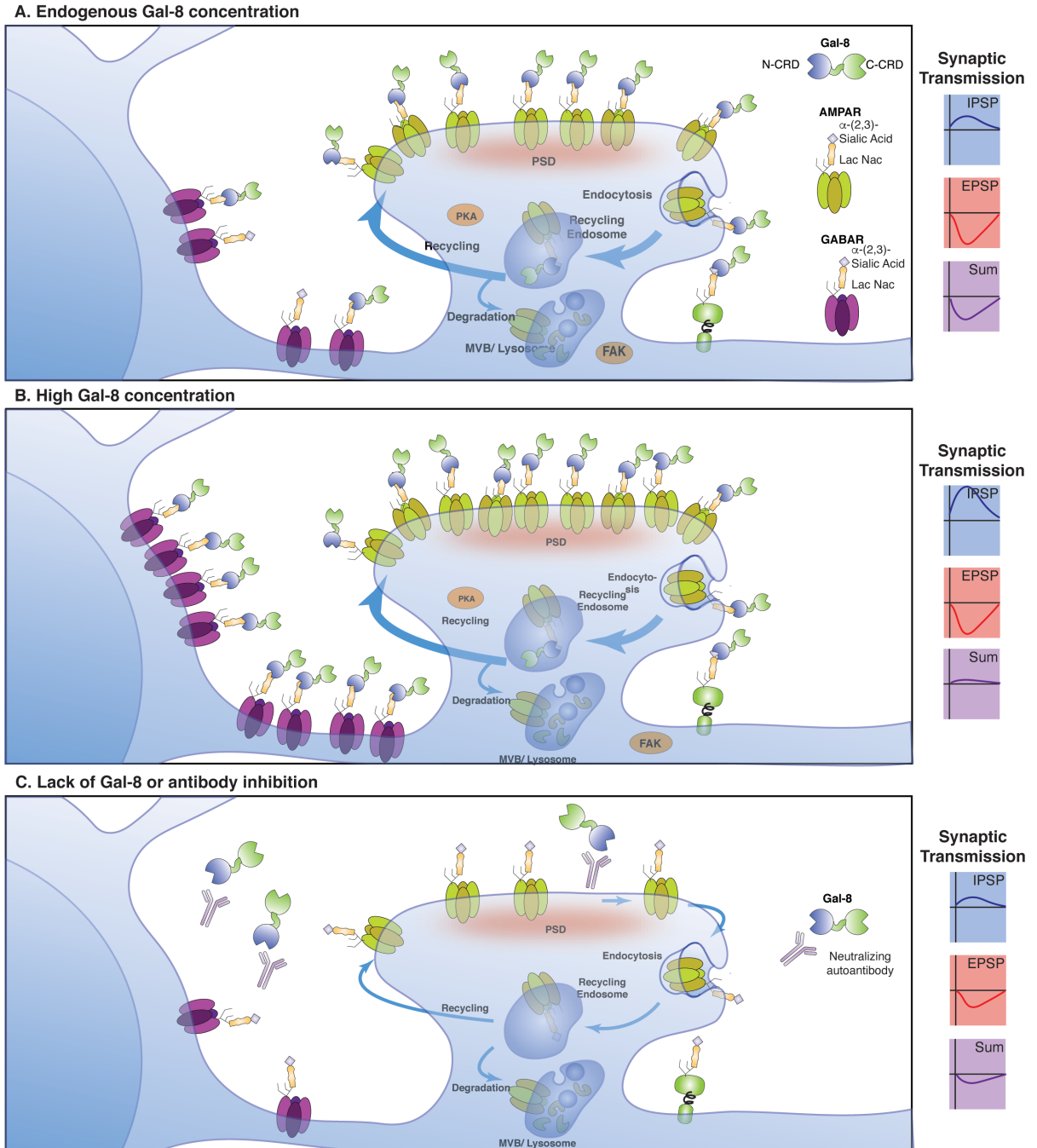


Figure 15. Model of Gal-8 glutamatergic functions: **A.** Endogenous Gal-8 levels binds AMPAR through sialic acid glycosylations (α -2,3-sialic acid-Lac NAc) recognized by the Gal-8 N-terminal carbohydrate recognition domain (N-CRD) and increase AMPAR endocytosis and recycling to the cell surface, involving focal adhesion kinase (FAK) and protein kinase A (PKA). **B.** High Gal-8 concentrations bind and increase the cell surface levels of GABA_AR, thus reducing synaptic transmission. **C.** Lack of Gal-8 or its inhibition by anti-Gal-8 antibodies leads to a reduced synaptic transmission, resulting from disbalanced excitatory postsynaptic potentials (EPSP) and inhibitory postsynaptic potentials (IPSP), presumably due to AMPAR and GABA_AR reduction at the cell surface.

5. CONCLUSIONS

Gal-8 function in the brain includes modulation of glutamatergic synaptic transmission and is required for LTP and memory processes.

Electrophysiology studies indicate that Gal-8 enhances AMPAR transmission at low levels while at high concentrations can inhibit this transmission due to stimulation of the GABA system.

Gal-8 binds both AMPAR and GABA_AR through carbohydrate interactions and can increase their levels at the cell surface.

Gal-8 increases AMPAR recycling from intracellular compartments to the cell surface through a mechanism that involves PKA and FAK and is independent of AMPAR or NMDAR activity.

Anti-Gal-8 antibodies purified from MS patients impair synaptic plasticity, indicating a neuropathogenic potential that can result in cognitive dysfunction.

These findings are completely novel regarding Gal-8 functions in the brain. Gal-8 emerges as a lectin with regulating properties upon AMPAR and GABA_AR functions, which are essential for many cognitive processes and several neurological diseases. Future work should address this new function under physiologic and therapeutic contexts, including pathogenic consequence of anti-Gal-8 antibodies entering the brain in MS and SLE.

ADDENDUM: Generation of mice and human monoclonal antibodies against ribosomal P-epitope and their effect on hippocampal glutamatergic transmission

A.1. INTRODUCTION

Several autoantibodies have been described to recognize elements of glutamatergic receptors and alter their function leading to neuropsychiatric manifestations including cognitive dysfunction (CD) (Gibson et al., 2020).

In SLE, the prototype of autoimmune disease where more than a hundred different autoantibodies have been described, two sets of antibodies have been identified with neuropathogenic potential which mediate diffuse cognitive alterations provided that the blood brain barrier (BBB) is permeated (Kello et al., 2019). The first, belong to a subset of anti-double stranded DNA (anti-dsDNA) antibodies that cross-react with NMDAR (DNRab) that target subunit GluN2 recognizing a peptide sequence D/EWD/EYS/G (DWEYS) (DeGiorgio et al., 2001). DNRab antibodies bind GluN2A and GluN2B subunits when NMDAR is in an open configuration (Faust et al., 2010), but prolongs the activity of the receptor exclusively through GluN2A subunits, resulting in increased postsynaptic glutamatergic transmission (Chan et al., 2020). These antibodies can induce apoptosis by excitotoxicity and alter spatial memory or emotional processes depending on the region where the BBB is permeable (Chan et al., 2020; Chang et al., 2015; Faust et al., 2010; Huerta et al., 2006; Kowal et al., 2006). In SLE patients, DNRab have been associated with impaired spatial memory (Chang et al., 2015; Kello et al., 2019; Mackay et al., 2019), spatial planning and rapid visual processing (Massardo et al., 2014). The pathogenesis of DNRab extends beyond the period of BBB

opening and antibody presence in the brain parenchyma involving excessive synaptic pruning by activated microglia, explaining chronic manifestations (Nestor et al., 2018).

Additionally, anti-ribosomal P (anti-P) antibodies originally described to associate to psychosis (Bonfa et al., 1987; González & Massardo, 2018) have more recently been associated also with CD (Massardo et al., 2014) in SLE patients. These anti-P antibodies recognize a sequence of 11 residues (SDEDMGFGLFD; the P-epitope) present in the carboxy-terminal region of three phosphorylated ribosomal proteins (P0, P1, P2) (Elkon et al., 1985; Mahler et al., 2003). However, an explanation for a neuropathogenic potential emerged from the finding that they cross-react with a high molecular weight membrane protein named Neuronal Surface P Antigen (NSPA) because it exposes a P-epitope at the surface of neurons (Matus et al., 2007). *In vitro* experiments and murine models are starting to elucidate anti-P neuropathologic effects (González & Massardo, 2018). In neurons, anti-P antibodies can induce calcium entrance and apoptosis, as well as increased synaptic transmission through AMPAR and NMDAR resulting in an impaired synaptic plasticity, as reflected in electrophysiological alterations of LTP (Bravo-Zehnder et al., 2014; Matus et al., 2007; Segovia-Miranda et al., 2015) and memory alterations, depressive behavior and smell perturbations in mice (Bravo-Zehnder et al., 2014; Katzav et al., 2008; Katzav et al., 2007). NSPA, is expressed at specific brain regions, including areas involved in memory, cognition and emotion, and is involved in adult neurogenesis, NMDAR synaptic transmission and plasticity and in spatial and object recognition memory (Espinoza et al., 2020; Matus et al., 2007; Segovia-Miranda et al., 2015). Our laboratory recently provided evidence NSPA is an ubiquitin ligase that regulates phosphatase PTPMEG, which in turn regulates NMDAR levels at the synaptic density (Espinoza et al., 2020). All these findings certainly link NSPA to NMDAR and suggest potential mechanisms of perturbation by anti-P antibodies, which deserve intense exploration. We initially propose to obtain monoclonal anti-P antibodies and

to study the neuropathogenic mechanisms of anti-P, however, methodological problems led us to change our focus. Despite the change in the theme of this thesis, we decided to present the results of the original objective regarding the obtention of murine and human monoclonal anti-P antibodies. This, as an important tool that would avoid the need of continuously screen patients with SLE and immunize rabbits to study the damaging mechanisms of these antibodies.

A.2. MATERIALS AND METHODS

A.2.1. Materials

A.2.1.1. Animals

BALB/c, C57/B6 H2B and C57BL/6 H2D mice for immunization were purchased from The Jackson Laboratory and housed at the Center for Comparative Physiology at the Feinstein Institute for Medical Research. Mice for electrophysiology were housed at the Faculty of Biological Sciences of the Pontificia Universidad Católica de Chile. All protocols were approved by the Institutional Animal Care and Use Committee of the corresponding facility. All animals were maintained under conditions of strict confinement, which included automatic control of temperature (21°C) and photoperiod (12 h light / 12 h dark) and received water and food *ad libitum*.

A.2.1.2. Patients Samples

Blood samples were collected from SLE patients and healthy controls according to protocols approved by the Northwell Health institutional review board and the Faculty of Medicine, Pontificia Universidad Católica de Chile ethics committee with written informed consent from all participants.

A.2.1.3. Antibodies

Anti-CD27-PE from Invitrogen. Anti-CD3-AF-700, anti-CD14-AF-700, anti-CD16-AF-700 anti-IgM-PerCP Cy5.5, anti-CD19-APC and anti-CD19-BV421 from BioLegend.

Primary antibodies were recognized with horseradish peroxidase (HRP) conjugated antibodies (Rockland) for western blots (1:5,000 dilution), with Alexa conjugated antibodies (Molecular Probes) for immunofluorescence (1:500 dilution) or western blots (1:1,000 dilution) or with alkaline phosphatase conjugated antibodies (Southern Biotech, Birmingham, AL) for ELISAs (1:1,000 dilution).

A.2.1.4. Reagents

RT Superscript III (200U/ μ l), HotStar Taq, 0.1M DTT, One shot E. coli and S.O.C. medium, Freestyle 293 Expression Medium, Lipofectamine 2000, Opti-MEM medium, Penicillin/Streptomycin (P/S), B27 supplement, Glutamine, NCTC-109 medium, nonessential amino acids (NEAA), Dulbecco's Modified Eagle Medium (DMEM), Isopropyl-1-thio-h-d-galactopyranoside (IPTG) (15529-010), nitrocellulose membrane (88018), Fetal bovine serum (FBS) from Invitrogen. SeaPlaque agarose from BioWhittaker Molecular Applications. Streptavidin BV421 (0.1mg/ml) from BioLegend. Bio-Spin 30 Chromatography columns (732-6006), Microseal Foil MSF1001, Bradford reagent, Affi-15 resin and Affi-10 resin from Bio-Rad. Compensation Beads NC (FBS) (BD 51-90-9001291) and Compensation Beads anti Mouse Ig (BD 51-90-9001229) from BD. Thermo-grid Optically Clear PCR Plates 96 well (C18096) from Denville Scientific. PrimeRNase inhibitor (4U/ μ l) (129916), 10x CoralLoad PCR Buffer, QIAquick PCR Purification Kit and QIAGEN prep Spin miniprep kit from QIAGEN. Dimethyl sulfoxide (DMSO) and polyethylene glycol (PEG)- 4000 (9727) from MERK. Random Hexamer (3 μ g/ μ l) (27-2166-01) from Amersham Biosciences. Prime RNase Inhibitor (1U/ μ l) (0032-005-403) from Eppendorf. DNTPs: Primer Nucleotide mix (25nM each) (77119) from Affymetrix. Age IHF, Sal IHF, Xho 1, BSA 100x and Ligase from New England Biolabs. Dimethyl sulfoxide Hybri-Max (DMSO-Hybri-Max), Igepal CA-630 (N-P40), ampicillin, Thrombin from human plasma (T1063) and AP solution in tablets from Sigma. Protein-G-Sepharose (200209) and Biotinylated peptides custom made at GenScript. MAP-core and MAP-P-Epitope custom made at ANASPEC. Amicon Ultra 0.5 ml 30,000 Da, Immobilon Forte Western HRP substrate (WBLUF0500) from Millipore. Glutathione Sepharose 4 Fast Flow Media from GE.

A.2.1.5. Plasmids

Human expression vectors Igy1 or Igk were a gift of M.C. Nussenzweig, Rockefeller University and described in (Wardemann et al., 2003).

A.2.2 Methods

A.2.2.1. Mouse Monoclonal

A.2.2.1.1. Mice immunization. Mice were immunized following procedures previously described (Kowal & Diamond, 2012). The Multiple Antigenic Peptide-P-epitope (MAP-P-Epitope) for immunization consisted in a poly-lysine core with 8 branches (MAP-core) where each branch binds a modified P-Epitope (SDEDMGFGLFD-AK-core). Peptides were resuspended in sterile saline. For MAP-P-Epitope saturated TRIS was added until complete resuspension. Emulsion was prepared with a volume of 50% adjuvant 50% peptide in glass syringes at 1 mg/ml final peptide concentration. 6 to 8 weeks old BALB/c, C57/B6 H2B and C57/B6 H2D strains of mice were immunized with 100 µg of MAP-P-Epitope or MAP-Core intraperitoneally every two weeks. The first immunization was with Complete Freund's Adjuvant and the other two with Incomplete Freund's Adjuvant. Mice were bled at indicated timepoints and blood was spun at 5000 rpm for 15 min to obtain sera.

A.2.2.1.2. Hybridomas. Spleen cells of an BALB/c immunized mouse (immunized 4 times and 3 days after the last immunization) were removed by balloon technique into ice cold DMEM (High Glucose DMEM 1% P/S). Debris was allowed to separate from cells by 5 min sedimentation. Top cells were transferred to a clean tube and spun. Supernatant was removed and ice cold NH₄Cl pH 7 was added to lyse red blood cells for 10 min. Afterwards, cells were washed and resuspended in ice cold DMEM. NSO (Myeloma cells) previously grown in DMEM with 1% Sodium pyruvate, 1% Glutamine, 1% P/S, 1% NEEA and 10% FBS, were centrifuged at 400 g for 10 min, washed and resuspended in ice cold DMEM. Cells were mixed at a ratio of 3 spleen cells to 1 myeloma cell (450x10⁵/ml:150x10⁵/ml) and the

remainder spleen cells were frozen in 10% DMSO / 90% FBS. Cells were pelleted and fused in 0.5 ml of PEG in 50% saline (0.8% NaCl, 0.04% Na₂HPO₄, 0.06% NaH₂PO₄, 0.2% Glucose, 0.001% phenol red pH 7.2) for 90 s at 37°C. Afterwards, 20 ml of saline was added and left for 10 min at RT, then spun at 400 g at room temperature (RT). Cells were resuspended in complete HAT media (20% FBS, 10% NCTC-109, 1% NEEA, Hypoxanthine, Thymidine, Aminopterin, 1%P/S, in DMEM) at 3x10⁵ cells/ml. 100 µl of cell suspension was plated in 20 96-well plates and placed in a 7% CO₂ incubator at 37°C. After 7 days, cells were fed with 100 µl of HAT media. Supernatants of visible colonies were screened for P-Epitope and P0 reactivity and IgG secretion in ELISA assays. Triple positive supernatants were amplified into 24-well plates and re-screened. Positive colonies were cloned in soft agarose as follows. Warm agarose cloning media (0.28% Sea Plaque agarose in 20% FBS, 10% NCTC-109, 1% NEEA, 1% P/S, 2% HT in High Glucose DMEM with 10% J774.2 cells supernatant (mouse macrophage cell line)) was added to a 60 mm Petri dish and incubated 15 min at 4°C as an underlayer until jellification. 1,000 - 2,000 cells were re-suspended in 3 ml of warm agarose cloning media and dropped gently on top of each underlayer and placed at 4°C for 15 min and then grown in the incubator for one week. 30 clones per cell line were picked and grown into 96-well plates in cloning media and grown until supernatants were screened. Positive clones were grown into 24-well plates, then expanded to 6-well plates and then frozen in 90% FBS, 10% DMSO-Hybri-Max or complete DMEM with 20% FBS and 10%DMSO-Hybri-Max. HAT medium was used for 3 weeks then only HT then only complete DMEM.

A.2.2.2. Human Monoclonal

To obtain P-Epitope reactive memory B cells and then cloning their heavy and light chains we followed the procedures previously described with modifications (Malkiel et al., 2016; Wardemann et al., 2003)

A.2.2.2.1. Fluorescent P-Epitope preparation. 2 μg of P-Epitope-Biotin (SDEDMGFGLFDAK-biotin) was incubated with 2 μg of SAV-BV421 at 4°C overnight (ON). The unbound peptide was discarded by gel filtration using a Bio-Spin 30 column. This column was resuspended by taping and inverting, then it was opened and let stand until it was dry. The column was spun at 1,000 g for 4 min, then the fluorescent peptide was added and spun again. The flow through contained the fluorescent peptide used for staining.

A.2.2.2.2. Sorting. Frozen peripheral blood mononuclear cells (PBMCs) were thawed at 37°C and washed twice with staining buffer (HBSS, 5% FBS) spinning them at 1,300 rpm for 6 min. Cells were resuspended in 20 μl of staining buffer with the Fluorescent P-Epitope at the indicated dilution and incubated on ice for 20 min. Then, the cells were stained for 20 min on ice with the following antibody cocktail: 6 μl of CD27-PE, 2 μl of CD3/14/16-AF-700 each, 1.25 μl of IgM-PerCP Cy5.5, and 6 μl CD19-APC. Cells were washed by gently shaking them with staining buffer then spun and resuspended in 200 μl of staining buffer. For each antibody, the compensation control was prepared with one drop of negative control beads and anti-mouse Ig beads with 1 μl of antibody. The compensation of SAV-BV421 was 1 μl of CD19-BV421. The mix was incubated for 15 min then washed with 3 ml of staining buffer, then spun and resuspended in 300 μl of staining buffer. The cells were single sorted in a FACSAria II (Becton Dickinson). The sorting parameters were set with 10,000 to 15,000 cells. Then, the rest of the sample was single sorted into 96-well plates which already contained 4 μl of Lysis solution (11 units of PrimeRNase Inhibitor, 0.5x PBS, 10 mM DTT and water). The plate was immediately frozen on dry ice, sealed and stored at -80°C until further use.

A.2.2.2.3. Complementary DNA (cDNA) Preparation. To each well of single sorted cell, 3.5 μl of the following was added on ice: 150 ng of Random Hexamer, 0.5 μl of NP-40, 0.6 U of Prime RNase Inhibitor, and 2.35 μl of water. The plates were sealed and incubated

at 65°C for 60 s. Then 7 µl of PCR mix was added (3 µl of 5x RT buffer, 0.5 µl of dNTPs, 1 µl of DTT, 2.8 µl of water, 0.250 µl of Prime RNase Inhibitor (1 U/µl) and 0.25 µl of RT Superscript III). The reverse transcriptase reaction was done in a thermo cycler considering a total of 15 µl per well with the following parameters: 42°C for 5 min, 25°C for 10 min, 40°C for 60 min and 94°C for 5 min. After the reaction the plate was stored at -20°C until further use.

A.2.2.2.4. Immunoglobulin variable region amplification. Immunoglobulin heavy chain (IgH) (γ only) and immunoglobulin light chain (IgL) (κ and λ) transcripts were amplified in 2 rounds of PCR as follows. First amplification round: To each well, 2 µl of cDNA were added with 38 µl of the corresponding PCR mix (32.7 µl of water, 4.5 µl of 10x Taq buffer, 0.28 µl of dNTPs, 0.15 µl of 5' primer mix, 0.15 µl of 3' primer mix and 0.21 µl of HotStar Taq). Primer mixes were prepared at equal concentrations of indicated primers from a 50 µM stock solution. Primers and their sequences are detailed in Table A.1. For γ chain amplification the 5' primer mix was: 5'LVH1, 5'LVH3, 5'LVH4/6 and 5'LVH5 primers. For 3' the primer was 3'CyCH1. For κ chain amplification the 5' primer mix was: 5' LVκ1/2, 5' LVκ3 and 5' LVκ4. For 3' the primer was 3'Cκ543. For λ chain amplification the 5' primer mix was: 5' L Vλ1, 5' L Vλ2, 5' L Vλ3, 5' L Vλ4/5, 5' L Vλ6, 5' L Vλ7 and 5' L Vλ8 primers. For 3' the primer was 3' Cλ. The amplification reaction was done in a thermo cycler with the following parameters: 94°C for 5 min, 50 cycles at 94°C for 30 s, 57°C for 30 s (60°C for λ) and 72°C for 55 s and finally 10 min at 72°C and then 4°C. Second amplification round: To each well, 5 µl of the product for the first amplification were added with 38 µl of the corresponding PCR mix (33 µl of water, 4.5 µl of 10x Coral Buffer, 0.48 µl of dNTPs, 0.15 µl of 5' primer mix, 0.15 µl of 3' primer mix and 0.21 µl of HotStar Taq). For γ chain amplification the 5' primer mix was: 5' Agel VH1, 5' Agel VH1/5, 5' Agel VH3, 5' Agel VH4, 5' Agel VH3-23 and 5' Agel VH4-34 primers. For 3' the primer was 3'IgG Internal. For κ chain amplification the 5' primer was 5' Pan Vκ. For 3' the primer was 3' Cκ494. For λ chain amplification the 5' primer mix was: 5'

Agel V λ 1, 5' Agel V λ 2, 5' Agel V λ 3, 5' Agel V λ 4/5, 5' Agel V λ 6, 5' Agel V λ 7/8. For 3' the primer was 3' XhoI C λ . The amplification reaction was done in a thermo cycler with the following parameters: 94°C for 5 min, 50 cycles at 94°C for 30 s, 57°C for 30 s (60°C for lambda) and 72°C for 55 s and finally 72°C for 10 min and then 4°C. The PCR products were run in a TBE 1.5% Agarose gel. PCR products were sequenced at Keck DNA Sequencing Facility, Yale University and analyzed using IgBLAST (<http://www.ncbi.nlm.nih.gov/igblast/>).

A.2.2.2.5. Cloning amplification round. Complete in-frame sequences were cloned into human expression vectors Igy1 or Igk as previously described (Wardemann et al., 2003). To each well 5 μ l of immunoglobulin cDNA were added with 38 μ l of PCR mix (33 μ l of water, 4.5 μ l of 10x Coral buffer, 0.48 μ l of dNTPs, 0.23 μ l of HotStar Taq). Finally, 1 μ l of 5' or 3' specific primers from Table A.1 were used according to the V or J specific sequence of each obtained cDNA. If the sequence did not match a primer on the list, a mix of primers was used with all the primers at the same concentration. The plate was spun and sealed with foil. The reaction was done in a thermo cycler with the following parameters: 94°C for 5 min, then 50 cycles at 94°C for 30 s, 57°C for 30 s (60°C for Lambda) and 72°C for 45 s then 72°C for 10 min and finally 4°C. The products were run in a TBE 1.5% Agarose gel.

A.2.2.2.6. Cloning. The products obtained on the cloning round were purified with QIAquick PCR Purification Kit following manufacturer's instructions. For the digestion, 30 μ l of purified PCR product was incubated with 20 μ l of digestion mix (5 μ l of 10x corresponding buffer, 0.5 μ l of BSA, 0.5 μ l of each corresponding enzyme and 13.5 μ l of water). For γ chains: buffer 4 and Age IHF and Sall IHF enzymes. For λ chains: buffer 4 and Age IHF and XHO1 enzymes. For κ chains: buffer 1 and Age IHF enzymes. The reaction was incubated for 2 h at 37°C then at 4°C. For κ chains a second digestion was needed adding to the reaction 2 μ l of BsiWI and then the reaction was incubated at 55°C for 2 h then at 4°C. The digested DNA was purified with QIAquick PCR Purification Kit following manufacturer's

instructions. The ligation reaction was prepared with 30 ng of DNA in 10 μ l of water and 2 μ l of 10x Ligase buffer, 0.3 μ l of Vector (either γ or κ , λ chains can be cloned on κ), 0.5 μ l of Ligase and 7.5 μ l of water. The plate was sealed and incubated at 16°C for 4 h then 4°C.

A.2.2.2.7. Transformation. 6 μ l of One shot E. coli competent bacteria was added per well into a 96 well plate with 2 μ l of ligation product. The plate was incubated on ice for 30 min then 30 s at 42°C. 100 μ l of S.O.C. medium was added per well and then the plate was incubated in a shaker for 1 hour at 37°C. Finally, all the reaction was spread into Luria Broth (LB)/Agar plates with Carbamacepin (100 μ g/ml) and incubated ON at 37°C. Positive colonies were checked with a PCR reaction as follows. For each well, a sample of each colony was mixed with: 22.37 μ l of water, 2.5 μ l of 10x Coral buffer, 0.125 μ l of DNTPs, 0.2 μ l of HotStar Taq, and 0.2 μ l of 5' and 0.2 μ l of 3' specific primers. For γ the 5' primer was 5Ab sense and 3' primer was 3 IgG (internal). For κ the 5' primer was 5Ab sense and the 3' primer was 3 Ck 494. The reaction was done in a thermo cycler with the following parameters: 5 min at 95°C, 25 cycles at 94°C for 30 s, 58°C for 30 s and 72°C for 59 s, then 10 min at 72°C and then 4°C. 5 μ l of product was run on an Agarose gel.

A.2.2.2.8. Miniprep. Positive colonies were grown in 3 ml of LB Carbamazepine (100 μ g/ml) ON at 37°C in the shaker. Colonies were centrifuged at 3200 rpm for 10 min and plasmids were obtained using QIAGEN prep Spin miniprep kit following manufacturer's instructions. The plasmids were analyzed by sequencing and IgBlast. Plasmids chosen for transfection were those with correct product length and in-frame sequences.

A.2.2.2.9. HEK 293-T transfections for antibody production. Cells were plated (3 to 5 million cells) the day before in 10 cm culture dishes in complete media (DMEM, 5% FBS, P/S). Few hours before the transfection, cells were washed with PBS and the media was changed to 10 ml Freestyle293, a protein-free expression medium, supplemented with P/S. The transfection reaction was prepared in 1 ml of OPTI-MEM adding 5 μ g of each heavy

chain and light chain plasmid. The solution was mixed and then 25 μ l of Lipofectamine 2000 was added. The mix was incubated for 15-30 min at RT then added on top of the cells in drops. Transfected cells were maintained in the incubator and supernatants were collected after 7 days.

A.2.2.3. Cellular biology techniques

A.2.2.3.1. HEK-293 Immunofluorescence. HEK-293T were plated the day before (30,000 cells per 12 mm cover). Cells were softly rinsed with PBS with 0.1 mM CaCl_2 and 1 mM MgCl_2 (PBS-CM) and fixed in freshly prepared 4% paraformaldehyde (PFA) in PBS for 30 min at RT. Then, cells were washed and permeabilized, only if indicated, with 0.2% Triton X-100 in PBS and then incubated in blocking buffer (0.2% Gelatin PBS) for 30 min at room temperature (RT). Supernatants, purified antibody or sera, as indicated, were incubated for 30 min at 37°C, washed and then incubated with anti-human-555 for 30 min at 37°C, then washed and mounted with Fluoromont. Digital images were acquired on a Zeiss Axiophot microscope using the 63x immersion objective and a 14 bit Axiocam camera and a Axiovision imaging software.

A.2.2.4. Biochemical techniques

A.2.2.4.1. Fusion protein-GST and recombinant protein production.

Recombinant proteins and fusion proteins were obtained following previously described procedures (Carcamo et al., 2006). Transformed Bacteria with pGEX-4T-3 (Pharmacia Biotech) plasmid with P0 protein were grown ON in LB supplemented with ampicillin (50-100 μ g/ml) (LB-amp) at 37°C in agitation. Then a 1:100 dilution was made also in LB-amp and grown for 2.5 h. Afterwards, IPTG was added at 0.1 mM final concentration for 4 h at 30°C for P0-GST. Medium was centrifuged in 250 ml aliquots at 5000 rpm for 10 min, the supernatants were discarded, and the bacterial pellets were frozen at -80°C until further use. Pellets were resuspended in 2 ml of STE buffer (10 mM Tris-Cl pH 8, 150 mM NaCl and 1 mM EDTA) with

bacterial antiproteases cocktail concentration of 1x per 100 ml of initial culture. Lysozyme was added for 30 min at 100 µg/ml on ice. DTT at 5 mM and Sarkosyl at 1.5% final concentration was added. The resuspension was sonicated and then incubated for 30 min at 4°C in agitation. Lysates were centrifuged at 12,000 g for 10 min and the supernatants were collected. Triton 100x was added at a final 4% concentration. Lysates were incubated with 125 µl Glutathion-Sepharose per 250 ml of initial culture previously washed twice with PBS, for 2 h at 4°C in rotation. Afterwards, the beads were washed at least 5 times with PBS and centrifuged at 500 g. If elution was needed, 1 U of Thrombin is used per 50 µl of beads for 30 min for P0. The beads are centrifuged at 500 g for 5 min and the protein was measured with Bradford.

A.2.2.4.2. Gel electrophoresis and western blot. Protein samples were resolved in sodium dodecyl sulfate polyacrylamide gel electrophoresis (SDS-PAGE) at different percentages depending on the protein of interest. Loading buffer contained DTT as a reducing agent except for antibody samples as indicated. After electrophoresis, samples were transferred into a nitrocellulose membrane in 25 mM Tris-HCl, Glycine 192 mM and 20% methanol at 450 mA for 1-2 h depending on the analyzed protein. After transferring, membranes were blocked with PBS-5% skim milk for 1 h at RT. Primary antibodies were incubated 2 h at RT in blocking buffer and then washed five times for 10 min with PBS 0.5% Tween 20. Secondary antibodies conjugated with horseradish peroxidase (HRP) or Alexa were incubated 1 h in blocking buffer then washed. HRP conjugated antibodies were developed with chemiluminescent HRP substrate following manufacturer's instructions. Chemiluminescent or fluorescent images were acquired in G:Box gene tools detection system (Syngene) with the corresponding filter.

A.2.2.4.3. Enzyme-linked immunosorbent (ELISA) assays. ELISA assays were performed following procedures as previously described (Kowal & Diamond, 2012) with some

modifications. For biotinylated peptides, plates were pre-coated with 50 μ l of unlabeled Streptavidin (25 μ g/ml) in Carbonated buffer (0.1 M NaHCO₃, pH 8.6), ON at 4°C then washed once in PBS 0.05% Tween-20 (PBS-T). Plates were blocked with 200 μ l of blocking buffer (1 x PBS, 1% BSA) for 1 h at RT and in agitation. Biotinylated peptides were added in 100 μ l at 5 μ g/ml in 1 x PBS, 0.2% BSA for 1 h at RT in agitation. For non-biotinylated coating, 100 μ l of P-Epitope (15 μ g/ml), anti-mouse or human IgG (5 μ g/ml) or P0 (0.5 μ g/ml) in carbonated buffer were incubated ON at 4°C then washed and blocked as above. All antigens were washed once, then 100 μ l of sample was added at the following dilutions: sera 1:200, plasma 1:100, supernatant or purified antibody as indicated in blocking buffer. After 1 hour at RT in agitation, samples were washed 4 times and then anti-human or mouse, accordingly, coupled to Alkaline phosphatase was incubated in 100 μ l per well for 1 h at RT in agitation. Secondary was washed 4 times and developed with 100 μ l of developing solution (5 ml of 0.05 M Na₂CO₃ and 0.001 M MgCl₂ in water and 1 tablet of AP solution) then absorbance was read at 405 nm.

A.2.2.4.4. Antibody purification. The resin for affinity purification was prepared as follows. 1 ml of Affi-15 was washed once with 15 ml of isopropanol then twice with DMSO with centrifugations at 1000 rpm for 5 min. Then, the resin was incubated with 1 mg of peptide in DMSO for 3 h at 4°C then centrifuged and washed with PBS. 1 ml of PBS and 200 μ L of ethanolamine/1 M HCl (freshly prepared with 61 μ l ethanolamine and 939 μ l HCl 1 N) was added for 1 h at 4°C then extensively washed with PBS and stored in 0.05% sodium azide PBS until further use. Before use, the resin was washed extensively with PBS and then, patient serum was incubated at 4°C ON. The resin and sera were centrifuged at 1000 rpm, serum was recuperated, and the resin was washed extensively with PBS. 10 ml of 0.1-0.2 M Glycine HCl pH 2.5-3 was added and eluates were collected in 400 μ L fractions with 125 μ L of 1M K₂HPO₄. The fractions were vortexed and rapidly put on ice. To determine the fractions

to be concentrated 5 μ l of each elution was sampled on a dot blot. Fractions were spun on Amicon Ultra 0.5 ml 30,000 Da at 14,000 g for 5 min. After concentrating the fractions of interest, the buffer was exchanged for PBS 3 times. Concentration was measured with Bradford. The procedure was similar for monoclonal antibody purification or control immunoglobulin, but supernatants or control sera were incubated with 100 μ l of Protein G-Sepharose previously washed 3 times with PBS ON at 4°C, the elution procedure was the same as above.

A.2.2.5. Animal procedures

A.2.2.5.1. Electrophysiology. Acute coronal slices from adult wild type male and female mice were prepared and recorded as described in (Oliva & Inestrosa, 2015). Immediately after removal, the brains were placed in ice cold cutting solution (85 mM NaCl, 75 mM Sucrose, 3 mM KCl, 1.25 mM NaH₂PO₄, 25 mM NaHCO₃, 10 mM Glucose, 3.5 mM MgSO₄, 0.5 mM CaCl₂, 3 mM Na-Pyruvate, 0.5 mM Na-Ascorbate, 305 mOsm, pH 7.4) thoroughly oxygenated with 95% O₂/5% CO₂. 350 μ m brain slices were obtained and left at 36°C for 30 min for recovery then placed in oxygenated recording solution (126 mM NaCl, 3.5 mM KCl, 1.25 mM NaH₂PO₄, 25 mM NaHCO₃, 10 mM Glucose, 2 mM MgSO₄, 2 mM CaCl₂, 3 mM Na-Pyruvate, 0.5 mM Na-Ascorbate, 305 mOsm, pH 7.4) at RT. For recording, slices were placed in a submerged-style chamber in recording solution at 30-32°C. Schaffer collaterals between CA3 and CA1 were stimulated with a bipolar concentric electrode (World Precision Instruments, Sarasota, FL, United States) connected to an ISO-Flex stimulus generator (A.M.P.I., Jerusalem, Israel). Evoked field excitatory postsynaptic potentials (fEPSPs) were recorded in the stratum radiatum of CA1, using a borosilicate glass electrode (World Precision Instruments, United States) of 0.5-1 M Ω pulled on a P-97 Flaming/Brown Micropipette Puller (Sutter Instruments, United States) filled with the recording solution. The signals were recorded using a MultiClamp 700B amplifier (Axon CNS, Molecular Devices

LLC, United States), and digitally sampled at 30 kHz using a Digidata-1440A interface (Axon CNS, Molecular Devices). Two pulses (R1 and R2) separated 50 ms each, were applied with the stimulus generator every 15 s for monoclonal antibodies supernatants or 60 s for the purified antibody. The fEPSP slope of the first pulse (R1) was averaged during 15 to 20 min and once a stable basal signal was obtained, the corresponding treatments were added. The analyses were done offline using pClamp 10.3 (Molecular Devices LLC, United States).

Table A.1: Primer sequences for amplification and cloning of the variable regions of heavy and light immunoglobins chains.

Primer	Sequence	Nucleotides
Heavy Chain 1st PCR		
5 L-VH 1	ACAGGTGCCCACTCCCAGGTGCAG	24
5 L-VH 3	AAGGTGTCCAGTGTGARGTGCAG	23
5 L-VH 4/6	CCCAGATGGGTCTCTGCCAGGTGCAG	27
5 L-VH 5	CAAGGAGTCTGTTCCGAGGTGCAG	24
3 C γ CH1	GGAAGGTGTGCACGCCGCTGGTC	23
Heavy Chain 2nd PCR		
5 AgeI VH1	CTGCAACCGGTGTACATTCCCAGGTGCAGCTGGTGCAG	38
5 AgeI VH1/5	CTGCAACCGGTGTACATTCCGAGGTGCAGCTGGTGCAG	38
5 AgeI VH 1-18	CTGCAACCGGTGTACATTCCCAGGTTCAGCTGGTGCAG	38
5 AgeI VH 1-24	CTGCAACCGGTGTACATTCCCAGGTCCAGCTGGTACAG	38
5 AgeI VH3	CTGCAACCGGTGTACATTCTGAGGTGCAGCTGGTGGAG	38
5 AgeI VH3-11	CTGCAACCGGTGTACATTCTCAGGTGCAGCTGGTGGAG	38
5 AgeI VH3-23	CTGCAACCGGTGTACATTCTGAGGTGCAGCTGTTGGAG	38
5 AgeI VH3-33	CTGCAACCGGTGTACATTCTCAGGTGCAGCTGGTGGAG	38
5 AgeI VH 3-9	CTGCAACCGGTGTACATTCTGAAGTGCAGCTGGTGGAG	38
5 AgeI VH4	CTGCAACCGGTGTACATTCCCAGGTGCAGCTGCAGGAG	38
5 AgeI VH 4-34	CTGCAACCGGTGTACATTCCCAGGTGCAGCTACAGCAGTG	40
5 AgeI VH4-39	CTGCAACCGGTGTACATTCCCAGGTGCAGCTGCAGGAG	38
5 AgeI VH 6-1	CTGCAACCGGTGTACATTCCCAGGTACAGCTGCAGCAG	38
3 Sall JH 1/2	TGCGAAGTCGACGCTGAGGAGACGGTGACCAG	32
3 Sall JH 3	TGCGAAGTCGACGCTGAAGAGACGGTGACCATTG	34
3 Sall JH 4/5	TGCGAAGTCGACGCTGAGGAGACGGTGACCAG	32
3 Sall JH 6	TGCGAAGTCGACGCTGAGGAGACGGTGACCGTG	33
3 IgG (internal)	GTTCCGGGAAGTAGTCCCTTGAC	22
λ Light Chain 1st PCR		
5 L VL1	GGTCCTGGGCCAGTCTGTGCTG	23
5 L VL2	GGTCCTGGGCCAGTCTGCCCTG	23
5 L VL3	GCTCTGTGACCTCCTATGAGCTG	23
5 L VL4/5	GGTCTCTCTCSCAGCYTGTGCTG	23
5 L VL6	GTTCTTGGGCCAATTTTATGCTG	23
5 L VL7	GGTCCAATTCYCAGGCTGTGGTG	23
5 L VL8	GAGTGGATTCTCAGACTGTGGTG	23
3 CL	CACCAGTGTGGCCTTGTGGCTTG	24
λ Light Chain 2nd PCR		
5 AgeI VL1	CTGCTACCGGTTCCCTGGGCCAGTCTGTGCTGACKCAG	38
5 AgeI VL2	CTGCTACCGGTTCCCTGGGCCAGTCTGCCCTGACTCAG	38
5 AgeI VL3	CTGCTACCGGTTCTGTGACCTCCTATGAGCTGACWCAG	38
5 AgeI VL4/5	CTGCTACCGGTTCTCTCTCSCAGCYTGTGCTGACTCA	37
5 AgeI VL6	CTGCTACCGGTTCTTGGGCCAATTTTATGCTGACTCAG	38
5 AgeI VL7/8	CTGCTACCGGTTCCAATTCYCAGRCTGTGGTGACYCAG	38
3 XhoI CL	CTCCTCACTCGAGGGYGGGAACAGAGTG	28
κ Light Chain 1st PCR		
5 L Vk1/2	ATGAGGSTCCCYGCTCAGCTGCTGG	25
5 L Vk3	CTCTTCTCCTGCTACTCTGGCTCCCAG	28
5 L Vk4	ATTTCTCTGTTGCTCTGGATCTCTG	25
3 Ck543	GTTTCTCGTAGTCTGCTTTGCTCA	24
κ Light Chain 2nd PCR		
5 Pan Vk	ATGACCCAGWCTCCABYCWCCCTG	24
3 Ck 494	GTGCTGTCTTGTCTGCTCTGCT	22
Insert check - PCR		
5 Ab-sense	GCTTCGTTAGAACGCGGCTAC	21
3 IgG (Internal)	GTTCCGGGAAGTAGTCCCTTGAC	22

A.3. RESULTS

A.3.1 Murine monoclonal antibodies

BALB/c, C57/B6 H2B and C57/B6 H2D strains of mice were immunized with a multiple antigenic peptide consisting in a poly-lysine core that has 8 branches of synthetic P-Epitope (MAP-P-Epitope). Between the lysine core and the P-Epitope we added an alanine for space. The immunization protocol included an intraperitoneal injection of 100 µg of MAP-P-Epitope or only the MAP-Core as control. These reagents were injected every two weeks, one time in complete Freund's Adjuvant and twice with Incomplete Freund's Adjuvant. We tested sera for reactivity against P0 and P-Epitope using ELISA or immunoblot assays and found that BALB/c, but not C57/B6 H2B or C57/B6 H2D mice, generated anti-P antibodies (Fig. A.1A and A.1B). After fusing splenocytes from a BALB/c mouse with NSO cells, we screened ~880 colonies and amplified 97 positives for mouse IgG production and P-Epitope and P0 recognition. Next, we subcloned 38 colonies and then chose 13 of them for further analysis. Finally, considering the highest binding on ELISA tested against the P-Epitope, we chose 2 hybridomas (8A1 and 8C1) (Fig. A.1C). Supernatants blotted against anti-mouse secondary antibodies demonstrated that only 8C1 had assembled antibody (Fig. A.1D). Supernatant of 8C1 cells did not show immunoblot reaction against P0 protein (Fig. A.1E), but nevertheless it increased field excitatory post synaptic potentials (fEPSP) in the CA3-CA1 hippocampal circuit in mouse brain slices, contrasting with the negative result of 8A1 supernatant used as control (Fig. A.1F). This effect mimicked the effect previously described for polyclonal human-anti-P antibodies (Segovia-Miranda et al., 2015).

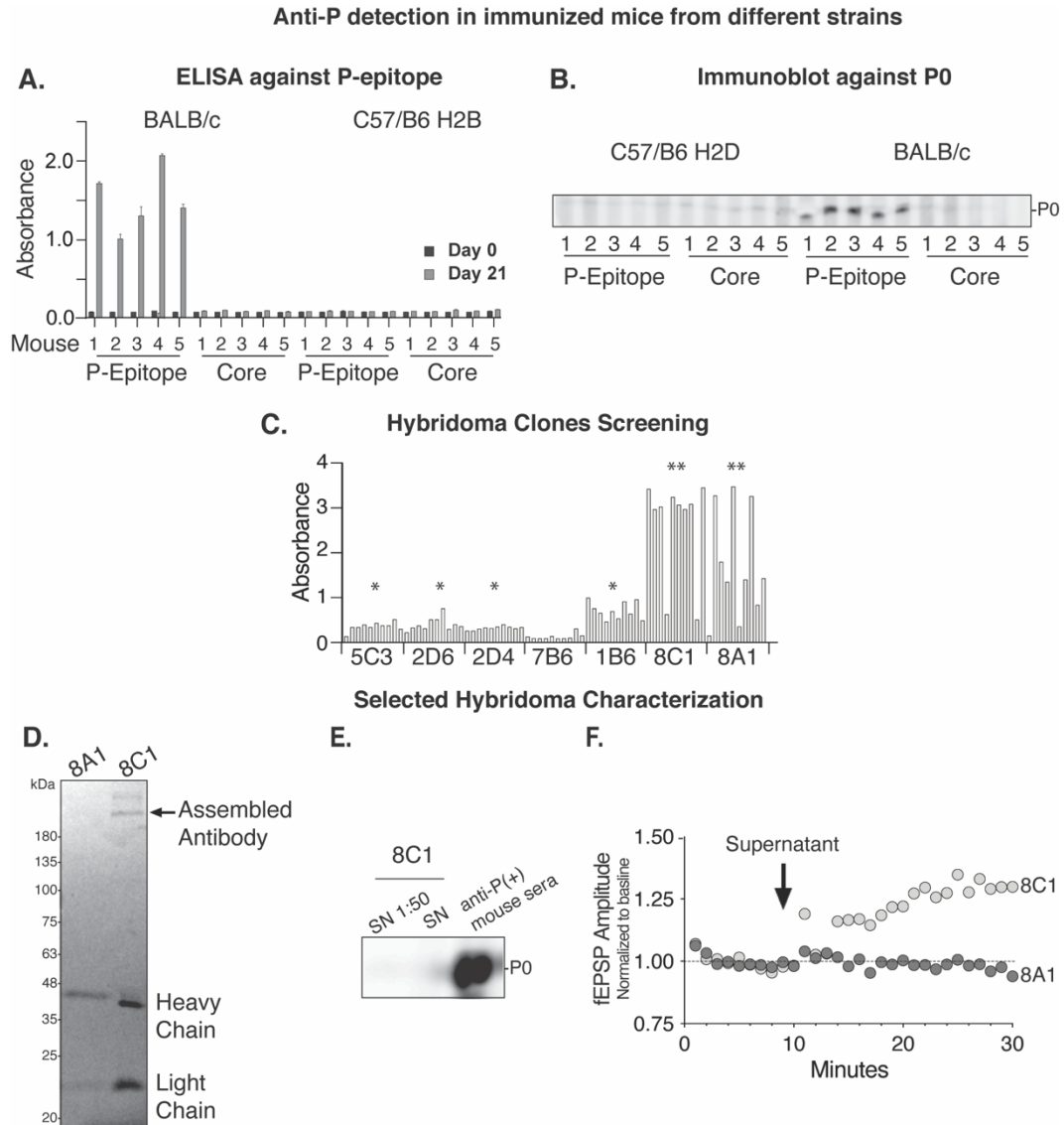


Figure A.1: Mouse monoclonal antibodies. Mice immunization. **A** and **B**. BALB/c, C57/B6 H2B and C57/B6 H2D mice were immunized with MAP-Core or MAP-P-Epitope and tested after 21 days for anti-P antibodies by ELISA against P-Epitope (**A**) and immunoblot against P0 (**B**). Only BALB/c immunized with MAP-P-Epitope produced anti-P antibodies (n=3; Graph shows absorbance of mean and SEM of duplicates of representative experiment). **C**. Hybridoma clones screening. The graph illustrates an example of absorbance in supernatants from different clones tested with P-Epitope ELISA after subcloning. (*) Indicates clones chosen for expansion and freezing. (**) Indicates clones further characterized for anti-P reactivity. **D**, **E** and **F** depict characterization of hybridomas 8A1 and 8C1. **D**. Non-reducing immunoblot of 40 μ l of supernatant probed with anti-mouse-555 secondary antibody shows assembled immunoglobulin (arrow) only in 8C1 sample (n=3). **E**. 8C1 supernatant at 1:50 dilution or directly tested does not recognize P0 in an immunoblot (n=3). **F**. Electrophysiology of hippocampal CA3-CA1 circuit in mouse brain slices shows that only 8C1 supernatant (1:10 dilution) increases fEPSP (n=1; Graph shows mean and SEM of amplitude normalized to baseline).

A.3.2 Human monoclonal antibodies

To obtain human monoclonal antibodies we isolated memory B cells expressing anti-P IgG at the cell surface from a SLE patient, performed single cell RT-PCR to obtain their cDNA from which we amplified the encoding variable regions of the heavy and light immunoglobulin chains, and cloned each cDNA into a human immunoglobulin expression vector for transfection in HEK-293 cells.

To select and sort the anti-P memory B cells, we incubated peripheral blood mononuclear cells (PBMC) from a SLE patient positive for anti-P antibodies, with a biotinylated P-Epitope coupled to a streptavidin fluorophore and sorted them by FACS. Firstly, we screened the best biotinylated peptide with an ELISA assay including Biotin-GLESEE-SDEDMGFGLFD, SDEDMGFGLFD-AK-Biotin and Biotin-SDEDMGFGLFD-AK. SDEDMGFGLFD-AK-Biotin gave the best detection signal (Fig. A.2). To set the sorting parameters, we used PBMCs from an anti-P (-) SLE sample for background setting and we isolated by cell sorting the subpopulation of memory B cells expressing anti-P IgG at the cell surface (Fig. A.3 and Table A.2). The amplification of the heavy and light chain of single cells is shown in Figure A.4A. After an additional round of cDNA amplification, we finally subcloned 13 antibody cDNAs (Fig. A.4B), which then were tested for immunoglobulin production by co-transfection into HEK-293 cells (Fig. A.4C and A.4D). We analyzed the supernatants for anti-P reactivity by ELISA using P0 and P-Epitope and by immunoblot using P0 (Fig. A.4E and A.4F). The sequences of the hypervariable region of the obtained immunoglobulins are shown in Figure A.4G. We chose human clone 12 (hmabC12) for further analysis.

Indirect immunofluorescence of permeabilized HEK-293 cells stained with hmabC12 showed perinuclear and speckled staining compatible with anti-P ribosomal pattern (Fig. A.5A). Cell surface hmabC12 staining in non-permeabilized cells showed the typical

regionalized pattern of the staining with human affinity purified anti-P antibodies (Fig. A.5B) (Bravo-Zehnder et al., 2014; Matus et al., 2007).

Finally, we examined the supernatant of hmabC12 on CA3-CA1 hippocampal synaptic transmission fEPSP. The supernatant of hmabC12 transfected HEK-293 cells, used at 1/10 dilution, increased synaptic transmission, similar to anti-P (+) serum (Fig. A.5C). Purified monoclonal (0.25 µg/ml) showed similar results (Fig. A.5D).

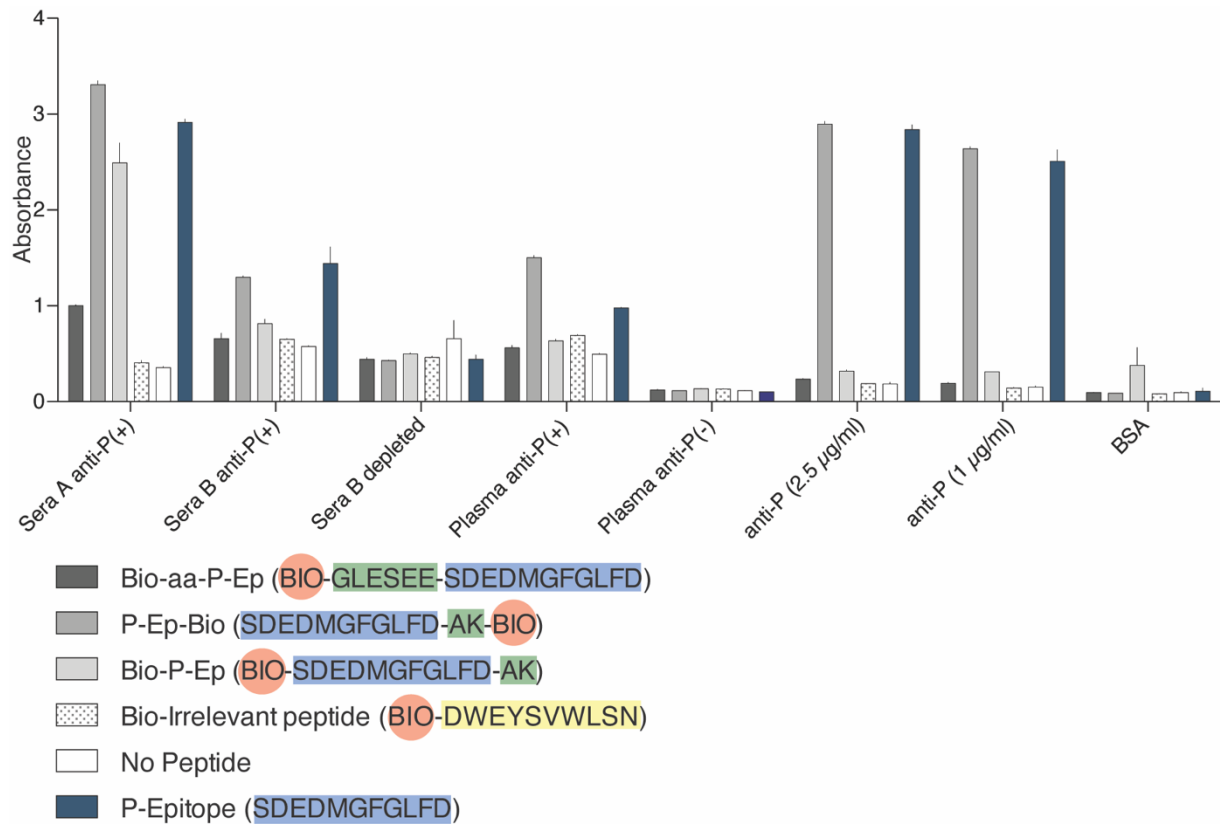


Figure A.2: C-terminal biotinylated P-Epitope as the best choice for detecting anti-P memory B cells. Three different biotinylated P-epitope peptides were compared with an irrelevant biotinylated peptide and the P-epitope without biotinylation in an ELISA assay using positive and negative anti-P antibodies samples, as indicated. SDEDMGFGLFD-AK-BIO was the biotinylated peptide recognized with highest affinity (n=2, Graph shows mean and SEM of duplicates representative of a experiment).

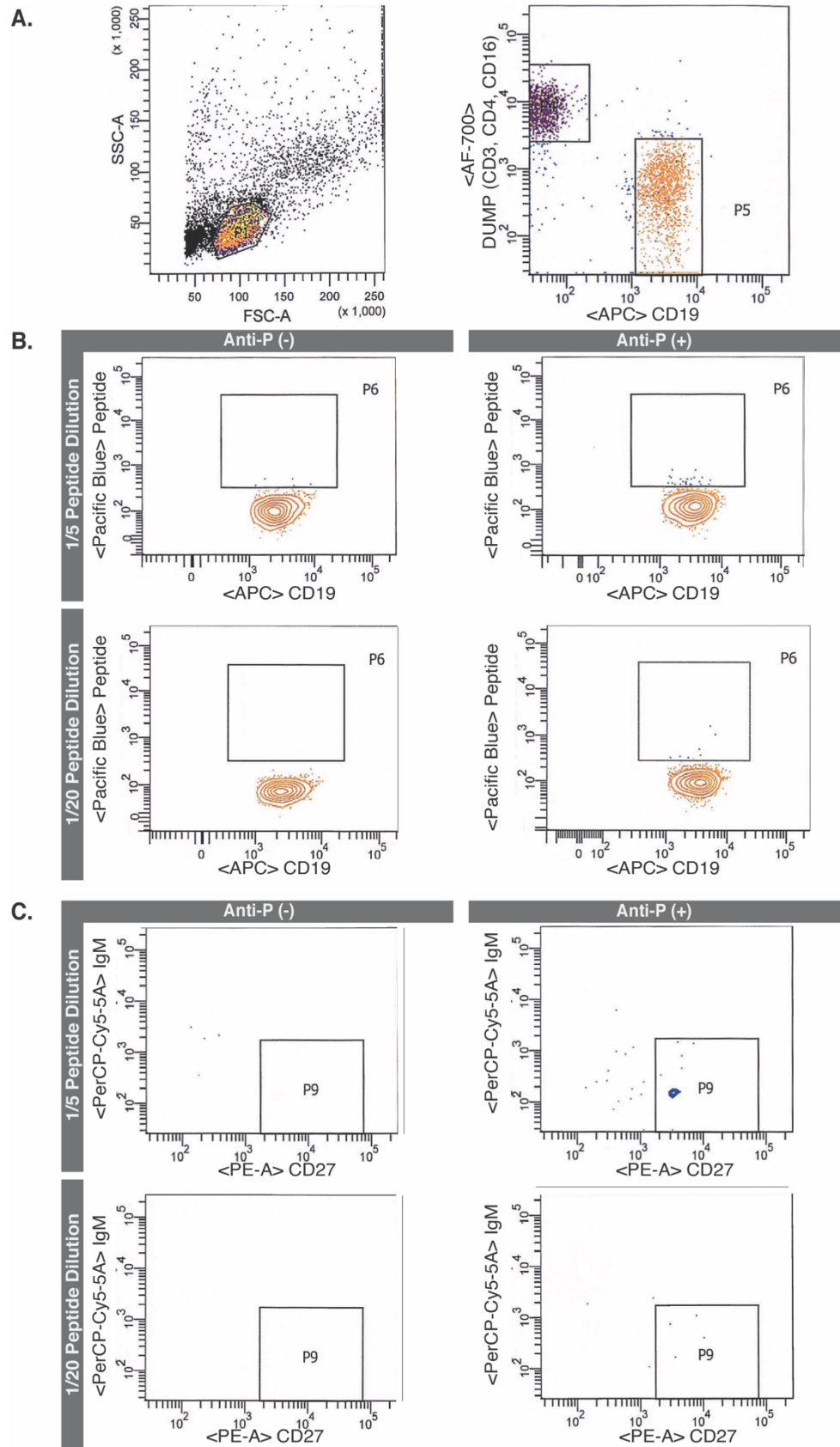
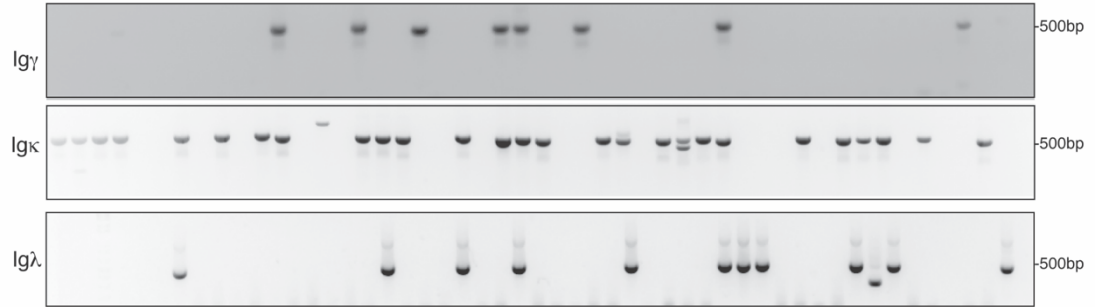


Figure A.3: Cell sorter setup for the identification of memory B cells expressing cell surface anti-P-IgG. PBMCs (10,000 to 15,000 cells) from an anti-P (+) and an anti-P (-) SLE patient were used to set the sorting parameters. **A.** Gate for B cells. After gating by size (P1) and eliminating doublets, CD19+ (B cells) population (P5) was gated against a dump gate consisting in anti-CD3+ (T cells), CD4+ (T helper cells, monocytes, macrophages and dendritic cells) and CD16+ antibodies (neutrophils, natural killer cells and macrophages). **B.** Anti-P (+)-B cells identification. Anti-P (+) cells were identified with the biotinylated P-Epitope (SDEDMGFGLFD-AK-BIO) coupled to Brilliant Violet streptavidin (Pacific Blue channel) at two dilutions, 1/5 and 1/20 as indicated (P6). False positives were excluded by using the anti-P (-) patient's PBMCs to establish the gate. **C.** Anti-P-IgG (+) memory B cells identification. From the peptide positive population (P6), IgG (+) memory B cells were identified as IgM (-) and CD27+ (memory B cells) (P9). These parameters were used to single sort cells into a 96 well plate.

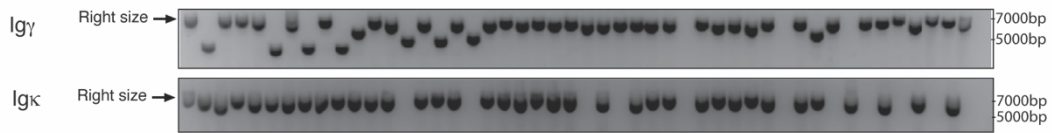
Table A.2: Summary of populations obtained when setting the cell sorting parameters.

Sera	Anti-P (-)	Anti-P (+)	Anti-P (-)	Anti-P (+)
Peptide dilution	Dilution 1/5	Dilution 1/5	Dilution 1/20	Dilution 1/20
Events	10,000 (100%)	10,000 (100%)	15,000 (100%)	10,360 (100%)
Non-B cells	5,049 (50.5%)	3,977 (39.8%)	6,460 (43.1%)	3,679 (35.5%)
B-cells	1,010 (10.1%)	1,947 (19.5%)	1,111 (7.4%)	1,980 (19.1%)
Tetramer (+) B cells	5 (<0.1%)	24 (0.2%)	0 (0%)	7 (0.1%)
Tetramer (+) Memory B cells	0 (0%)	9 (0.1%)	0 (0%)	4 (<0.1%)

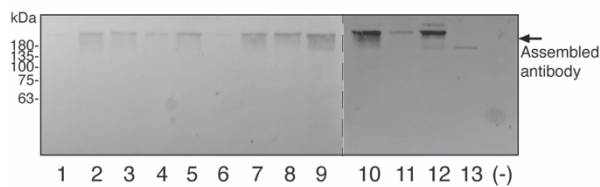
A. Heavy and light chain variable region amplification



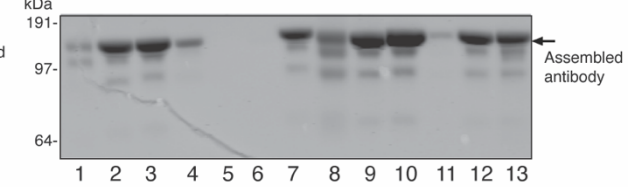
B. Plasmids



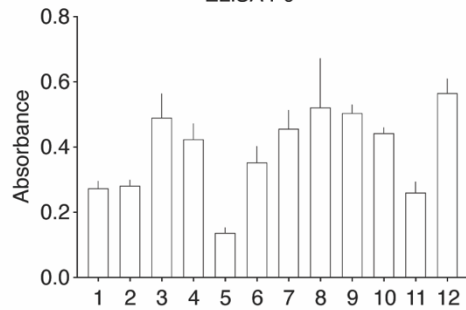
C. Immunoblot of antibodies secreted by HEK-293 cells



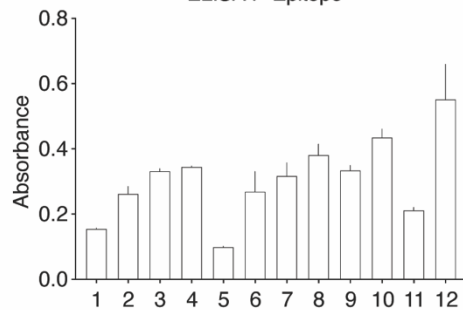
D. Purified IgGs secreted by HEK-293 cells



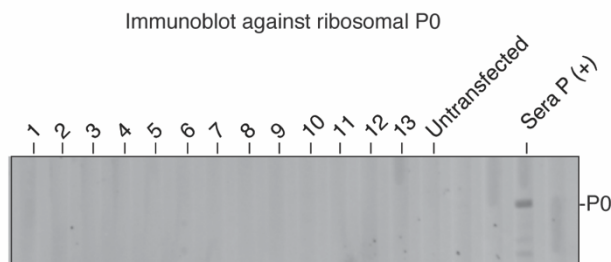
E. ELISA P0



ELISA P-Epitope



F.



G. Hypervariable region sequences for each cloned antibody

#	Gamma CDR3	Kappa CDR3
1	CGAPNLYYDFD	QQCSNWPRT
2	AREHSYGLDN	MQGIQLYS
3	AAYCSSTNCHQGTYAFDI	QQYGSSSHYS
4	ARTDY	QQYGNSPRYS
5	MTKGRDIGDNSVPH	HQYYSPPFA
6	VRVDILVVPAGDLDFDI	QQSYSPPLT
7	ARSPTLNSGWYVYYMDV	QQTHTPYT
8	ARGDYVAGYFDY	QQYNYWPRT
9	ARVLGKYRGEVFWHGVFDP	QQYSSHSPYS
10	DYGRILLSEQRPRISLPRILPA	QQYNSYSPLT
11	ARGSGSYGSDY	QQSYTTPET
12	ARRGEYCSSVNCPDFDY	QQSYSKFRS
13	TTKTGIVGGQGFY	QQYNNWPPGDS

Figure A.4: Human anti-P monoclonal antibody cDNAs cloned from single sorted memory B cells. **A.** PCR-amplified immunoglobulin cDNAs. Single memory B cells isolated from the cell sorter were subjected to RNA reverse transcription and two amplification rounds of Ig γ , Ig λ and Ig κ variable region using specific combination of primers. The products are shown by agarose gel electrophoresis. **B.** Cloned products. After another round of amplification, the products were cloned in expression vectors that contain the constant region of heavy or light chains. Figure shows different cloned heavy and light chain plasmids. **C** and **D.** Antibody production in transfected HEK-293 cells. Heavy and light chain plasmids paired from an initial cell, were co-transfected in HEK-293 cells and after 7 days the supernatants were analyzed by non-reducing immunoblot and probed with anti-Human-555 secondary antibody. High molecular bands reflect assembled human antibody (arrow) (**C**). **D.** Antibodies purified with Protein G and stained with Coomassie blue after gel electrophoresis in non-reducing conditions. Bands correspond to assembled antibody. **E.** ELISA against P-Epitope and P0. Recombinant antibodies generated in transfected HEK-293 recognize the P-Epitope and P0 in ELISA. (n=3; Graph shows absorbance of mean and SEM of duplicates of representative experiment). **F.** Immunoblot against P0 show no reactivity (n=3). **G.** Sequence of hypervariable region (CDR3) of cloned antibodies. Heavy and light chains were sequenced and blasted in IgG blast. The table shows the CDR3 of each pair of the obtained antibodies.

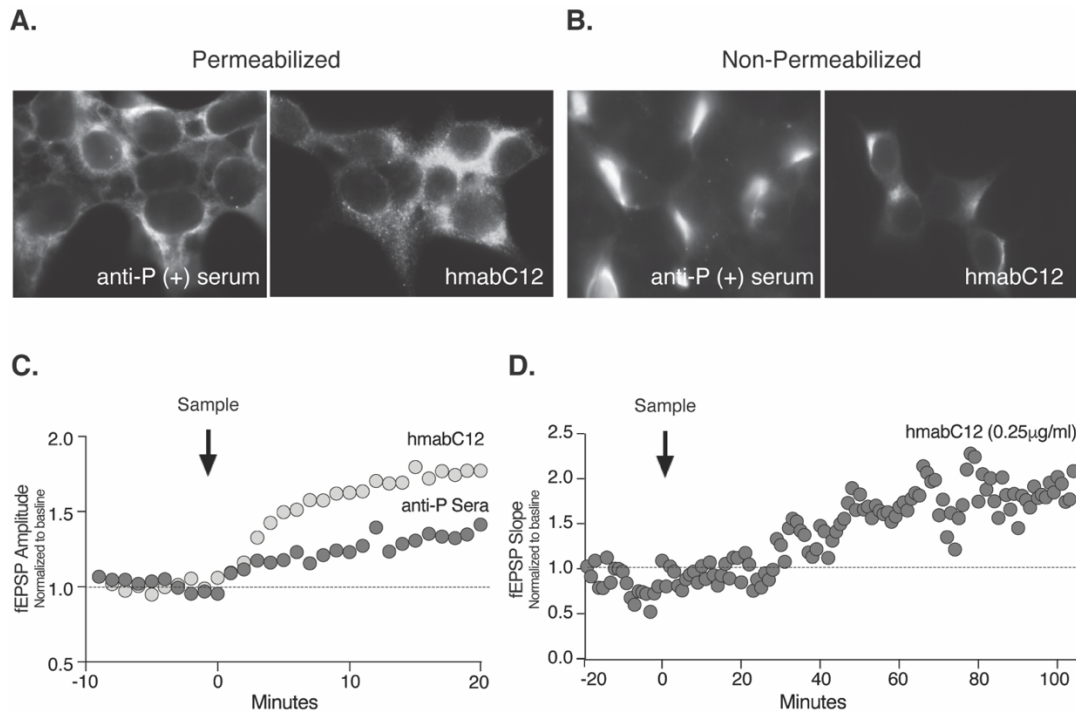


Figure A.5: Properties of human monoclonal antibody C12 (hmabC12) that resemble anti-P antibodies. **A** and **B**. Indirect immunofluorescence of HEK-293 cells. HmabC12 supernatant shows a perinuclear speckled staining pattern compatible with ribosomal staining in permeabilized cells (**A**). Purified hmabC12 (50 $\mu\text{g}/\text{ml}$) shows a regionalized cell surface staining pattern similar to anti-P (+) serum (1:500 dilution) in non-permeabilized cells (**B**). **C** and **D**. Enhancement of hippocampal synaptic transmission. Brain slices incubated with dialyzed supernatant or human anti-P (+) (**C**) or with purified hmabC12 (**D**) increases fEPSP at the hippocampal CA3-CA1 circuit ($n=1$; Graph shows mean and SEM of amplitude or slope as indicated, normalized to baseline).

A.4. DISCUSSION

In this part of the thesis corresponding to objectives of the former proposal we obtained and characterized murine and human monoclonal antibodies that will facilitate future studies on the pathogenic mechanisms of these antibodies. Current strategies to study the pathogenic role of anti-P antibodies have been the screening and identification of sera bearing these antibodies in patients with SLE. Monoclonal antibodies from murine and human origin indeed might provide more convenient tools.

A.4.1 Murine monoclonal anti-P antibodies

Our studies with anti-P antibodies that cross-react with NSPA have been done with human or rabbit antibodies purified using the P-epitope of only 11 amino acids (Bravo-Zehnder et al., 2014; Matus et al., 2007; Segovia-Miranda et al., 2015). We immunized mice with the 11-residue P-Epitope as this approach creates fewer confounding antibodies compared with immunization with ribosomal proteins (Hines et al., 1991; Shor et al., 2014; Sun et al., 2001; Towbin et al., 1982; Uchiumi et al., 1990), or with models of lupus prone mice that produce several antibodies, including anti-P (Kello et al., 2019). We first observed that BALB/c strain but not the C57/B6H2B or H2D strains generate antibodies against the P-Epitope and obtained 13 hybridomas. Due to technical difficulties in the transport from the laboratory in USA, we only partially characterized the 8C1 hybridoma. This 8C1 hybridoma showed binding in ELISA assay to the P-Epitope and gave no reaction in western blot against the P0 protein, contrasting with polyclonal antibodies (Bravo-Zehnder et al., 2014; Matus et al., 2007). We also provide evidence that this antibody increases synaptic transmission in the CA3-CA1 of the hippocampus, a functional assay that resembles the effect of human and rabbit anti-P antibodies (Segovia-Miranda et al., 2015). Indeed, for further experiments of

passive transfer *in vivo*, it would be necessary to produce these antibodies in large amounts, ideally using the ascites method.

A.4.2 Human monoclonal anti-P antibodies

In addition, we also obtained recombinant 13 monoclonal human antibodies using single cell sorting and cloning. When we tested different biotinylated peptides with the sequence of the P-Epitope that is recognized by anti-P, we observed that C-terminal biotinylation provided the best binding in ELISA tests. Most likely the biotin in the N-terminal blocks the binding of antibodies in this test. Afterwards we used flow cytometry to identify memory B cells with P-Epitope affinity applying a sorting strategy that resulted effective in detecting anti-P positive cells. Among the 13 antibodies cloned and produced by transfection in HEK-293 cells some had affinity for the P-Epitope and P0 in ELISAs assay, but none recognized P0 on western blots, similar to our mouse monoclonal. Both the MAP-P-Epitope used for the immunization and the biotinylated P-Epitope for the cell sorting are bound to the core or the biotin, respectively, through the carboxy terminal. This may expose an epitope favorable for ELISA but not for western blot testing. However, we find that the hmabC12 antibody resembles anti-P antibodies in immunofluorescence, ELISA and synaptic transmission effects (Bravo-Zehnder et al., 2014; Matus et al., 2007; Segovia-Miranda et al., 2015).

A.4.3. Conclusions

In conclusion, the monoclonal antibodies generated in mice and obtained from a SLE patient elicit glutamatergic synaptic alterations that mimic previous effects of circulating human polyclonal anti-P antibodies, thus providing a powerful tool to investigate their pathogenic mechanisms. Anti-P antibodies have been associated to psychosis and cognitive dysfunction (Elkon et al., 1985; González & Massardo, 2018; Massardo et al., 2014). A

pathogenic mechanism relies on their cross reactivity with NPSA (Matus et al., 2007). We recently showed that NSPA can ubiquitinate the phosphatase PTPMEG that controls NMDAR phosphorylation impacting on memory processes (Espinoza et al., 2020). This opens the possibility that anti-P antibodies perturb the function of PTPMEG. Therefore, our hmabC12 human antibodies may facilitate future studies regarding the pathogenic mechanism of anti-P antibodies in the brain, especially regarding the NSPA/PTPMEG system that stabilizes NMDAR at the synapse (Espinoza et al., 2020).

BIBLIOGRAPHY

- Allendorf, D. H., Franssen, E. H., & Brown, G. C. (2020). Lipopolysaccharide activates microglia via neuraminidase 1 desialylation of Toll-like Receptor 4. *J Neurochem*, *155*(4), 403-416. doi:10.1111/jnc.15024
- Allendorf, D. H., Puigdellivol, M., & Brown, G. C. (2020). Activated microglia desialylate their surface, stimulating complement receptor 3-mediated phagocytosis of neurons. *Glia*, *68*(5), 989-998. doi:10.1002/glia.23757
- Anacker, C., & Hen, R. (2017). Adult hippocampal neurogenesis and cognitive flexibility - linking memory and mood. *Nat Rev Neurosci*, *18*(6), 335-346. doi:10.1038/nrn.2017.45
- Arancibia-Cárcamo, L., Fairfax, B. P., Moss, S. J., & Kittler, J. (2006). Studying the Localization, Surface Stability and Endocytosis of Neurotransmitter Receptors by Antibody Labeling and Biotinylation Approaches - The Dynamic Synapse - NCBI Bookshelf. *The Dynamic Synapse: Molecular Methods in Ionotropic Receptor Biology*. doi:NBK2552 [bookaccession]
- Armada-Moreira, A., Gomes, J. I., Pina, C. C., Savchak, O. K., Goncalves-Ribeiro, J., Rei, N., . . . Vaz, S. H. (2020). Going the Extra (Synaptic) Mile: Excitotoxicity as the Road Toward Neurodegenerative Diseases. *Front Cell Neurosci*, *14*, 90. doi:10.3389/fncel.2020.00090
- Babayan, A. H., Kramar, E. A., Barrett, R. M., Jafari, M., Haettig, J., Chen, L. Y., . . . Lynch, G. (2012). Integrin Dynamics Produce a Delayed Stage of Long-Term Potentiation and Memory Consolidation. *Journal of Neuroscience*, *32*(37), 12854-12861. doi:10.1523/JNEUROSCI.2024-12.2012
- Barake, F., Soza, A., & González, A. (2020). Galectins in the brain: advances in neuroinflammation, neuroprotection and therapeutic opportunities. *Current Opinion in Neurology*, *33*(3), 381-390. doi:10.1097/WCO.0000000000000812
- Beggs, H. E., Baragona, S. C., Hemperly, J. J., & Maness, P. F. (1997). NCAM140 interacts with the focal adhesion kinase p125(fak) and the SRC-related tyrosine kinase p59(fyn). *J Biol Chem*, *272*(13), 8310-8319. doi:10.1074/jbc.272.13.8310
- Bidon, N., Brichory, F., Bourguet, P., Le Pennec, J. P., & Dazard, L. (2001). Galectin-8: a complex sub-family of galectins (Review). *Int J Mol Med*, *8*(3), 245-250.
- Bonfa, E., Golombek, S. J., Kaufman, L. D., Skelly, S., Weissbach, H., Brot, N., & Elkon, K. (1987). Association between lupus psychosis and anti-ribosomal P protein antibodies. *N Engl J Med*, *317*, 265-271.
- Bowen, A. B., Bourke, A. M., Hiester, B. G., Hanus, C., & Kennedy, M. J. (2017). Golgi-Independent secretory trafficking through recycling endosomes in neuronal dendrites and spines. *eLife*, *6*, 1-27. doi:10.7554/eLife.27362
- Bravo-Zehnder, M., Toledo, E. M., Segovia-Miranda, F., Serrano, F. G., Benito, M. J., Metz, C., . . . González, A. (2014). Anti-Ribosomal P Protein Autoantibodies From Patients With Neuropsychiatric Lupus Impair Memory in Mice. *Arthritis & Rheumatology*, *67*(1), 204-214.
- Brimberg, L., Mader, S., Fujieda, Y., Arinuma, Y., Kowal, C., Volpe, B. T., & Diamond, B. (2015). Antibodies as Mediators of Brain Pathology. *Trends in Immunology*.

- Brinker, T., Stopa, E., Morrison, J., & Klinge, P. (2014). A new look at cerebrospinal fluid circulation. *Fluids and barriers of the CNS*, *11*, 10-10. doi:10.1186/2045-8118-11-10
- Buller, A. L., Larson, H. C., Schneider, B. E., Beaton, J. A., Morrisett, R. A., & Monaghan, D. T. (1994). The molecular basis of NMDA receptor subtypes: native receptor diversity is predicted by subunit composition. *The Journal of neuroscience : the official journal of the Society for Neuroscience*, *14*(9), 5471-5484.
- Buonarati, O. R., Hammes, E. A., Watson, J. F., Greger, I. H., & Hell, J. W. (2019). *Mechanisms of postsynaptic localization of AMPA-type glutamate receptors and their regulation during long-term potentiation*. Retrieved from
- Burgaya, F., Menegon, A., Menegoz, M., Valtorta, F., & Girault, J. A. (1995). Focal adhesion kinase in rat central nervous system. *Eur J Neurosci*, *7*(8), 1810-1821. doi:10.1111/j.1460-9568.1995.tb00700.x
- Cagnoni, A. J., Troncoso, M. F., Rabinovich, G. A., Marino, K. V., & Elola, M. T. (2020). Full-length galectin-8 and separate carbohydrate recognition domains: the whole is greater than the sum of its parts? *Biochem Soc Trans*. doi:10.1042/BST20200311
- Carcamo, C., Pardo, E., Oyanadel, C., Bravo-Zehnder, M., Bull, P., Caceres, M., . . . Soza, A. (2006). Galectin-8 binds specific beta1 integrins and induces polarized spreading highlighted by asymmetric lamellipodia in Jurkat T cells. *Exp Cell Res*, *312*(4), 374-386. doi:10.1016/j.yexcr.2005.10.025
- Carlsson, S., Carlsson, M. C., & Leffler, H. (2007). Intracellular sorting of galectin-8 based on carbohydrate fine specificity. *Glycobiology*, *17*(9), 906-912. doi:10.1093/glyco/cwm059
- Carola, V., D'Olimpio, F., Brunamonti, E., Mangia, F., & Renzi, P. (2002). Evaluation of the elevated plus-maze and open-field tests for the assessment of anxiety-related behaviour in inbred mice. *Behav Brain Res*, *134*, 49-57.
- Carvajal, F. J., Mira, R. G., Rovegno, M., Minniti, A. N., & Cerpa, W. (2018). Age-related NMDA signaling alterations in SOD2 deficient mice. *Biochimica et Biophysica Acta (BBA) - Molecular Basis of Disease*. doi:10.1016/j.bbadis.2018.03.019
- Chan, K., Nestor, J., Huerta, T. S., Certain, N., Moody, G., Kowal, C., . . . Wollmuth, L. P. (2020). Lupus autoantibodies act as positive allosteric modulators at GluN2A-containing NMDA receptors and impair spatial memory. *Nat Commun*, *11*(1), 1403. doi:10.1038/s41467-020-15224-w
- Chang, E. H., Volpe, B. T., Mackay, M., Aranow, C., Watson, P., Kowal, C., . . . Diamond, B. (2015). Selective Impairment of Spatial Cognition Caused by Autoantibodies to the N-Methyl-d-Aspartate Receptor. *EBioMedicine*, *2*(7), 755-764. doi:10.1016/j.ebiom.2015.05.027
- Chen, Y.-C., Ma, Y.-L., Lin, C.-H., Cheng, S.-J., Hsu, W.-L., & Lee, E. H. Y. (2017). Galectin-3 Negatively Regulates Hippocampus-Dependent Memory Formation through Inhibition of Integrin Signaling and Galectin-3 Phosphorylation. *Frontiers in Molecular Neuroscience*, *10*(July), 1-15. doi:10.3389/fnmol.2017.00217
- Cho, B. G., Veillon, L., & Mechref, Y. (2019). N-Glycan Profile of Cerebrospinal Fluids from Alzheimer's Disease Patients Using Liquid Chromatography with Mass Spectrometry. *J Proteome Res*, *18*(10), 3770-3779. doi:10.1021/acs.jproteome.9b00504
- Choquet, D., & Hossy, E. (2020). AMPA receptor nanoscale dynamic organization and synaptic plasticities. *Curr Opin Neurobiol*, *63*, 137-145. doi:10.1016/j.conb.2020.04.003
- Chowdhury, S., Shepherd, J. D., Okuno, H., Lyford, G., Petralia, R. S., Plath, N., . . . Worley, P. F. (2006). Arc/Arg3.1 interacts with the endocytic machinery to regulate AMPA receptor trafficking. *Neuron*, *52*(3), 445-459. doi:10.1016/j.neuron.2006.08.033

- Cingolani, L. A., & Goda, Y. (2008). Differential involvement of beta3 integrin in pre- and postsynaptic forms of adaptation to chronic activity deprivation. *Neuron Glia Biol*, 4(3), 179-187. doi:10.1017/S1740925X0999024X
- Cingolani, L. A., Thalhammer, A., Yu, L. M., Catalano, M., Ramos, T., Colicos, M. A., & Goda, Y. (2008). Activity-dependent regulation of synaptic AMPA receptor composition and abundance by beta3 integrins. *Neuron*, 58(5), 749-762. doi:10.1016/j.neuron.2008.04.011
- Citri, A., & Malenka, R. C. (2008). Synaptic plasticity: multiple forms, functions, and mechanisms. *Neuropsychopharmacology*, 33(1), 18-41. doi:1301559 [pii] 10.1038/sj.npp.1301559
- Collingridge, G. L., Isaac, J. T., & Wang, Y. T. (2004). Receptor trafficking and synaptic plasticity. *Nat Rev Neurosci*, 5(12), 952-962. doi:nrn1556 [pii] 10.1038/nrn1556
- Copits, B. A., Vernon, C. G., Sakai, R., & Swanson, G. T. (2014). Modulation of ionotropic glutamate receptor function by vertebrate galectins. *J Physiol*, 592.10(592.10), 2079-2096. doi:10.1113/jphysiol.2013.269597
- de Jong, C. G. H. M., Gabius, H. J., & Baron, W. (2019). The emerging role of galectins in (re)myelination and its potential for developing new approaches to treat multiple sclerosis. *Cellular and Molecular Life Sciences*(0123456789). doi:10.1007/s00018-019-03327-7
- DeGiorgio, L. A., Konstantinov, K. N., Lee, S. C., Hardin, J. A., Volpe, B. T., & Diamond, B. (2001). A subset of lupus anti-DNA antibodies cross-reacts with the NR2 glutamate receptor in systemic lupus erythematosus. *Nature Medicine*, 7(11), 1189-1193.
- Díaz-Alonso, J., Sun, Y. J., Granger, A. J., Levy, J. M., Blankenship, S. M., & Nicoll, R. A. (2017). Subunit-specific role for the amino-terminal domain of AMPA receptors in synaptic targeting. *Proceedings of the National Academy of Sciences*, 114(27), 7136-7141. doi:10.1073/pnas.1707472114
- Diering, G. H., & Huganir, R. L. (2018). The AMPA Receptor Code of Synaptic Plasticity. *Neuron*, 100(2), 314-329. doi:10.1016/j.neuron.2018.10.018
- Diskin, S., Cao, Z., Leffler, H., & Panjwani, N. (2009). The role of integrin glycosylation in galectin-8-mediated trabecular meshwork cell adhesion and spreading. *Glycobiology*, 19(1), 29-37. doi:10.1093/glycob/cwn100
- Doherty, G. J., Ahlund, M. K., Howes, M. T., Moren, B., Parton, R. G., McMahon, H. T., & Lundmark, R. (2011). The endocytic protein GRAF1 is directed to cell-matrix adhesion sites and regulates cell spreading. *Mol Biol Cell*, 22(22), 4380-4389. doi:10.1091/mbc.E10-12-0936
- Edvardson, S., Baumann, A. M., Muhlenhoff, M., Stephan, O., Kuss, A. W., Shaag, A., . . . Elpeleg, O. (2013). West syndrome caused by ST3Gal-III deficiency. *Epilepsia*, 54(2), e24-27. doi:10.1111/epi.12050
- Ehlers, M. D. (2000). Reinsertion or Degradation of AMPA Receptors Determined by Activity-Dependent Endocytic Sorting. *Neuron*, 28(2), 511-525. doi:10.1016/S0896-6273(00)00129-X
- Elkon, K. B., Parnassa, A. P., & Foster, C. L. (1985). Lupus autoantibodies target ribosomal P proteins. *The Journal of experimental medicine*, 162(2), 459-471.
- Espinoza, S., Arredondo, S. B., Barake, F., Carvajal, F., Guerrero, F. G., Segovia-Miranda, F., . . . Gonzalez, A. (2020). Neuronal surface P antigen (NSPA) modulates postsynaptic NMDAR stability through ubiquitination of tyrosine phosphatase PTPMEG. *BMC Biol*, 18(1), 164. doi:10.1186/s12915-020-00877-2

- Esteban, J. A., Shi, S. H., Wilson, C., Nuriya, M., Huganir, R. L., & Malinow, R. (2003). PKA phosphorylation of AMPA receptor subunits controls synaptic trafficking underlying plasticity. *Nat Neurosci*, *6*(2), 136-143. doi:10.1038/nn997
- Everts, I., Villmann, C., & Hollmann, M. (1997). N-Glycosylation Is Not a Prerequisite for Glutamate Receptor Function but Is Essential for Lectin Modulation. *Molecular Pharmacology*, *52*(5). Retrieved from <http://www.molpharm.org>
- Ezratty, E. J., Partridge, M. A., & Gundersen, G. G. (2005). Microtubule-induced focal adhesion disassembly is mediated by dynamin and focal adhesion kinase. *Nat Cell Biol*, *7*(6), 581-590. doi:10.1038/ncb1262
- Fang, P., Xie, J., Sang, S., Zhang, L., Liu, M., Yang, L., . . . Shen, H. (2020). Multilayered N-Glycoproteome Profiling Reveals Highly Heterogeneous and Dysregulated Protein N-Glycosylation Related to Alzheimer's Disease. *Anal Chem*, *92*(1), 867-874. doi:10.1021/acs.analchem.9b03555
- Faust, T. W., Chang, E. H., Kowal, C., Berlin, R., Gazaryan, I. G., Bertini, E., . . . Huerta, P. T. (2010). Neurotoxic lupus autoantibodies alter brain function through two distinct mechanisms. *Proceedings of the National Academy of Sciences*, *107*(43), 18569-18574.
- Filippi, M., Bar-Or, A., Piehl, F., Preziosa, P., Solari, A., Vukusic, S., & Rocca, M. A. (2018). Multiple sclerosis. *Nat Rev Dis Primers*, *4*(1), 43. doi:10.1038/s41572-018-0041-4
- Fraussen, J., Claes, N., de Bock, L., & Somers, V. (2014). Targets of the humoral autoimmune response in multiple sclerosis. *Autoimmun Rev*, *13*(11), 1126-1137. doi:10.1016/j.autrev.2014.07.002
- Gardoni, F., Stanic, J., Scheggia, D., Benussi, A., Borroni, B., & Di Luca, M. (2021). NMDA and AMPA Receptor Autoantibodies in Brain Disorders: From Molecular Mechanisms to Clinical Features. *Cells*, *10*(1). doi:10.3390/cells10010077
- Gaunitz, S., Tjernberg, L. O., & Schedin-Weiss, S. (2020). The N-glycan profile in cortex and hippocampus is altered in Alzheimer s disease. *J Neurochem*. doi:10.1111/jnc.15202
- Gibson, L. L., McKeever, A., Coutinho, E., Finke, C., & Pollak, T. A. (2020). Cognitive impact of neuronal antibodies: encephalitis and beyond. *Translational Psychiatry*, *10*(1), 304-304. doi:10.1038/s41398-020-00989-x
- Gleichman, A. J., Panzer, J. A., Baumann, B. H., Dalmau, J., & Lynch, D. R. (2014). Antigenic and mechanistic characterization of anti-AMPA receptor encephalitis. *Ann Clin Transl Neurol*, *1*(3), 180-189. doi:10.1002/acn3.43
- González, A., & Massardo, L. (2018). Antibodies and the brain: Antiribosomal P protein antibody and the clinical effects in patients with systemic lupus erythematosus. *Current Opinion in Neurology*, *31*(3), 300-305. doi:10.1097/WCO.0000000000000549
- Grant, B. D., & Donaldson, J. G. (2009). Pathways and mechanisms of endocytic recycling. *Nat Rev Mol Cell Biol*, *10*(9), 597-608. doi:10.1038/nrm2755
- Gurba, K. N., Hernandez, C. C., Hu, N., & Macdonald, R. L. (2012). GABRB3 mutation, G32R, associated with childhood absence epilepsy alters alpha1beta3gamma2L gamma-aminobutyric acid type A (GABAA) receptor expression and channel gating. *J Biol Chem*, *287*(15), 12083-12097. doi:10.1074/jbc.M111.332528
- Hadari, Y. R., Arbel-Goren, R., Levy, Y., Amsterdam, A., Alon, R., Zakut, R., & Zick, Y. (2000). Galectin-8 binding to integrins inhibits cell adhesion and induces apoptosis. *J Cell Sci*, *113* (Pt 13), 2385-2397.
- Hanley, J. G. (2018). The Regulation of AMPA Receptor Endocytosis by Dynamic Protein-Protein Interactions. *Frontiers in Cellular Neuroscience*, *12*(October), 1-10. doi:10.3389/fncel.2018.00362

- Hanus, C., Geptin, H., Tushev, G., Garg, S., Alvarez-Castelao, B., Sambandan, S., . . . Schuman, E. M. (2016). Unconventional secretory processing diversifies neuronal ion channel properties. *eLife*, 5(September2016), 1-27. doi:10.7554/eLife.20609.001
- Henley, J. M., & Wilkinson, K. A. (2016). Synaptic AMPA receptor composition in development, plasticity and disease. *Nature Reviews*, 17, 337-350. doi:10.1038/nrn.2016.37
- Herguedas, B., Watson, J. F., Ho, H., Cais, O., Garcia-Nafria, J., & Greger, I. H. (2019). Architecture of the heteromeric GluA1/2 AMPA receptor in complex with the auxiliary subunit TARP gamma8. *Science*, 364(6438). doi:10.1126/science.aav9011
- Hidalgo, A., Burgos, V., Viola, H., Medina, J., & Argibay, P. (2006). Differential expression of glycans in the hippocampus of rats trained on an inhibitory learning paradigm. *Neuropathology*, 26(6), 501-507. doi:10.1111/j.1440-1789.2006.00718.x
- Hildick, K. L., González-González, I. M., Jaskolski, F., & Henley, J. M. (2012). Lateral Diffusion and Exocytosis of Membrane Proteins in Cultured Neurons Assessed using Fluorescence Recovery and Fluorescence-loss Photobleaching. *Journal of Visualized Experiments*(60), 1-8. doi:10.3791/3747
- Hines, J. J., Weissbach, H., Brot, N., & Elkon, K. (1991). Anti-P autoantibody production requires P1/P2 as immunogens but is not driven by exogenous self-antigen in MRL mice. *Journal of immunology (Baltimore, Md. : 1950)*, 146(10), 3386-3395.
- Hoftberger, R., van Sonderen, A., Leyboldt, F., Houghton, D., Geschwind, M., Gelfand, J., . . . Dalmau, J. (2015). Encephalitis and AMPA receptor antibodies: Novel findings in a case series of 22 patients. *Neurology*, 84(24), 2403-2412. doi:10.1212/WNL.0000000000001682
- Hu, H., Eggers, K., Chen, W., Garshasbi, M., Motazacker, M. M., Wrogemann, K., . . . Kuss, A. W. (2011). ST3GAL3 mutations impair the development of higher cognitive functions. *Am J Hum Genet*, 89(3), 407-414. doi:10.1016/j.ajhg.2011.08.008
- Huerta, P. T., Kowal, C., DeGiorgio, L. A., Volpe, B. T., & Diamond, B. (2006). Immunity and behavior: antibodies alter emotion. *Proceedings of the National Academy of Sciences of the United States of America*, 103(3), 678-683. doi:10.1073/pnas.0510055103
- Hwang, H., & Rhim, H. (2019). Acutely elevated O-GlcNAcylation suppresses hippocampal activity by modulating both intrinsic and synaptic excitability factors. *Sci Rep*, 9(1), 7287. doi:10.1038/s41598-019-43017-9
- Ideo, H., Matsuzaka, T., Nonaka, T., Seko, A., & Yamashita, K. (2011). Galectin-8-N-domain Recognition Mechanism for Sialylated and Sulfated Glycans. doi:10.1074/jbc.M110.195925
- Iliff, J. J., Wang, M., Liao, Y., Plogg, B. A., Peng, W., Gundersen, G. A., . . . Nedergaard, M. (2012). A paravascular pathway facilitates CSF flow through the brain parenchyma and the clearance of interstitial solutes, including amyloid beta. *Sci Transl Med*, 4(147), 147ra111. doi:10.1126/scitranslmed.3003748
- Imaizumi, Y., Sakaguchi, M., Morishita, T., Ito, M., Poirier, F., Sawamoto, K., & Okano, H. (2011). Galectin-1 is expressed in early-type neural progenitor cells and down-regulates neurogenesis in the adult hippocampus. *Molecular Brain*, 4(1), 7-7. doi:10.1186/1756-6606-4-7
- Jacob, T. C., Moss, S. J., & Jurd, R. (2008). GABA(A) receptor trafficking and its role in the dynamic modulation of neuronal inhibition. *Nat Rev Neurosci*, 9(5), 331-343. doi:10.1038/nrn2370
- Johannes, L., Jacob, R., & Leffler, H. (2018). Galectins at a glance. *Journal of Cell Science*, 131(9), jcs208884-jcs208884. doi:10.1242/jcs.208884

- Johannes, L., Wunder, C., & Shafaq-Zadah, M. (2016). Glycolipids and Lectins in Endocytic Uptake Processes. *Journal of Molecular Biology*, 428(24), 4792-4818. doi:10.1016/j.jmb.2016.10.027
- Kaltner, H., Abad-Rodriguez, J., Corfield, A. P., Kopitz, J., & Gabius, H. J. (2019). The sugar code: letters and vocabulary, writers, editors and readers and biosignificance of functional glycan-lectin pairing. *Biochem J*, 476(18), 2623-2655. doi:10.1042/BCJ20170853
- Kanno, T., Yaguchi, T., Nagata, T., Mukasa, T., & Nishizaki, T. (2010). Regulation of AMPA receptor trafficking by O-glycosylation. *Neurochemical Research*, 35(5), 782-788. doi:10.1007/s11064-010-0135-1
- Katzav, A., Ben-Ziv, T., Chapman, J., Blank, M., Reichlin, M., & Shoenfeld, Y. (2008). Anti-P ribosomal antibodies induce defect in smell capability in a model of CNS -SLE (depression). *Journal of Autoimmunity*, 31(4), 393-398. doi:10.1016/j.jaut.2008.09.002
- Katzav, A., Solodeev, I., Brodsky, O., Chapman, J., Pick, C. G., Blank, M., . . . Shoenfeld, Y. (2007). Induction of autoimmune depression in mice by anti-ribosomal P antibodies via the limbic system. *Arthritis & Rheumatism*, 56(3), 938-948. doi:10.1002/art.22419
- Keable, R., Leshchyns'ka, I., & Sytnyk, V. (2020). Trafficking and Activity of Glutamate and GABA Receptors: Regulation by Cell Adhesion Molecules. *Neuroscientist*, 26(5-6), 415-437. doi:10.1177/1073858420921117
- Kello, N., Anderson, E., & Diamond, B. (2019). Cognitive Dysfunction in Systemic Lupus Erythematosus: A Case for Initiating Trials. *Arthritis Rheumatol*, 71(9), 1413-1425. doi:10.1002/art.40933
- Kessels, H. W., & Malinow, R. (2009). Synaptic AMPA receptor plasticity and behavior. *Neuron*, 61(3), 340-350. doi:10.1016/j.neuron.2009.01.015
- Kleene, R., Mzoughi, M., Joshi, G., Kalus, I., Bormann, U., Schulze, C., . . . Schachner, M. (2010). NCAM-induced neurite outgrowth depends on binding of calmodulin to NCAM and on nuclear import of NCAM and fak fragments. *J Neurosci*, 30(32), 10784-10798. doi:10.1523/JNEUROSCI.0297-10.2010
- Kleene, R., & Schachner, M. (2004). Glycans and neural cell interactions. *Nature reviews. Neuroscience*, 5(3), 195-208. doi:10.1038/nrn1349
- Kleinschmidt, E. G., & Schlaepfer, D. D. (2017). Focal adhesion kinase signaling in unexpected places. *Curr Opin Cell Biol*, 45, 24-30. doi:10.1016/j.ceb.2017.01.003
- Kolkova, K., Novitskaya, V., Pedersen, N., Berezin, V., & Bock, E. (2000). Neural cell adhesion molecule-stimulated neurite outgrowth depends on activation of protein kinase C and the Ras-mitogen-activated protein kinase pathway. *J Neurosci*, 20(6), 2238-2246.
- Kopec, C. D. (2006). Glutamate Receptor Exocytosis and Spine Enlargement during Chemically Induced Long-Term Potentiation. *Journal of Neuroscience*, 26(7), 2000-2009. doi:10.1523/JNEUROSCI.3918-05.2006
- Kowal, C., Degiorgio, L. A., Lee, J. Y., Edgar, M. A., Huerta, P. T., Volpe, B. T., & Diamond, B. (2006). Human lupus autoantibodies against NMDA receptors mediate cognitive impairment. *Proceedings of the National Academy of Sciences of the United States of America*, 103(52), 19854-19859. doi:10.1073/pnas.0608397104
- Kowal, C., & Diamond, B. (2012). Aspects of CNS lupus: mouse models of anti-NMDA receptor antibody mediated reactivity. *Methods in molecular biology (Clifton, N.J.)*, 900, 181-206. Retrieved from <http://eutils.ncbi.nlm.nih.gov/entrez/eutils/elink.fcgi?dbfrom=pubmed&id=22933070&rtmode=ref&cmd=prlinks>

- Lakshminarayan, R., Wunder, C., Becken, U., Howes, M. T., Benzing, C., Arumugam, S., . . . Johannes, L. (2014). Galectin-3 drives glycosphingolipid-dependent biogenesis of clathrin-independent carriers. *Nat Cell Biol*, *16*(6), 595-606. doi:10.1038/ncb2970 ncb2970 [pii]
- Lau, K. S., Partridge, E. A., Grigorian, A., Silvescu, C. I., Reinhold, V. N., Demetriou, M., & Dennis, J. W. (2007). Complex N-Glycan Number and Degree of Branching Cooperate to Regulate Cell Proliferation and Differentiation. *Cell*, *129*(1), 123-134. doi:10.1016/j.cell.2007.01.049
- Lee, E., Lee, J., & Kim, E. (2017). Excitation/Inhibition Imbalance in Animal Models of Autism Spectrum Disorders. *Biol Psychiatry*, *81*(10), 838-847. doi:10.1016/j.biopsych.2016.05.011
- Lekishvili, T., Hesketh, S., Brazier, M. W., & Brown, D. R. (2006). Mouse galectin-1 inhibits the toxicity of glutamate by modifying NR1 NMDA receptor expression. *European Journal of Neuroscience*, *24*(11), 3017-3025. doi:10.1111/j.1460-9568.2006.05207.x
- Levy, Y., Arbel-Goren, R., Hadari, Y. R., Eshhar, S., Ronen, D., Elhanany, E., . . . Zick, Y. (2001). Galectin-8 functions as a matricellular modulator of cell adhesion. *J Biol Chem*, *276*(33), 31285-31295. doi:10.1074/jbc.M100340200
- Lilja, J., & Ivaska, J. (2018). Integrin activity in neuronal connectivity. *J Cell Sci*, *131*(12). doi:10.1242/jcs.212803
- Limon, I. D., Ramirez, E., Diaz, A., Mendieta, L., Mayoral, M. A., Espinosa, B., . . . Zenteno, E. (2011). Alteration of the sialylation pattern and memory deficits by injection of Abeta(25-35) into the hippocampus of rats. *Neurosci Lett*, *495*(1), 11-16. doi:10.1016/j.neulet.2011.03.006
- Lo, W. Y., Lagrange, A. H., Hernandez, C. C., Harrison, R., Dell, A., Haslam, S. M., . . . Macdonald, R. L. (2010). Glycosylation of β 2 subunits regulates GABAA receptor biogenesis and channel gating. *J Biol Chem*, *285*(41), 31348-31361. doi:10.1074/jbc.M110.151449
- Luscher, B., Fuchs, T., & Kilpatrick, C. L. (2011). GABAA receptor trafficking-mediated plasticity of inhibitory synapses. *Neuron*, *70*(3), 385-409. doi:10.1016/j.neuron.2011.03.024
- Luscher, C., Xia, H., Beattie, E. C., Carroll, R. C., von Zastrow, M., Malenka, R. C., & Nicoll, R. A. (1999). Role of AMPA receptor cycling in synaptic transmission and plasticity. *Neuron*, *24*(3), 649-658. doi:10.1016/s0896-6273(00)81119-8
- Lutowski, D., Joubert-Caron, R., Lefebvre, C., Salama, J., Belin, C., Bladier, D., & Caron, M. (1997). Anti-galectin-1 autoantibodies in serum of patients with neurological diseases. *Clin Chim Acta*, *262*(1-2), 131-138.
- Mackay, M., Vo, A., Tang, C. C., Small, M., Anderson, E. W., Ploran, E. J., . . . Eidelberg, D. (2019). Metabolic and microstructural alterations in the SLE brain correlate with cognitive impairment. *JCI Insight*, *4*(1). doi:10.1172/jci.insight.124002
- Mahler, M., Kessenbrock, K., Raats, J., Williams, R., Fritzler, M. J., & Blüthner, M. (2003). Characterization of the human autoimmune response to the major C-terminal epitope of the ribosomal P proteins. *Journal of molecular medicine (Berlin, Germany)*, *81*(3), 194-204. doi:10.1007/s00109-003-0423-1
- Malkiel, S., Jeganathan, V., Wolfson, S., Manjarrez Orduno, N., Marasco, E., Aranow, C., . . . Diamond, B. (2016). Checkpoints for Autoreactive B Cells in the Peripheral Blood of Lupus Patients Assessed by Flow Cytometry. *Arthritis Rheumatol*, *68*(9), 2210-2220. doi:10.1002/art.39710

- Massardo, L., Bravo-Zehnder, M., Calderon, J., Flores, P., Padilla, O., Aguirre, J. M., . . . Gonzalez, A. (2014). Anti-N-methyl-D-aspartate receptor and anti-ribosomal-P autoantibodies contribute to cognitive dysfunction in systemic lupus erythematosus. *Lupus*. doi:10.1177/0961203314555538
- Massardo, L., Bravo-Zehnder, M., Calderon, J., Flores, P., Padilla, O., Aguirre, J. M., . . . Gonzalez, A. (2015). Anti-N-methyl-D-aspartate receptor and anti-ribosomal-P autoantibodies contribute to cognitive dysfunction in systemic lupus erythematosus. *Lupus*, 24(6), 558-568. doi:10.1177/0961203314555538
- Massardo, L., Metz, C., Pardo, E., Mezzano, V., Babul, M., Jarpa, E., . . . Soza, A. (2009). Autoantibodies against galectin-8: their specificity, association with lymphopenia in systemic lupus erythematosus and detection in rheumatoid arthritis and acute inflammation. *Lupus*, 18(6), 539-546. doi:10.1177/0961203308099973
- Mathew, M. P., & Donaldson, J. G. (2019). Glycosylation and glycan interactions can serve as extracellular machinery facilitating clathrin-independent endocytosis. *Traffic*, 20(4), 295-300. doi:10.1111/tra.12636
- Matus, S., Burgos, P. V., Bravo-Zehnder, M., Kraft, R., Porras, O. H., Farías, P., . . . González, A. (2007). Antiribosomal-P autoantibodies from psychiatric lupus target a novel neuronal surface protein causing calcium influx and apoptosis. *The Journal of experimental medicine*, 204(13), 3221-3234. doi:10.1084/jem.20071285
- Meinohl, C., Barnard, S. J., Fritz-Wolf, K., Unger, M., Porr, A., Heipel, M., . . . Giehl, K. (2020). Galectin-8 binds to the Farnesylated C-terminus of K-Ras4B and Modifies Ras/ERK Signaling and Migration in Pancreatic and Lung Carcinoma Cells. *Cancers*, 12(1), 30.
- Menegon, A., Burgaya, F., Baudot, P., Dunlap, D. D., Girault, J. A., & Valtorta, F. (1999). FAK+ and PYK2/CAKbeta, two related tyrosine kinases highly expressed in the central nervous system: similarities and differences in the expression pattern. *Eur J Neurosci*, 11(11), 3777-3788. doi:10.1046/j.1460-9568.1999.00798.x
- Minami, A., Meguro, Y., Ishibashi, S., Ishii, A., Shiratori, M., Sai, S., . . . Suzuki, T. (2017). Rapid regulation of sialidase activity in response to neural activity and sialic acid removal during memory processing in rat hippocampus. *J Biol Chem*, 292(14), 5645-5654. doi:10.1074/jbc.M116.764357
- Minami, A., Saito, M., Mamada, S., Ieno, D., Hikita, T., Takahashi, T., . . . Suzuki, T. (2016). Role of Sialidase in Long-Term Potentiation at Mossy Fiber-CA3 Synapses and Hippocampus-Dependent Spatial Memory. *PLoS ONE*, 11(10), e0165257. doi:10.1371/journal.pone.0165257
- Monje, F. J., Kim, E. J., Pollak, D. D., Cabatic, M., Li, L., Baston, A., & Lubec, G. (2012). Focal adhesion kinase regulates neuronal growth, synaptic plasticity and hippocampus-dependent spatial learning and memory. *Neurosignals*, 20(1), 1-14. doi:10.1159/000330193
- Moretto, E., & Passafaro, M. (2018). Recent Findings on AMPA Receptor Recycling. *Frontiers in Cellular Neuroscience*, 12(September), 1-12. doi:10.3389/fncel.2018.00286
- Mudd, A. T., Fleming, S. A., Labhart, B., Chichlowski, M., Berg, B. M., Donovan, S. M., & Dilger, R. N. (2017). Dietary Sialyllactose Influences Sialic Acid Concentrations in the Prefrontal Cortex and Magnetic Resonance Imaging Measures in Corpus Callosum of Young Pigs. *Nutrients*, 9(12). doi:10.3390/nu9121297
- Mueller, T. M., Haroutunian, V., & Meador-Woodruff, J. H. (2014). N-Glycosylation of GABAA Receptor Subunits is Altered in Schizophrenia. *Neuropsychopharmacology*, 39(3), 528-537. doi:10.1038/npp.2013.190

- Nader, G. P., Ezratty, E. J., & Gundersen, G. G. (2016). FAK, talin and PIPK1gamma regulate endocytosed integrin activation to polarize focal adhesion assembly. *Nat Cell Biol*, *18*(5), 491-503. doi:10.1038/ncb3333
- Nestor, J., Arinuma, Y., Huerta, T. S., Kowal, C., Nasiri, E., Kello, N., . . . Diamond, B. (2018). Lupus antibodies induce behavioral changes mediated by microglia and blocked by ACE inhibitors. *The Journal of experimental medicine*, *215*(10), 2554-2566. doi:10.1084/jem.20180776
- Nicoll, R. A. (2017). A Brief History of Long-Term Potentiation. *Neuron*, *93*(2), 281-290. doi:10.1016/j.neuron.2016.12.015
- Niethammer, P., Delling, M., Sytnyk, V., Dityatev, A., Fukami, K., & Schachner, M. (2002). Cosignaling of NCAM via lipid rafts and the FGF receptor is required for neurogenesis. *J Cell Biol*, *157*(3), 521-532. doi:10.1083/jcb.200109059
- Nishi, N., Itoh, A., Shoji, H., Miyanaka, H., & Nakamura, T. (2006). Galectin-8 and galectin-9 are novel substrates for thrombin. *Glycobiology*, *16*(11), 15C-20C. doi:10.1093/glycob/cwl028
- Nishi, N., Shoji, H., Seki, M., Itoh, A., Miyanaka, H., Yuube, K., . . . Nakamura, T. (2003). Galectin-8 modulates neutrophil function via interaction with integrin alphaM. *Glycobiology*, *13*(11), 755-763. doi:10.1093/glycob/cwg102
- Nishihara, H., Shimizu, F., Kitagawa, T., Yamanaka, N., Akada, J., Kuramitsu, Y., . . . Kanda, T. (2017). Identification of galectin-3 as a possible antibody target for secondary progressive multiple sclerosis. *Mult Scler*, *23*(3), 382-394. doi:10.1177/1352458516655217
- Nomura, K., Vilalta, A., Allendorf, D. H., Hornik, T. C., & Brown, G. C. (2017). Activated Microglia Desialylate and Phagocytose Cells via Neuraminidase, Galectin-3, and Mer Tyrosine Kinase. *The Journal of Immunology*, *198*(12), 4792-4801. doi:10.4049/jimmunol.1502532
- Norambuena, A., Metz, C., Vicuna, L., Silva, A., Pardo, E., Oyanadel, C., . . . Soza, A. (2009). Galectin-8 induces apoptosis in Jurkat T cells by phosphatidic acid-mediated ERK1/2 activation supported by protein kinase A down-regulation. *J Biol Chem*, *284*(19), 12670-12679. doi:10.1074/jbc.M808949200
- Ohkawa, T., Fukata, Y., Yamasaki, M., Miyazaki, T., Yokoi, N., Takashima, H., . . . Fukata, M. (2013). Autoantibodies to epilepsy-related LGI1 in limbic encephalitis neutralize LGI1-ADAM22 interaction and reduce synaptic AMPA receptors. *J Neurosci*, *33*(46), 18161-18174. doi:10.1523/JNEUROSCI.3506-13.2013
- Oliva, C. A., & Inestrosa, N. C. (2015). A novel function for Wnt signaling modulating neuronal firing activity and the temporal structure of spontaneous oscillation in the entorhinal-hippocampal circuit. *Experimental Neurology*, *269*, 43-55. doi:10.1016/j.expneurol.2015.03.027
- Oliveros, E., Vazquez, E., Barranco, A., Ramirez, M., Gruart, A., Delgado-Garcia, J. M., . . . Martin, M. J. (2018). Sialic Acid and Sialylated Oligosaccharide Supplementation during Lactation Improves Learning and Memory in Rats. *Nutrients*, *10*(10). doi:10.3390/nu10101519
- Opazo, P., Labrecque, S., Tigaret, C. M., Frouin, A., Wiseman, P. W., De Koninck, P., & Choquet, D. (2010). CaMKII triggers the diffusional trapping of surface AMPARs through phosphorylation of stargazin. *Neuron*, *67*(2), 239-252. doi:10.1016/j.neuron.2010.06.007
- Oyanadel, C., Holmes, C., Pardo, E., Retamal, C., Shaughnessy, R., Smith, P., . . . Gonzalez, A. (2018). Galectin-8 induces partial epithelial-mesenchymal transition with invasive

- tumorigenic capabilities involving a FAK/EGFR/proteasome pathway in Madin-Darby canine kidney cells. *Mol Biol Cell*, 29(5), 557-574. doi:10.1091/mbc.E16-05-0301
- Paoletti, P., Bellone, C., & Zhou, Q. (2013). NMDA receptor subunit diversity: impact on receptor properties, synaptic plasticity and disease. *Nature reviews. Neuroscience*, 14(6), 383-400. doi:doi.org/10.1038/nrn3504
- Pardo, E., Barake, F., Godoy, J. A., Oyanadel, C., Espinoza, S., Metz, C., . . . Gonzalez, A. (2019). GALECTIN-8 Is a Neuroprotective Factor in the Brain that Can Be Neutralized by Human Autoantibodies. *Mol Neurobiol*, 56(11), 7774-7788. doi:10.1007/s12035-019-1621-3
- Pardo, E., Carcamo, C., Massardo, L., Mezzano, V., Jacobelli, S., Gonzalez, A., & Soza, A. (2006). [Antibodies against galectin-8 in patients with systemic lupus erythematosus]. *Rev Med Chil*, 134(2), 159-166. doi:10.4067/s0034-98872006000200004
- Pardo, E., Carcamo, C., Uribe-San Martin, R., Ciampi, E., Segovia-Miranda, F., Curkovic-Pena, C., . . . Gonzalez, A. (2017). Galectin-8 as an immunosuppressor in experimental autoimmune encephalomyelitis and a target of human early prognostic antibodies in multiple sclerosis. *PLoS ONE*, 12(6), e0177472. doi:10.1371/journal.pone.0177472
- Park, M. (2018). AMPA Receptor Trafficking for Postsynaptic Potentiation. *Frontiers in Cellular Neuroscience*, 12(October), 1-10. doi:10.3389/fncel.2018.00361
- Park, Y. K., & Goda, Y. (2016). Integrins in synapse regulation. *Nat Rev Neurosci*, 17(12), 745-756. doi:10.1038/nrn.2016.138
- Peng, X., Hughes, E. G., Moscato, E. H., Parsons, T. D., Dalmau, J., & Balice-Gordon, R. J. (2015). Cellular plasticity induced by anti-alpha-amino-3-hydroxy-5-methyl-4-isoxazolepropionic acid (AMPA) receptor encephalitis antibodies. *Ann Neurol*, 77(3), 381-398. doi:10.1002/ana.24293
- Penn, A. C., Zhang, C. L., Georges, F., Royer, L., Breillat, C., Hosy, E., . . . Choquet, D. (2017). Hippocampal LTP and contextual learning require surface diffusion of AMPA receptors. *Nature*, 549(7672), 384-388. doi:10.1038/nature23658
- Petrini, E. M., Lu, J., Cognet, L., Lounis, B., Ehlers, M. D., & Choquet, D. (2009). Endocytic trafficking and recycling maintain a pool of mobile surface AMPA receptors required for synaptic potentiation. *Neuron*, 63(1), 92-105. doi:10.1016/j.neuron.2009.05.025
- Petrini, E. M., Marchionni, I., Zacchi, P., Sieghart, W., & Cherubini, E. (2004). Clustering of extrasynaptic GABA(A) receptors modulates tonic inhibition in cultured hippocampal neurons. *J Biol Chem*, 279(44), 45833-45843. doi:10.1074/jbc.M407229200
- Phulera, S., Zhu, H., Yu, J., Claxton, D. P., Yoder, N., Yoshioka, C., & Gouaux, E. (2018). Cryo-EM structure of the benzodiazepine-sensitive $\alpha 1\beta 1\gamma 2S$ tri-heteromeric GABAA receptor in complex with GABA. *eLife*, 7, e39383. doi:10.7554/eLife.39383
- Pozo, K., Cingolani, L. A., Bassani, S., Laurent, F., Passafaro, M., & Goda, Y. (2012). $\beta 3$ integrin interacts directly with GluA2 AMPA receptor subunit and regulates AMPA receptor expression in hippocampal neurons. *Proceedings of the National Academy of Sciences*, 109(4), 1323-1328. doi:10.1073/pnas.1113736109
- Prato, C. A., Carabelli, J., Campetella, O., & Tribulatti, M. V. (2020). Galectin-8 Enhances T cell Response by Promotion of Antigen Internalization and Processing. *iScience*, 23(7), 101278. doi:10.1016/j.isci.2020.101278
- Puigdellivol, M., Allendorf, D. H., & Brown, G. C. (2020). Sialylation and Galectin-3 in Microglia-Mediated Neuroinflammation and Neurodegeneration. *Front Cell Neurosci*, 14, 162. doi:10.3389/fncel.2020.00162

- Purcell, A. L., & Carew, T. J. (2003). Tyrosine kinases, synaptic plasticity and memory: insights from vertebrates and invertebrates. *Trends Neurosci*, 26(11), 625-630. doi:10.1016/j.tins.2003.09.005
- Purkey, A. M., & Dell'Acqua, M. L. (2020). Phosphorylation-Dependent Regulation of Ca²⁺-Permeable AMPA Receptors During Hippocampal Synaptic Plasticity. *Front Synaptic Neurosci*, 12, 8. doi:10.3389/fnsyn.2020.00008
- Rabinovich, G. A., & Croci, D. O. (2012). Regulatory circuits mediated by lectin-glycan interactions in autoimmunity and cancer. *Immunity*, 36(3), 322-335. doi:10.1016/j.immuni.2012.03.004
- Rahimian, R., Lively, S., Abdelhamid, E., Lalancette-Hebert, M., Schlichter, L., Sato, S., & Kriz, J. (2019). Delayed Galectin-3-Mediated Reprogramming of Microglia After Stroke is Protective. *Molecular Neurobiology*, 3. doi:10.1007/s12035-019-1527-0
- Ramos-Martinez, I., Martinez-Loustalot, P., Lozano, L., Issad, T., Limon, D., Diaz, A., . . . Zenteno, E. (2018). Neuroinflammation induced by amyloid beta₂₅₋₃₅ modifies mucin-type O-glycosylation in the rat's hippocampus. *Neuropeptides*, 67, 56-62. doi:10.1016/j.npep.2017.11.008
- Regan, P., McClean, P. L., Smyth, T., & Doherty, M. (2019). Early Stage Glycosylation Biomarkers in Alzheimer's Disease. *Medicines (Basel)*, 6(3). doi:10.3390/medicines6030092
- Reily, C., Stewart, T. J., Renfrow, M. B., & Novak, J. (2019). Glycosylation in health and disease. *Nature Reviews Nephrology*, 15(6), 346-366. doi:10.1038/s41581-019-0129-4
- Renard, H. F., Tyckaert, F., Lo Giudice, C., Hirsch, T., Valades-Cruz, C. A., Lemaigre, C., . . . Morsomme, P. (2020). Endophilin-A3 and Galectin-8 control the clathrin-independent endocytosis of CD166. *Nat Commun*, 11(1), 1457. doi:10.1038/s41467-020-15303-y
- Rial Verde, E. M., Lee-Osbourne, J., Worley, P. F., Malinow, R., & Cline, H. T. (2006). Increased expression of the immediate-early gene *arc/arg3.1* reduces AMPA receptor-mediated synaptic transmission. *Neuron*, 52(3), 461-474. doi:10.1016/j.neuron.2006.09.031
- Roth, R. H., Zhang, Y., & Haganir, R. L. (2017). Dynamic imaging of AMPA receptor trafficking in vitro and in vivo. *Current Opinion in Neurobiology*, 45, 51-58. doi:10.1016/j.conb.2017.03.008
- Sakaguchi, M., Arruda-Carvalho, M., Kang, N. H., Imaizumi, Y., Poirier, F., Okano, H., & Frankland, P. W. (2011). Impaired spatial and contextual memory formation in galectin-1 deficient mice. *Mol Brain*, 4, 33. doi:10.1186/1756-6606-4-33
- Sakaguchi, M., Imaizumi, Y., & Okano, H. (2007). Expression and function of galectin-1 in adult neural stem cells. *Cell Mol Life Sci*, 64(10), 1254-1258. doi:10.1007/s00018-007-6476-5
- Sakaguchi, M., Imaizumi, Y., Shingo, T., Tada, H., Hayama, K., Yamada, O., . . . Okano, H. (2010). Regulation of adult neural progenitor cells by Galectin-1/beta1 Integrin interaction. *J Neurochem*, 113(6), 1516-1524. doi:10.1111/j.1471-4159.2010.06712.x
- Sakaguchi, M., & Okano, H. (2012). Neural stem cells, adult neurogenesis, and galectin-1: from bench to bedside. *Dev Neurobiol*, 72(7), 1059-1067. doi:10.1002/dneu.22023
- Salazar, G., & Gonzalez, A. (2002). Novel mechanism for regulation of epidermal growth factor receptor endocytosis revealed by protein kinase A inhibition. *Mol Biol Cell*, 13(5), 1677-1693.

- Schindelin, J., Arganda-Carreras, I., Frise, E., Kaynig, V., Longair, M., Pietzsch, T., . . . Cardona, A. (2012). Fiji: an open-source platform for biological-image analysis. *Nat Methods*, *9*(7), 676-682. doi:10.1038/nmeth.2019
- Segovia-Miranda, F., Serrano, F., Dyrda, A., Ampuero, E., Retamal, C., Bravo-Zehnder, M., . . . González, A. (2015). Pathogenicity of Lupus Anti-Ribosomal P Antibodies: Role of Cross-Reacting Neuronal Surface P Antigen in Glutamatergic Transmission and Plasticity in a Mouse Model. *Arthritis & Rheumatology*, *67*(6), 1598-1610. doi:10.1002/art.39081
- Seino, S., & Shibasaki, T. (2005). PKA-dependent and PKA-independent pathways for cAMP-regulated exocytosis. *Physiol Rev*, *85*(4), 1303-1342. doi:10.1152/physrev.00001.2005
- Sheng, N., Bemben, M. A., Diaz-Alonso, J., Tao, W., Shi, Y. S., & Nicoll, R. A. (2018). LTP requires postsynaptic PDZ-domain interactions with glutamate receptor/auxiliary protein complexes. *Proc Natl Acad Sci U S A*, *115*(15), 3948-3953. doi:10.1073/pnas.1800719115
- Shi, Y., Pontrello, C. G., DeFea, K. A., Reichardt, L. F., & Ethell, I. M. (2009). Focal adhesion kinase acts downstream of EphB receptors to maintain mature dendritic spines by regulating cofilin activity. *J Neurosci*, *29*(25), 8129-8142. doi:10.1523/JNEUROSCI.4681-08.2009
- Shi, Z. R., Cao, C. X., Tan, G. Z., & Wang, L. (2015). The association of serum anti-ribosomal P antibody with clinical and serological disorders in systemic lupus erythematosus: a systematic review and meta-analysis. *Lupus*, *24*(6), 588-596. doi:10.1177/0961203314560003
- Shor, D. B.-A., Blank, M., Reuter, S., Matthias, T., Beiglass, I., Volkov, A., . . . Shoenfeld, Y. (2014). Anti-ribosomal-P antibodies accelerate lupus glomerulonephritis and induce lupus nephritis in naïve mice. *Journal of Autoimmunity*, *54*(C), 118-126.
- Siciliano, J. C., Toutant, M., Derkinderen, P., Sasaki, T., & Girault, J. A. (1996). Differential regulation of proline-rich tyrosine kinase 2/cell adhesion kinase beta (PYK2/CAKbeta) and pp125(FAK) by glutamate and depolarization in rat hippocampus. *J Biol Chem*, *271*(46), 28942-28946. doi:10.1074/jbc.271.46.28942
- Siew, J. J., & Chern, Y. (2018). Microglial Lectins in Health and Neurological Diseases. *Frontiers in Molecular Neuroscience*, *11*(May), 1-17. doi:10.3389/fnmol.2018.00158
- Simon, M. J., & Iliff, J. J. (2016). Regulation of cerebrospinal fluid (CSF) flow in neurodegenerative, neurovascular and neuroinflammatory disease. *Biochim Biophys Acta*, *1862*(3), 442-451. doi:10.1016/j.bbadis.2015.10.014
- Smith, P. C., Metz, C., de la Pena, A., Oyanadel, C., Avila, P., Arancibia, R., . . . Soza, A. (2020). Galectin-8 mediates fibrogenesis induced by cyclosporine in human gingival fibroblasts. *J Periodontal Res*, *55*(5), 724-733. doi:10.1111/jre.12761
- Srikanth, K. D., Meirson, T., Sharan Sams, D., & Gil-Henn, H. (2018). FAK family kinases in brain health and disease. *Journal of Molecular and Clinical Medicine*, *1*(3), 177-190. doi:10.31083/j.jmcm.2018.03.007
- Standley, S., Tocco, G., Wagle, N., & Baudry, M. (1998). High- and low-affinity alpha-[³H]amino-3-hydroxy-5-methylisoxazole-4-propionic acid ([³H]AMPA) binding sites represent immature and mature forms of AMPA receptors and are composed of differentially glycosylated subunits. *Journal of Neurochemistry*, *70*(6), 2434-2445.
- Stevens, G. R., Zhang, C., Berg, M. M., Lambert, M. P., Barber, K., Cantalops, I., . . . Klein, W. L. (1996). CNS neuronal focal adhesion kinase forms clusters that co-localize with

- vinculin. *J Neurosci Res*, 46(4), 445-455. doi:10.1002/(SICI)1097-4547(19961115)46:4<445::AID-JNR6>3.0.CO;2-G
- Stock, A. D., Gelb, S., Pasternak, O., Ben-Zvi, A., & Putterman, C. (2017). The blood brain barrier and neuropsychiatric lupus: new perspectives in light of advances in understanding the neuroimmune interface. *Autoimmun Rev*, 16(6), 612-619. doi:10.1016/j.autrev.2017.04.008
- Straube, T., von Mach, T., Honig, E., Greb, C., Schneider, D., & Jacob, R. (2013). pH-dependent recycling of galectin-3 at the apical membrane of epithelial cells. *Traffic*, 14(9), 1014-1027. doi:10.1111/tra.12086
- Sulzmaier, F. J., Jean, C., & Schlaepfer, D. D. (2014). FAK in cancer: mechanistic findings and clinical applications. *Nat Rev Cancer*, 14(9), 598-610. doi:10.1038/nrc3792
- Sumowski, J. F., Benedict, R., Enzinger, C., Filippi, M., Geurts, J. J., Hamalainen, P., . . . Rao, S. (2018). Cognition in multiple sclerosis: State of the field and priorities for the future. *Neurology*, 90(6), 278-288. doi:10.1212/WNL.0000000000004977
- Sun, K. H., Tang, S. J., Lin, M. L., Wang, Y. S., Sun, G. H., & Liu, W. T. (2001). Monoclonal antibodies against human ribosomal P proteins penetrate into living cells and cause apoptosis of Jurkat T cells in culture. *Rheumatology (Oxford, England)*, 40(7), 750-756. doi:10.1093/rheumatology/40.7.750
- Tanaka, M., Olsen, R. W., Medina, M. T., Schwartz, E., Alonso, M. E., Duron, R. M., . . . Delgado-Escueta, A. V. (2008). Hyperglycosylation and reduced GABA currents of mutated GABRB3 polypeptide in remitting childhood absence epilepsy. *Am J Hum Genet*, 82(6), 1249-1261. doi:10.1016/j.ajhg.2008.04.020
- Tavalin, S. J., Colledge, M., Hell, J. W., Langeberg, L. K., Haganir, R. L., & Scott, J. D. (2002). Regulation of GluR1 by the A-kinase anchoring protein 79 (AKAP79) signaling complex shares properties with long-term depression. *J Neurosci*, 22(8), 3044-3051. doi:20026277
- Taylor, E. W., Wang, K., Nelson, A. R., Bredemann, T. M., Fraser, K. B., Clinton, S. M., . . . McMahon, L. L. (2014). O-GlcNAcylation of AMPA receptor GluA2 is associated with a novel form of long-term depression at hippocampal synapses. *J Neurosci*, 34(1), 10-21. doi:10.1523/JNEUROSCI.4761-12.2014
- ten Bruggencate, S. J., Bovee-Oudenhoven, I. M., Feitsma, A. L., van Hoffen, E., & Schoterman, M. H. (2014). Functional role and mechanisms of sialyllactose and other sialylated milk oligosaccharides. *Nutr Rev*, 72(6), 377-389. doi:10.1111/nure.12106
- Towbin, H., Ramjoué, H. P., Kuster, H., Liverani, D., & Gordon, J. (1982). Monoclonal antibodies against eucaryotic ribosomes. . *THE JOURNAL OF BIOLOGICAL CHEMISTRY*, 257(21), 12709-12715.
- Tribulatti, M. V., Carabelli, J., Prato, C. A., & Campetella, O. (2020). Galectin-8 in the onset of the immune response and inflammation. *Glycobiology*, 30(3), 134-142. doi:10.1093/glycob/cwz077
- Troncoso, M. F., Ferragut, F., Bacigalupo, M. L., Cardenas Delgado, V. M., Nugnes, L. G., Gentilini, L., . . . Elola, M. T. (2014). Galectin-8: a matricellular lectin with key roles in angiogenesis. *Glycobiology*, 24(10), 907-914. doi:10.1093/glycob/cwu054
- Tucholski, J., Pinner, A. L., Simmons, M. S., & Meador-Woodruff, J. H. (2014). Evolutionarily Conserved Pattern of AMPA Receptor Subunit Glycosylation in Mammalian Frontal Cortex. *PLoS ONE*, 9(4). doi:10.1371/journal.pone.0094255
- Tucholski, J., Simmons, M. S., Pinner, A. L., Haroutunian, V., McCullumsmith, R. E., & Meador-Woodruff, J. H. (2013). Abnormal N-linked glycosylation of cortical AMPA

- receptor subunits in schizophrenia. *Schizophr Res*, 146(1-3), 177-183. doi:10.1016/j.schres.2013.01.031
- Tucholski, J., Simmons, M. S., Pinner, A. L., McMillan, L. D., Haroutunian, V., & Meador-Woodruff, J. H. (2013). N-linked glycosylation of cortical N-methyl-D-aspartate and kainate receptor subunits in schizophrenia. *Neuroreport*, 24(12), 688-691. doi:10.1097/WNR.0b013e328363bd8a
- Uchiumi, T., Traut, R. R., & Kominami, R. (1990). Monoclonal antibodies against acidic phosphoproteins P0, P1, and P2 of eukaryotic ribosomes as functional probes. *THE JOURNAL OF BIOLOGICAL CHEMISTRY*, 265(1), 89-95.
- Vargas, L. M., Leal, N., Estrada, L. D., Gonzalez, A., Serrano, F., Araya, K., . . . Alvarez, A. R. (2014). EphA4 activation of c-Abl mediates synaptic loss and LTP blockade caused by amyloid-beta oligomers. *PLoS ONE*, 9(3), e92309. doi:10.1371/journal.pone.0092309
- Velasco, S., Diez-Revuelta, N., Hernandez-Iglesias, T., Kaltner, H., Andre, S., Gabius, H. J., & Abad-Rodriguez, J. (2013). Neuronal Galectin-4 is required for axon growth and for the organization of axonal membrane L1 delivery and clustering. *J Neurochem*, 125(1), 49-62. doi:10.1111/jnc.12148
- Vicuña, L., Pardo, E., Curkovic, C., Döger, R., Oyanadel, C., Metz, C., . . . Soza, A. (2013). Galectin-8 binds to LFA-1, blocks its interaction with ICAM-1 and is counteracted by anti-Gal-8 autoantibodies isolated from lupus patients. *Biol Res*, 46, 275-280.
- Vingtdeux, V., Chang, E. H., Frattini, S. A., Zhao, H., Chandakkar, P., Adrien, L., . . . Marambaud, P. (2016). CALHM1 deficiency impairs cerebral neuron activity and memory flexibility in mice. *Scientific Reports*, 6, 24250-24250. doi:10.1038/srep24250
- Volk, L., Chiu, S. L., Sharma, K., & Huganir, R. L. (2015). Glutamate synapses in human cognitive disorders. *Annu Rev Neurosci*, 38, 127-149. doi:10.1146/annurev-neuro-071714-033821
- Vorhees, C. V., & Williams, M. T. (2006). Morris water maze: procedures for assessing spatial and related forms of learning and memory. *Nature Protocols*, 1(2), 848-858.
- Wang, B. (2009). Sialic acid is an essential nutrient for brain development and cognition. *Annu Rev Nutr*, 29, 177-222. doi:10.1146/annurev.nutr.28.061807.155515
- Wang, B., McVeagh, P., Petocz, P., & Brand-Miller, J. (2003). Brain ganglioside and glycoprotein sialic acid in breastfed compared with formula-fed infants. *Am J Clin Nutr*, 78(5), 1024-1029. doi:10.1093/ajcn/78.5.1024
- Wang, B., Yu, B., Karim, M., Hu, H., Sun, Y., McGreevy, P., . . . Brand-Miller, J. (2007). Dietary sialic acid supplementation improves learning and memory in piglets. *Am J Clin Nutr*, 85(2), 561-569. doi:10.1093/ajcn/85.2.561
- Wang, Z., Edwards, J. G., Riley, N., Provance, D. W., Karcher, R., Li, X. d., . . . Ehlers, M. D. (2008). Myosin Vb Mobilizes Recycling Endosomes and AMPA Receptors for Postsynaptic Plasticity. *Cell*, 135(3), 535-548. doi:10.1016/j.cell.2008.09.057
- Wardemann, H., Yurasov, S., Schaefer, A., Young, J. W., Meffre, E., & Nussenzweig, M. C. (2003). Predominant autoantibody production by early human B cell precursors. *Science (New York, N.Y.)*, 301(5638), 1374-1377. Retrieved from <http://www.sciencemag.org/cgi/doi/10.1126/science.1086907>
- papers2://publication/doi/10.1126/science.1086907
- Watson, J. F., Ho, H., & Greger, I. H. (2017). Synaptic transmission and plasticity require AMPA receptor anchoring via its N-terminal domain. *eLife*, 6, 1-20. doi:10.7554/elife.23024

- Williams, S. E., Mealer, R. G., Scolnick, E. M., Smoller, J. W., & Cummings, R. D. (2020). Aberrant glycosylation in schizophrenia: a review of 25 years of post-mortem brain studies. *Mol Psychiatry*. doi:10.1038/s41380-020-0761-1
- Wu, X., Gan, B., Yoo, Y., & Guan, J. L. (2005). FAK-mediated src phosphorylation of endophilin A2 inhibits endocytosis of MT1-MMP and promotes ECM degradation. *Dev Cell*, 9(2), 185-196. doi:10.1016/j.devcel.2005.06.006
- Wyneken, U., Smalla, K. H., Marengo, J. J., Soto, D., De la Cerda, A., Tischmeyer, W., . . . Gundelfinger, E. D. (2001). Kainate-induced seizures alter protein composition and N-methyl-D-aspartate receptor function of rat forebrain postsynaptic densities. *Neuroscience*, 102(1), 65-74. doi:10.1016/S0306-4522(00)00469-3
- Yang, Y. C., Ma, Y. L., Chen, S. K., Wang, C. W., & Lee, E. H. (2003). Focal adhesion kinase is required, but not sufficient, for the induction of long-term potentiation in dentate gyrus neurons in vivo. *J Neurosci*, 23(10), 4072-4080.
- Yang, Y. R., Song, S., Hwang, H., Jung, J. H., Kim, S. J., Yoon, S., . . . Suh, P. G. (2017). Memory and synaptic plasticity are impaired by dysregulated hippocampal O-GlcNAcylation. *Sci Rep*, 7, 44921. doi:10.1038/srep44921
- Yoo, S. W., Motari, M. G., Susuki, K., Prendergast, J., Mountney, A., Hurtado, A., & Schnaar, R. L. (2015). Sialylation regulates brain structure and function. *FASEB J*, 29(7), 3040-3053. doi:10.1096/fj.15-270983
- Zamorano, P., Koning, T., Oyanadel, C., Mardones, G. A., Ehrenfeld, P., Boric, M. P., . . . Sanchez, F. A. (2019). Galectin-8 induces endothelial hyperpermeability through the eNOS pathway involving S-nitrosylation-mediated adherens junction disassembly. *Carcinogenesis*, 40(2), 313-323. doi:10.1093/carcin/bgz002
- Zappelli, C., van der Zwaan, C., Thijssen-Timmer, D. C., Mertens, K., & Meijer, A. B. (2012). Novel role for galectin-8 protein as mediator of coagulation factor V endocytosis by megakaryocytes. *J Biol Chem*, 287(11), 8327-8335. doi:10.1074/jbc.M111.305151
- Zhang, J., Yin, Y., Ji, Z., Cai, Z., Zhao, B., Li, J., . . . Guo, G. (2017). Endophilin2 Interacts with GluA1 to Mediate AMPA Receptor Endocytosis Induced by Oligomeric Amyloid-beta. *Neural Plast*, 2017, 8197085. doi:10.1155/2017/8197085
- Zhang, M., Patriarchi, T., Stein, I. S., Qian, H., Matt, L., Nguyen, M., . . . Hell, J. W. (2013). Adenylyl cyclase anchoring by a kinase anchor protein AKAP5 (AKAP79/150) is important for postsynaptic beta-adrenergic signaling. *J Biol Chem*, 288(24), 17918-17931. doi:10.1074/jbc.M112.449462
- Zheng, N., Jeyifous, O., Munro, C., Montgomery, J. M., & Green, W. N. (2015). Synaptic activity regulates AMPA receptor trafficking through different recycling pathways. *eLife*, 4. doi:10.7554/eLife.06878
- Zong, S., Hoffmann, C., Mane-Damas, M., Molenaar, P., Losen, M., & Martinez-Martinez, P. (2017). Neuronal Surface Autoantibodies in Neuropsychiatric Disorders: Are There Implications for Depression? *Front Immunol*, 8, 752. doi:10.3389/fimmu.2017.00752